MetOceanWorks

Metocean Analysis Overview

North Sea I Offshore Wind Farm

24 October 2024

MetOceanWorks Reference:

Energinet_C00001_R02_Metocean_Analysis_Overview

Commercial in Confidence

Andrew Watson MSc CSci CMarSci MIMarEST

Senior Metocean Consultant & Director

andrew.watson@metoceanworks.com

Contact +44 (0)7763 896635

Revision	Description	Prepared	Reviewed	Date
R02	Final	Jamie Hernon Andrew Watson	Andrew Watson	24 October 2024
R01	Draft	Andrew Berkeley Dave Quantrell	Andrew Watson	27 September 2024

Table of contents

List of Figures

List of Tables

1 Definitions

1.1   Units and Conventions

The following list describes the units and conventions used in this report. Unless stated otherwise, units have been expressed using the SI convention.

- Wind direction is expressed in compass points or degrees, relative to true North [°N], and describes the direction **from** which the winds are blowing.
- Wind speeds are expressed in metres per second [m/s].
- Wave direction is expressed in compass points or degrees, relative to true North [°N], and describes the direction **from** which the waves are propagating.
- Wave heights are expressed in metres [m].
- Wave periods are expressed in seconds [s].
- Current direction is expressed in compass points or degrees, relative to true North [°N], and describes the direction **towards** which the currents are flowing.
- Current speeds are expressed in metres per second [m/s].
- Water levels are expressed in metres [m].
- Temperature is expressed in degrees Celsius [°C].
- Salinity is expressed in practical salinity units [PSU].
- Density is expressed in kilograms per metre cubed [kg/m^3].
- Relative humidity unit is expressed as a percentage [%].
- Precipitation rate is expressed in millimetres per hour [mm/h].
- Solar radiation is expressed in watts per metre squared (W/m^2).
- Positions are quoted relative to WGS 84 except where stated.
- All times are quoted in Coordinated Universal Time [UTC].
- 'Hydrodynamics' refers to both water levels and currents.

1.2   Glossary of commonly used metocean terms

The following list describes common metocean terms used throughout this report.

Winds	Description
ASL	Above Sea Level. Refers to the height of the wind measurements above sea level.
U_{3-hr}	Mean wind speed averaged over a 3-hour period at 10 m ASL.
Wind gust	Wind speeds persisting for less than 1 minute are generally termed wind gusts.
Wind speed	Magnitude of local wind flow. Must be accompanied by an elevation ASL and averaging period for valid interpretation.
Waves	**Description**
Cmax	The maximum individual wave crest elevation occurring within a defined period.
Cmp	The most probable maximum individual wave crest elevation occurring within a storm.
Hmax	The maximum individual wave height occurring within a defined period.
Hmp	The most probable maximum individual wave height occurring within a storm.

Hm0	Significant wave height. Approximately the average height of the highest one third of the waves in a defined period, estimated from the wave spectrum as $4\sqrt{m_0}$.
m_0, m_1, m_2	The zeroth, first and second moments of the wave spectrum respectively.
Tp	The spectral peak period. The period at which most energy is present in the wave spectrum.
Tm02	The mean zero-crossing wave period. Estimated from the wave spectrum as $\sqrt{m_0/m_2}$.
Wave crest elevation	The vertical distance between the still water level and the maximum elevation of an individual wave.
Wave height	The vertical distance between the minimum and maximum elevations of an individual wave.
Levels	**Description**
HAT	Highest Astronomical Tide. Maximum level of sea surface due to tidal forcing alone.
LAT	Lowest Astronomical Tide. Minimum level of sea surface due to tidal forcing alone.
MHW	Mean High Water. Mean of all high water levels.
MHWN	Mean High Water Neap. Mean high water level during neap phase of tidal cycle.
MHWS	Mean High Water Spring. Mean high water level during spring phase of tidal cycle.
MLW	Mean Low Water. Mean of all low water levels.
MLWN	Mean Low Water Neap. Mean low water level during neap phase of tidal cycle.
MLWS	Mean Low Water Spring. Mean low water level during spring phase of tidal cycle.
MSL	Mean Sea Level. Mean sea surface elevation over a prolonged period of time.
Still water level	Instantaneous water level in the absence of waves, but including water level variations due to tide and meteorologically induced forcing.
Surge level	Difference between the tidal level estimated by harmonic analysis/prediction and the actual level. Includes any errors due to failure to adequately resolve the tidal signal. Includes meteorologically induced storm surge.
Tidal level	Still water level relative to a defined datum due to astronomical forcing. Tidal elevations exclude all meteorologically induced forcing.
Currents	**Description**
Current speed	Magnitude of local current flow.
Residual current	Current driven by processes excluding astronomical forcing and wave induced motions.
Tidal current	Current driven by astronomical forcing.
Total current	Combination of tidal and residual current.

2 Introduction

2.1 Background

The Danish Energy Agency has tasked Energinet with undertaking site metocean conditions assessments for the development of the offshore wind farm area North Sea I. Figure 2-1 shows the location of the wind farm area in the North Sea off the west coast of Jutland.

To support the development of offshore wind farms within the North Sea I area, Energinet has contracted MetOceanWorks to characterise the site metocean conditions for the area. The results of the Site Metocean Conditions Assessment will be used for the Front-End Engineering and Design (FEED) of offshore wind turbine generators (WTG) and other support structures for the offshore wind farms, particularly in early-stage integrated load analyses.
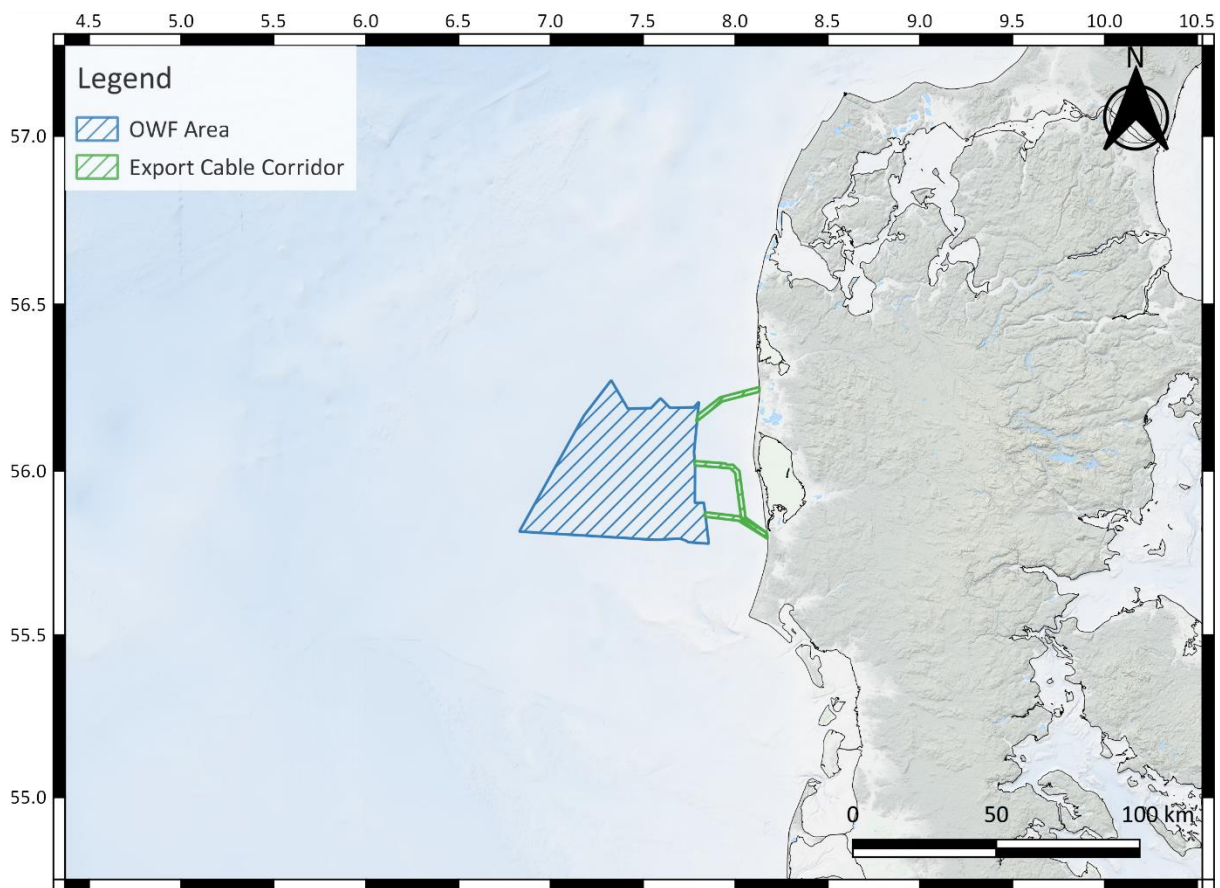
Figure 2-1: Project development area.

Energinet requires full metocean modelling, including wave and hydrodynamic modelling at a suitable resolution over a relevant time period, from which a suite of analyses will be conducted resulting in an appropriate level of information to enable FEED. The results will be issued to a certification body, who will give a feasibility statement related to the work. Hence, a full certification is not expected and in this manner the work differs from a full site metocean conditions assessment exercise.

2.2   Document Structure

For convenience, data sources, methodology details and design criteria and are split across several documents as follows:

- **NSI Metocean Data Overview (Energinet_C00001_Rxx_Metocean_Data_Overview):** Describes the data sources and models used to support this study, including numerous validations of models against measurements in the region of interest to demonstrate suitability in this regard.
- **NSI Metocean Analysis Overview (Energinet_C00001_Rxx_Metocean_Analysis_Overview):** Details analysis methods used to derive the criteria presented in all other documents, as well as including all spatial analyses which consider the project development area as a whole.
- **NSI *[LocationID]* Criteria (Energinet_C00001_Rxx_*[LocationID]*_Design_Criteria):** Metocean design criteria for individual locations, wherein *[LocationID]* should be replaced by the identifier for the location. For example, criteria for the A3W site can be found in the document **NSI A3W Criteria (Energinet_C00001_Rxx_A3W_Design_Criteria)**.

Throughout, Rxx denotes the report revision, for example R01 is used for the first revision, R02 the second, etc.

This Metocean Analysis Overview itself proceeds as follows:

- In Section 3, spatial maps illustrating variations in key parameters across the region of interest are included.
- In Section 4, the process of selecting the nine analysis locations is described, and the locations themselves summarized.
- Section 5 describes the analysis methods used to derive criteria for all locations.
- Section 6 describes expected marine growth as well as snow and ice.
- Section 7 provides a summary of possible changes to metocean conditions at the site driven by climate change.

The document concludes with a list of the references used throughout and various appendices providing more detail on a number of topics outlined in preceding sections.

3 Spatial Maps

3.1 Introduction

In this Section, map plots are provided to illustrate the spatial variability of metocean parameters across the lease area and surrounds. Maps of wave parameters are included in Section 3.2, followed by those for hydrodynamics (current speeds and water levels) in Section 3.3. The full duration of the hindcast period is used throughout.

Details of the methodology used to create extreme maps can be found in Appendix A. As outlined in more detail therein, note that the maps are intended to provide a general overview of behaviour in the region of interest, rather than detailed design criteria. In particular, the need to generate extreme values at many thousands of grid points means that results for individual locations are not subject to the same level of scrutiny as would generally be necessary in determining location-specific design criteria.

3.2 Waves

3.2.1 Operational Statistics

In Figure 3-1 through Figure 3-8, the following statistics are shown for significant wave height:

- Time-averaged **mean** significant wave height.
- Time-averaged power means of significant wave height **$<H_{m0}>_{(2)}$ and $<H_{m0}>_{(5)}$** whereby:

$$\langle H_{mo} \rangle_{(m)} = \left[\frac{1}{N} \sum_{n=1}^{N} \left(H_{m0,n} \right)^m \right]^{1/m}$$

   With $H_{m0,n}$ being the total significant wave height at time step n, m a coefficient (2 or 5), and the sum taken over all N steps of the dataset.

- **50th, 90th, 99th and 99.9th percentiles** of significant wave height.
- **Maximum** significant wave height.
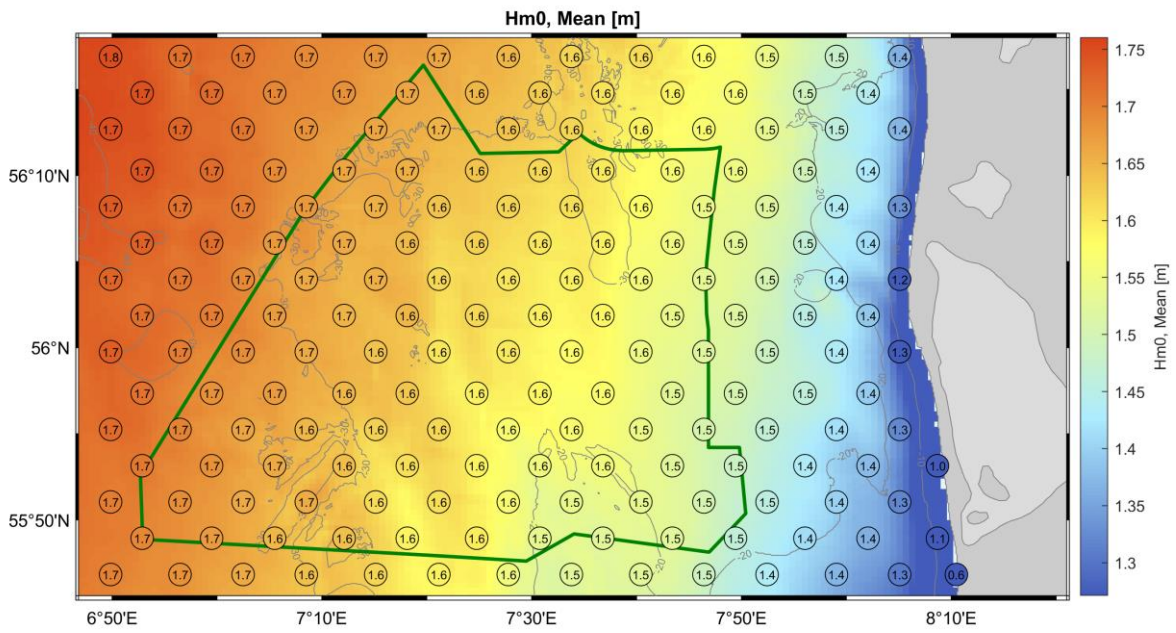
Figure 3-1:   Mean of Hm0.
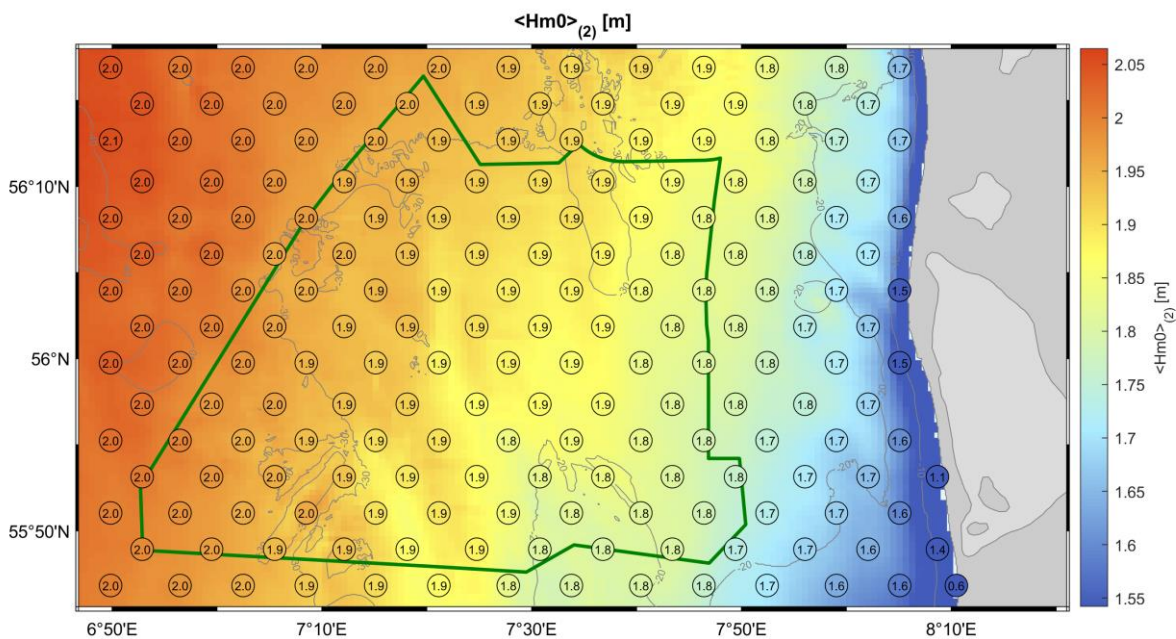
Figure 3-2:   2nd power mean of Hm0.
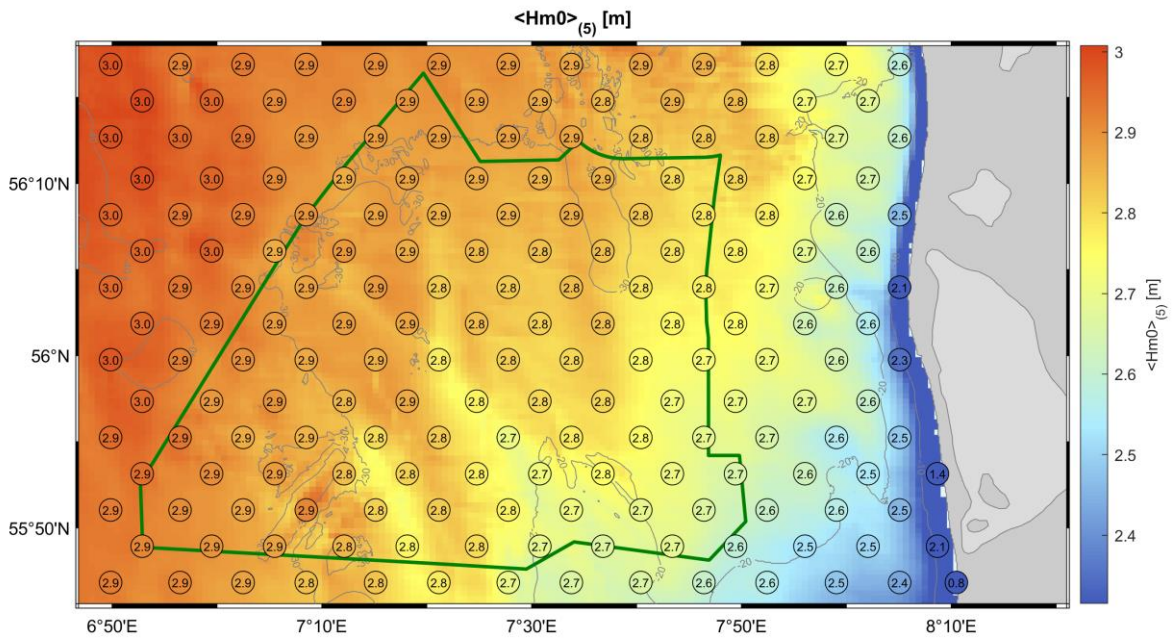
Figure 3-3:   5th power mean of Hm0.
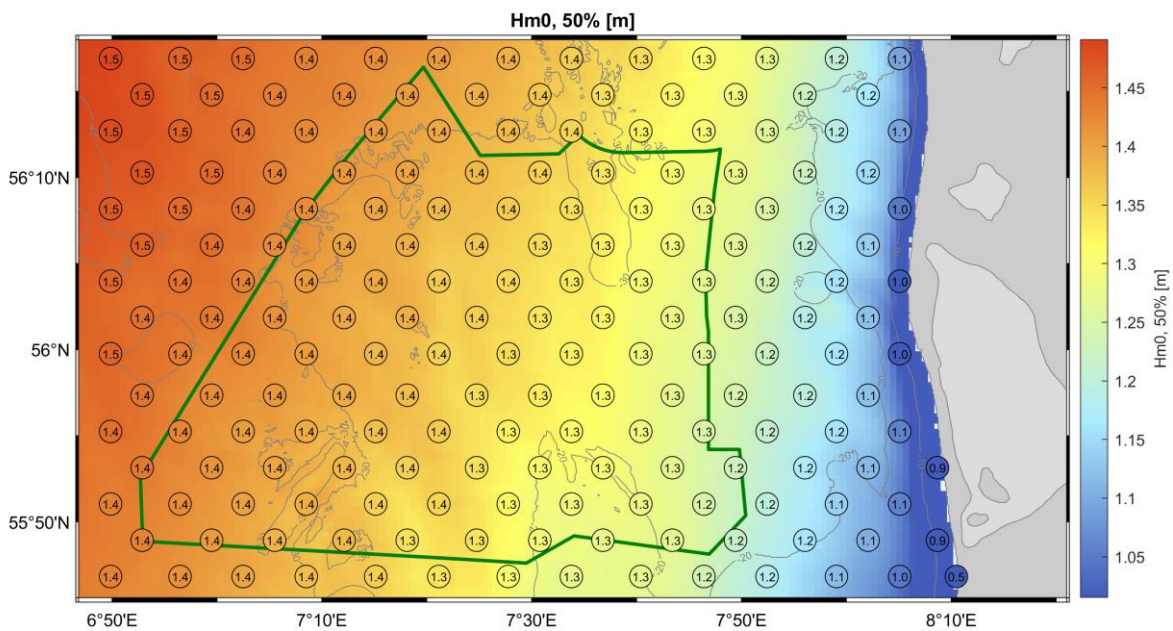
Figure 3-4:   50th percentile of Hm0.
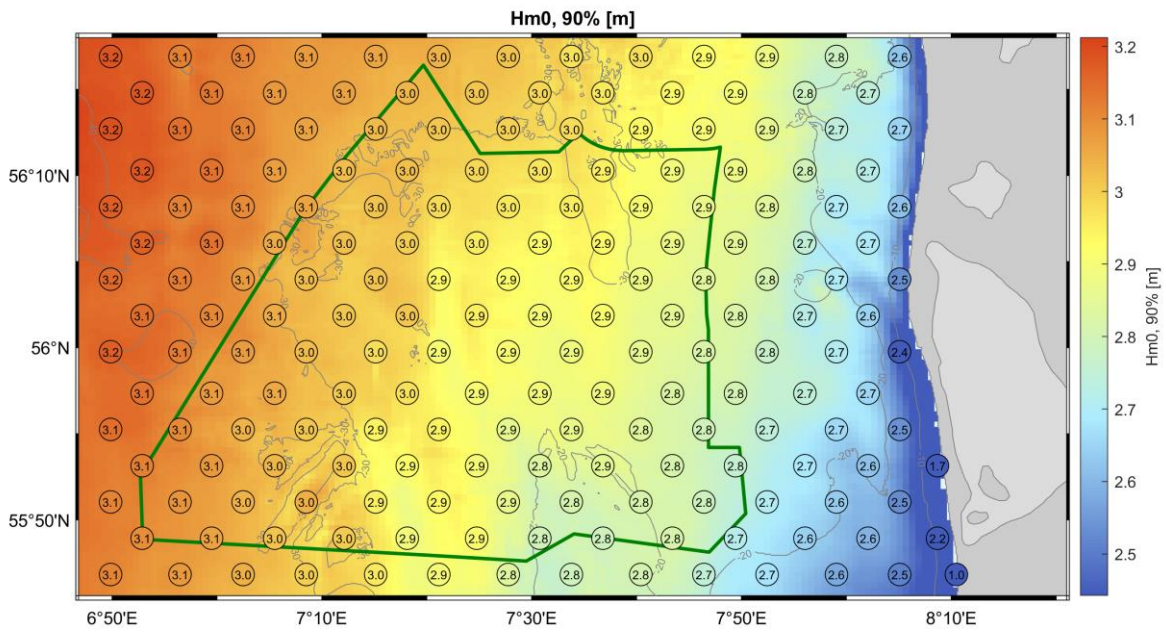
Figure 3-5:   90th percentile of Hm0.
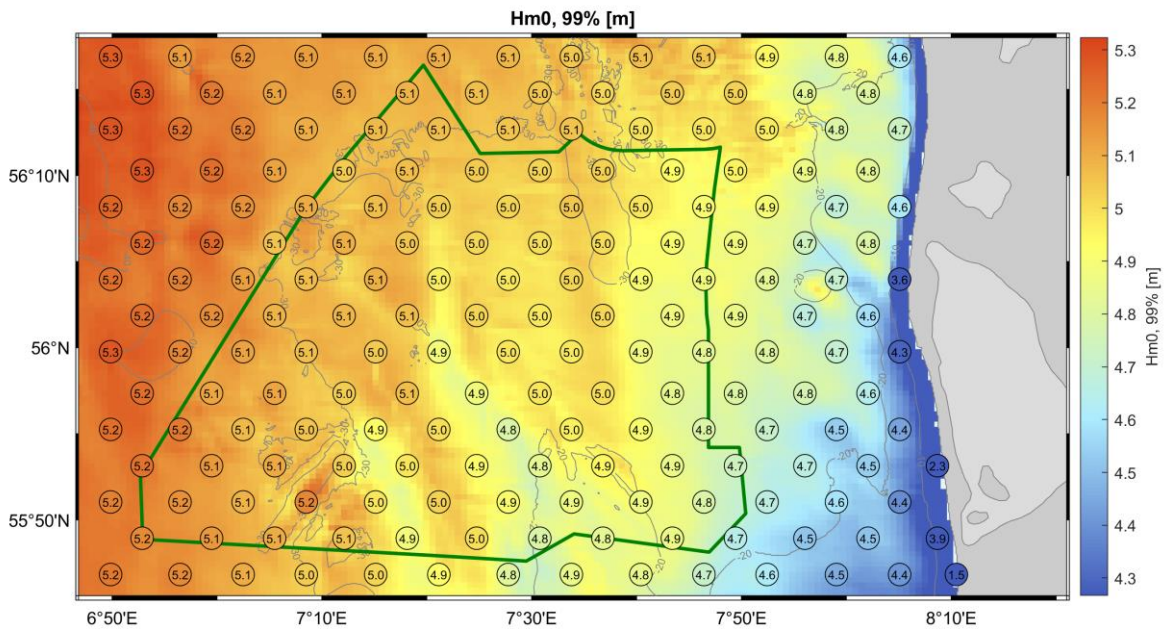
Figure 3-6:   99th percentile of Hm0.
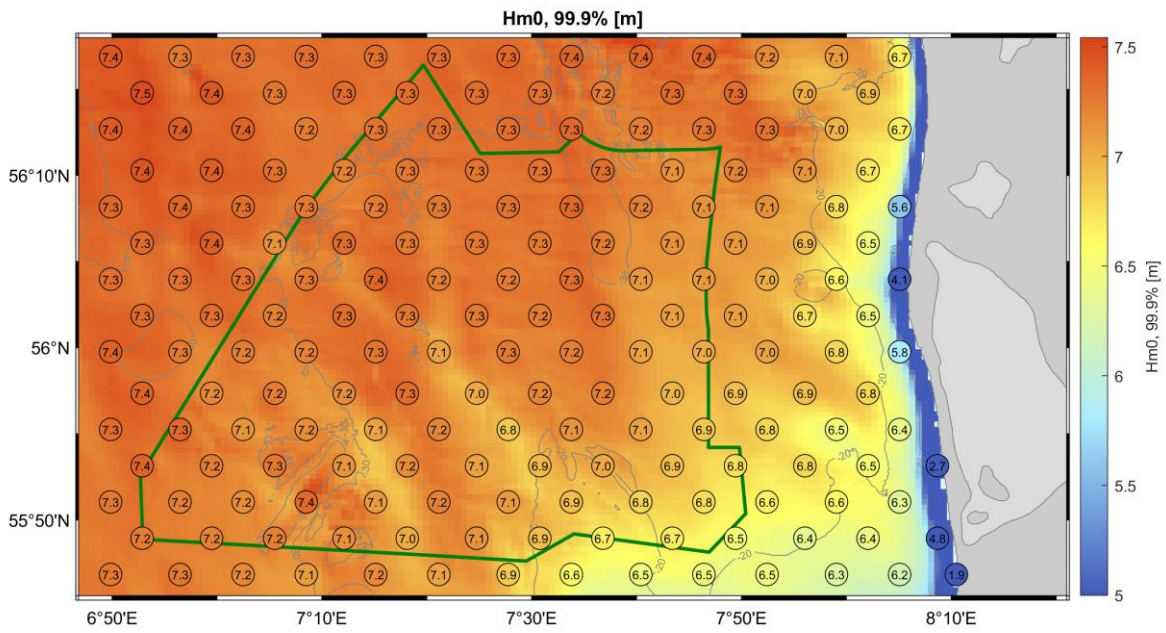
Figure 3-7:   99.9th percentile of Hm0.
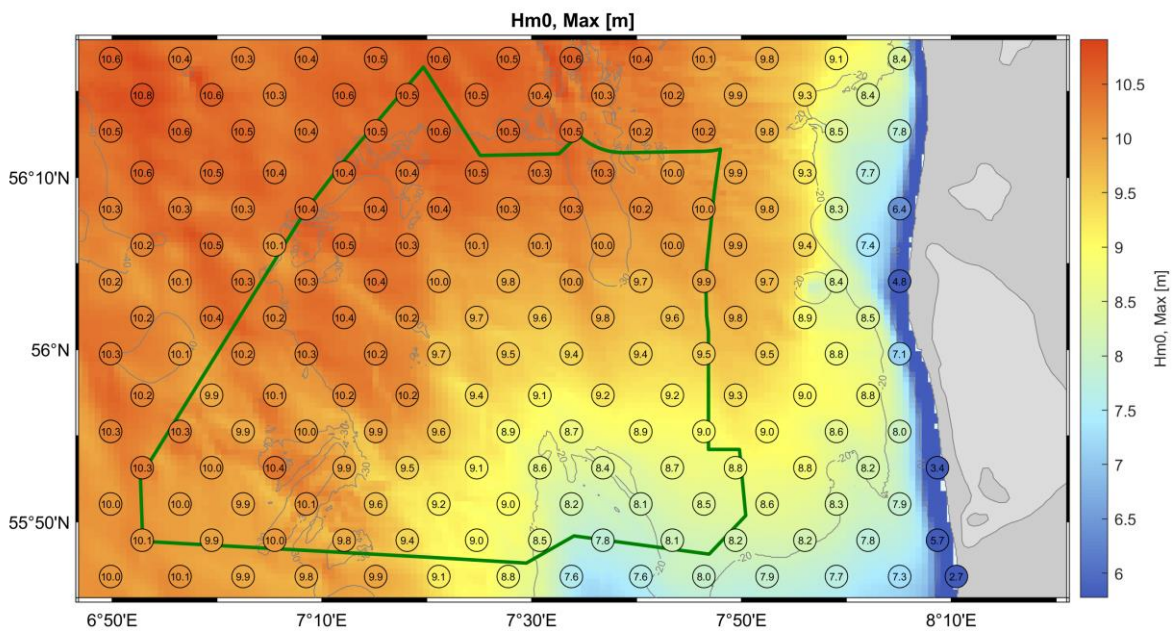
Figure 3-8:   Maximum Hm0.

3.2.2 Extreme Criteria

Maps showing extreme values associated with 1-, 5-, 10-, 25- and 50-year return periods are shown in Figure 3-9 through Figure 3-23 for the following parameters:

- **Significant wave height** (Figure 3-9 to Figure 3-13)

- **Maximum individual wave height** (Figure 3-14 to Figure 3-18)

- **Maximum individual crest height above still water level** (Figure 3-19 to Figure 3-23)
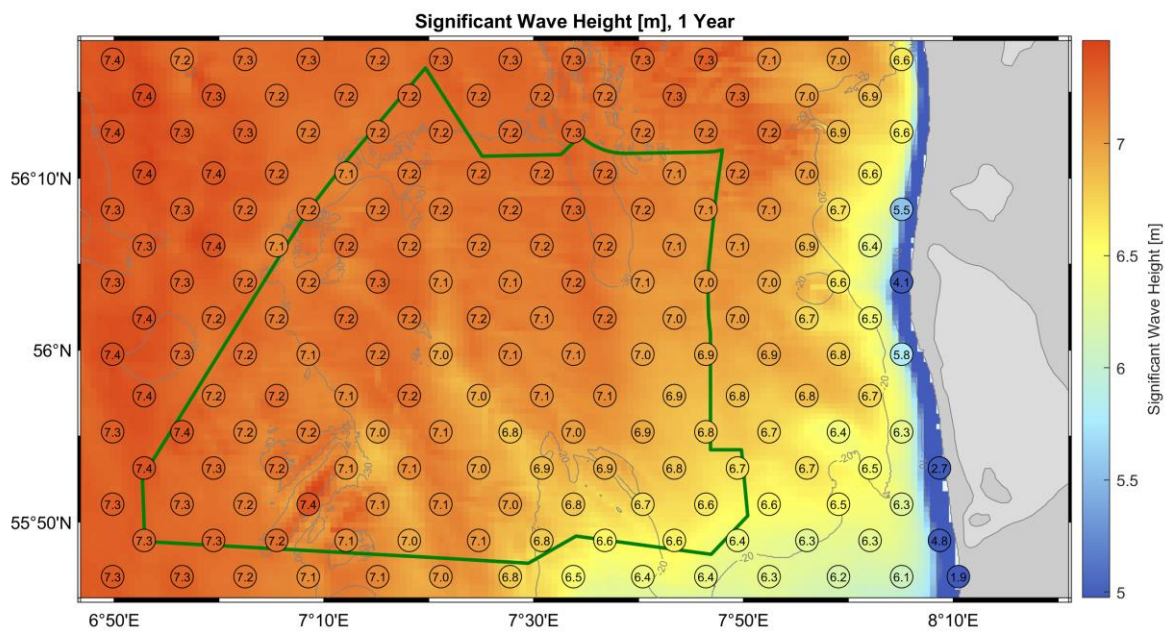
Figure 3-9: 1-year extreme values, Hm0.
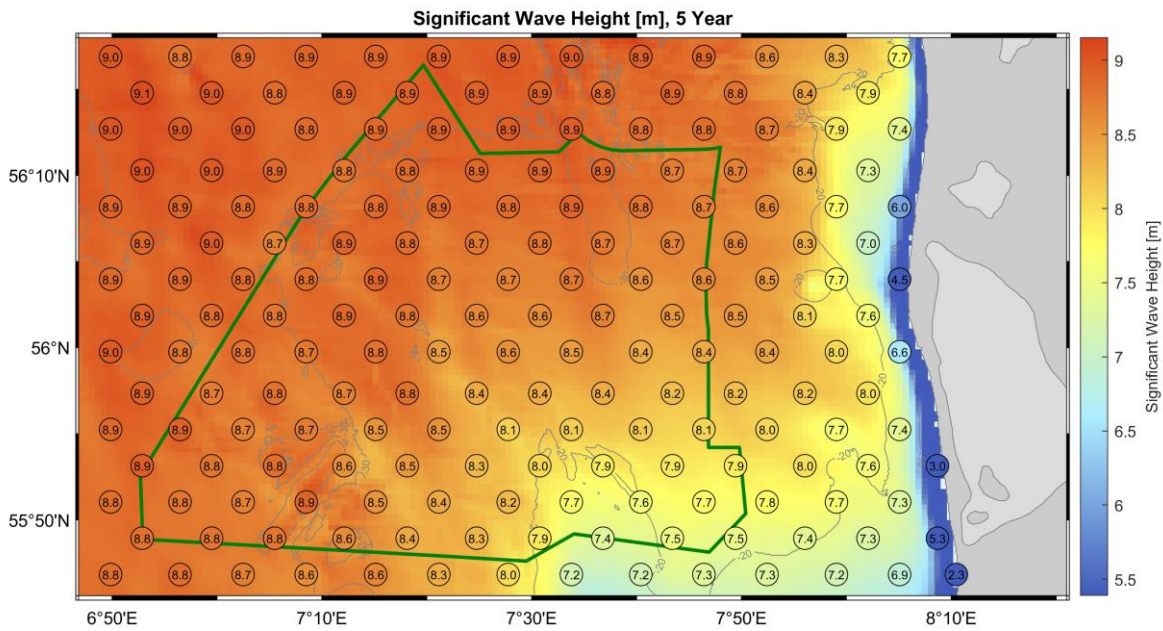
Figure 3-10: 5-year extreme values, Hm0.
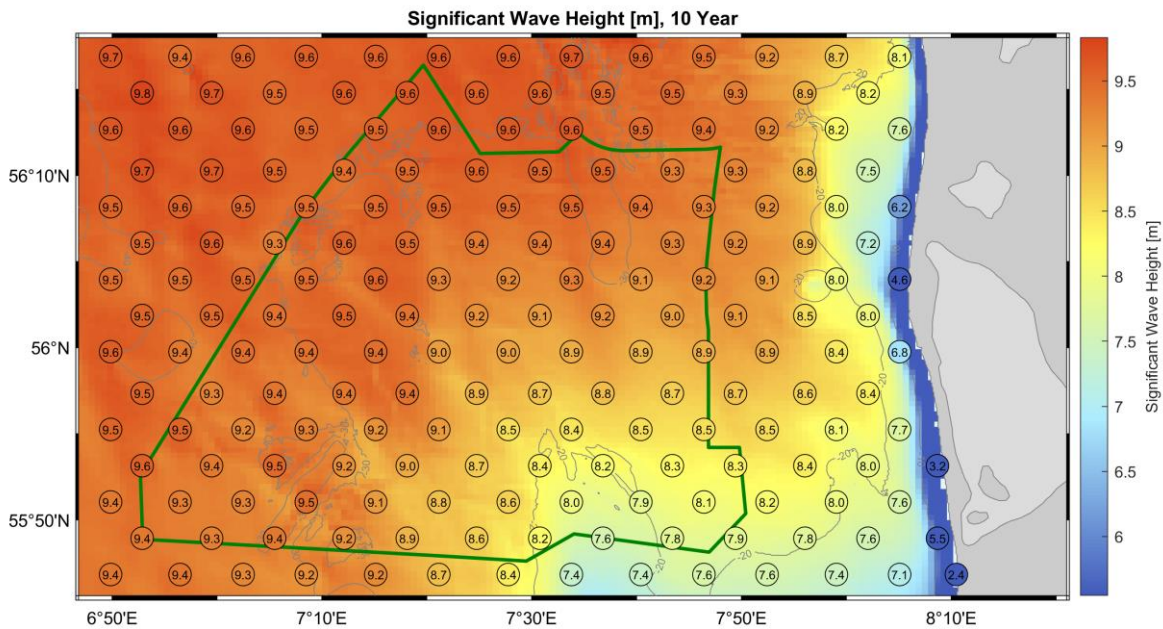
Figure 3-11: 10-year extreme values, Hm0.
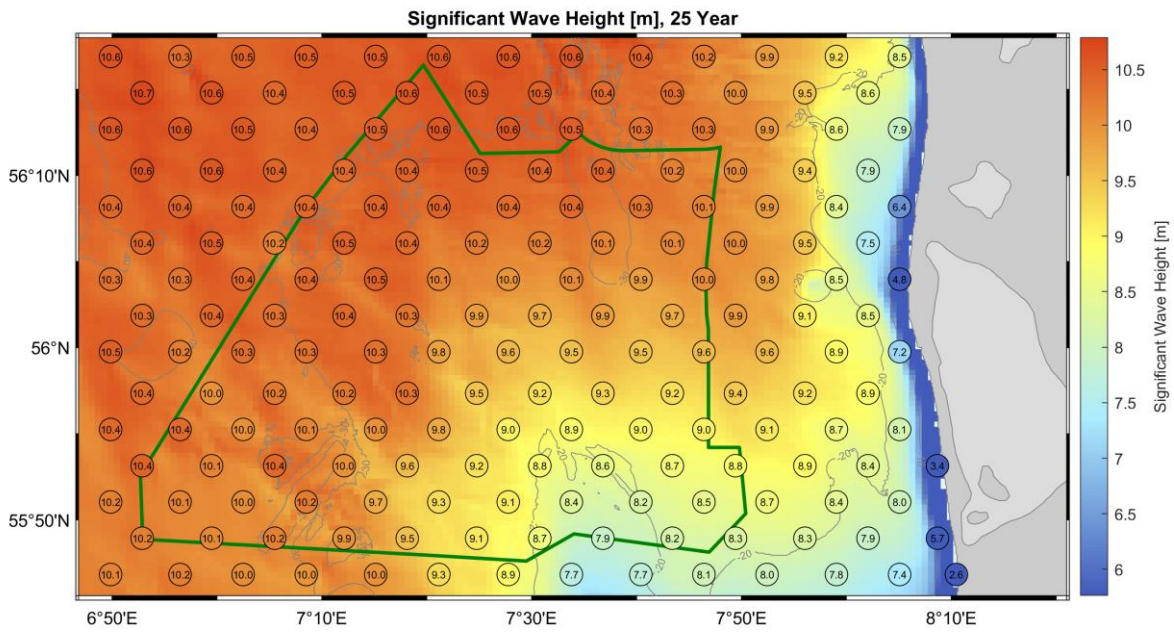
Figure 3-12: 25-year extreme values, Hm0.
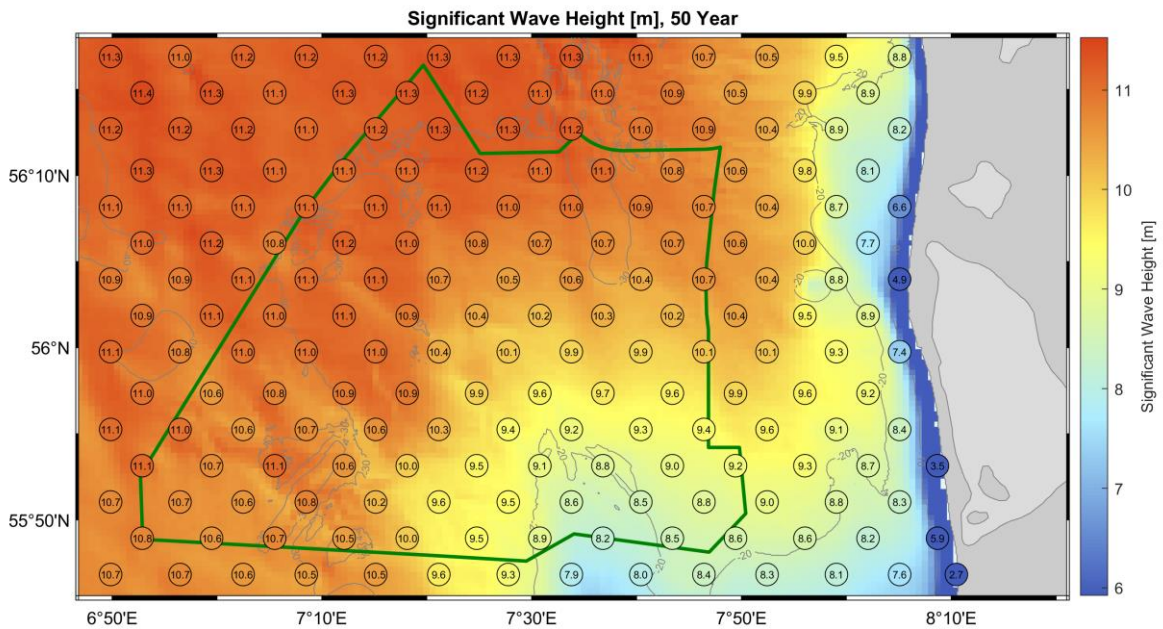
Figure 3-13: 50-year extreme values, Hm0.
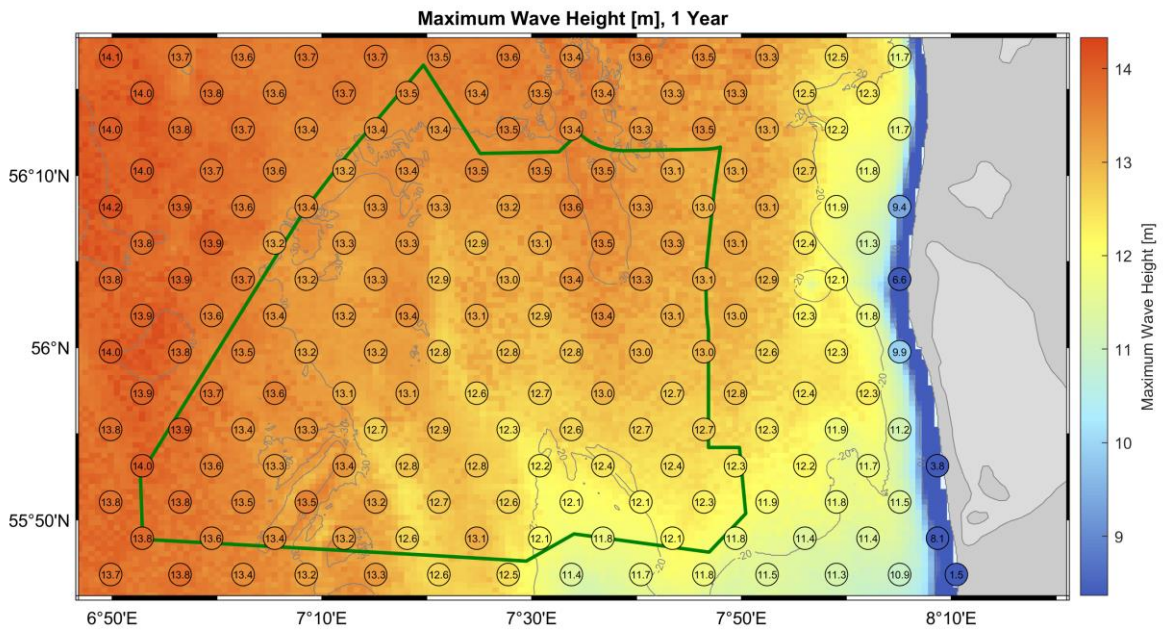
Figure 3-14: 1-year extreme values, Hmax.
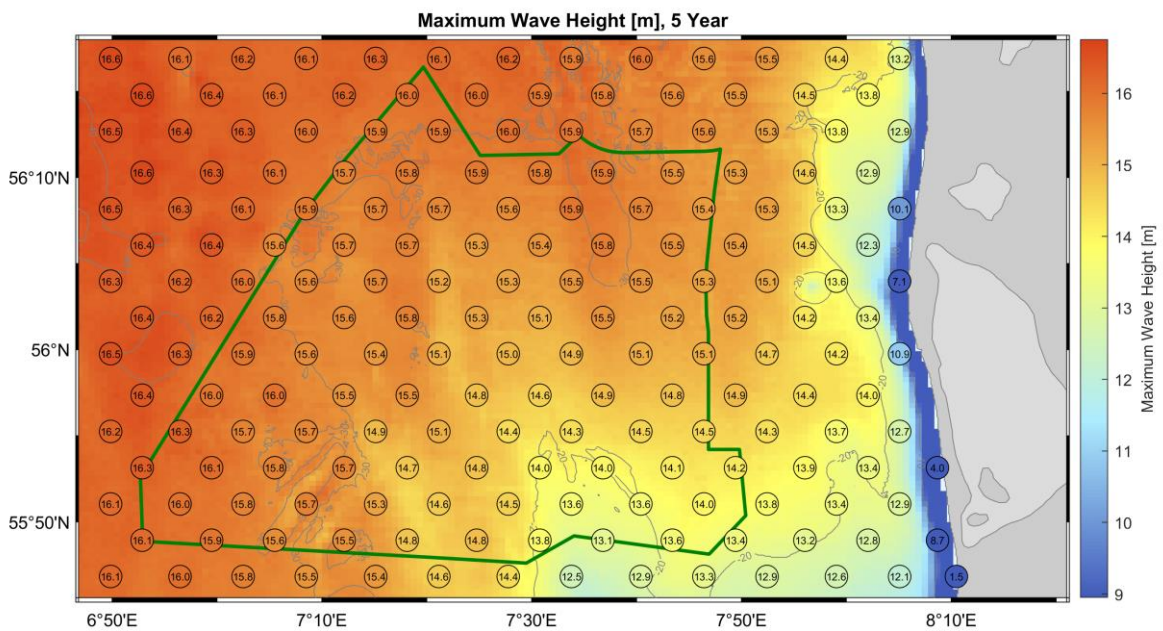
Figure 3-15: 5-year extreme values, Hmax.
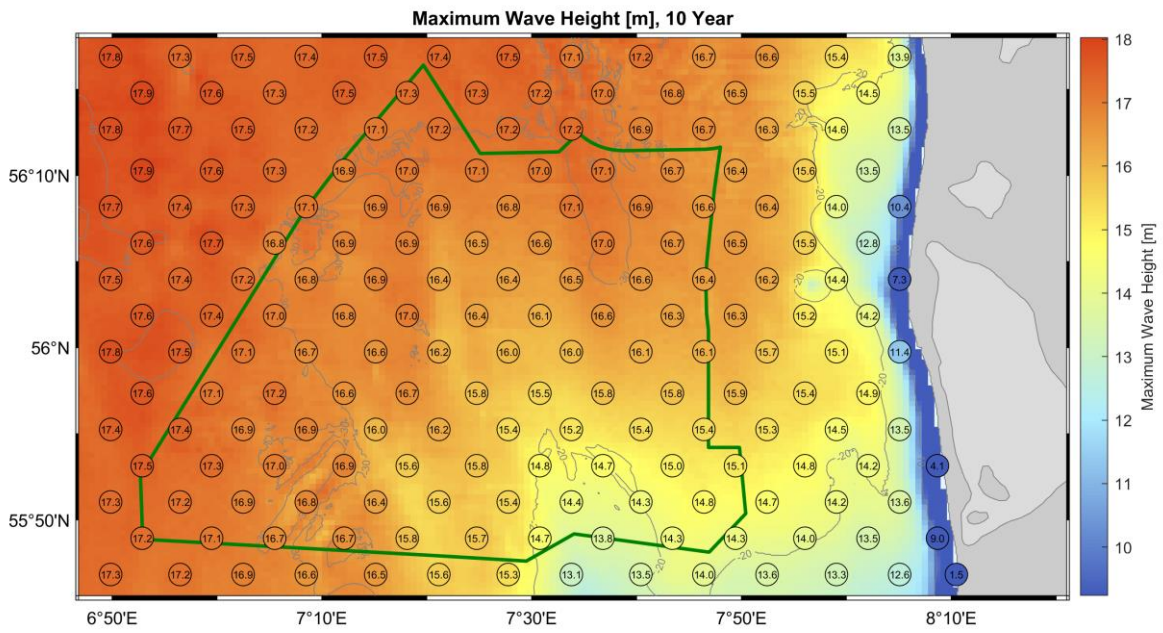
Figure 3-16: 10-year extreme values, Hmax.
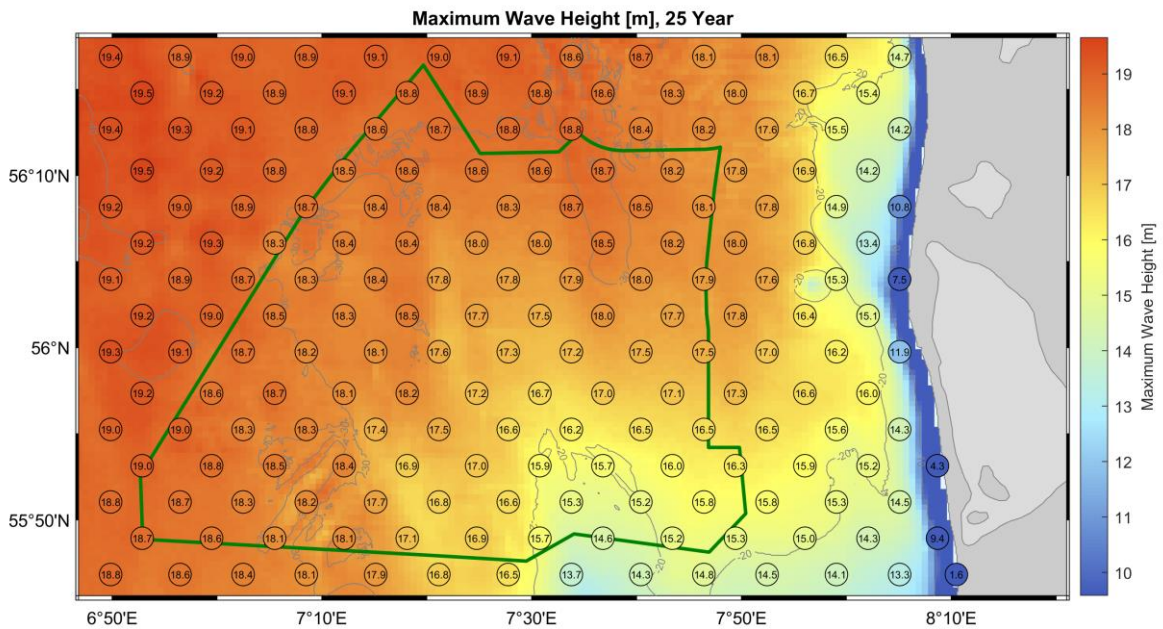
Figure 3-17: 25-year extreme values, Hmax.
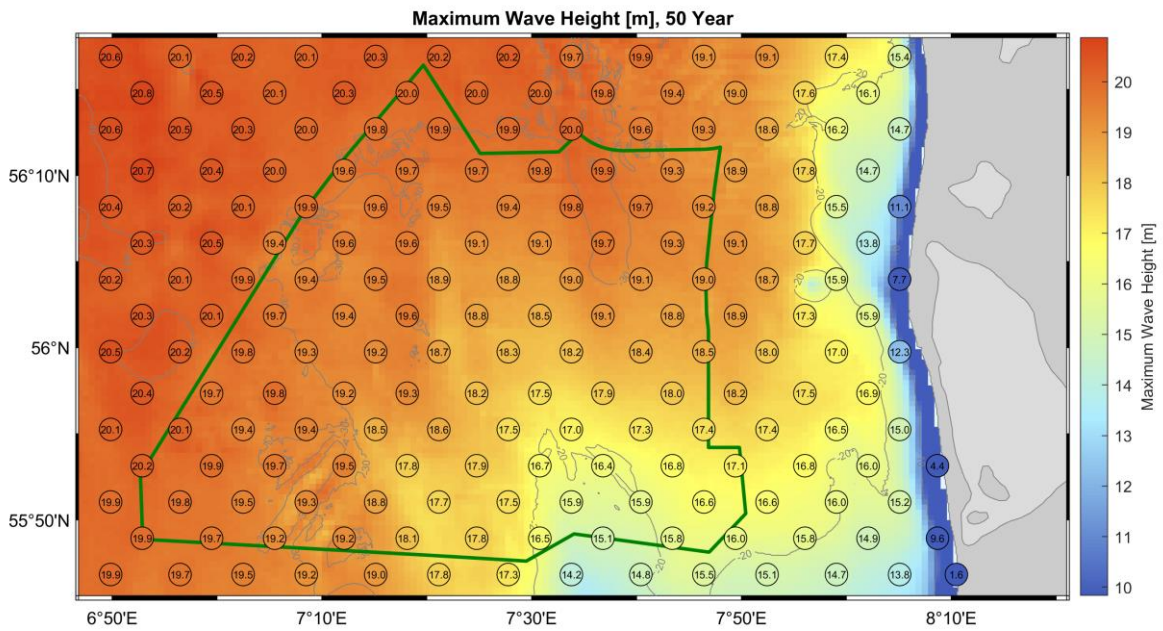
Figure 3-18: 50-year extreme values, Hmax.
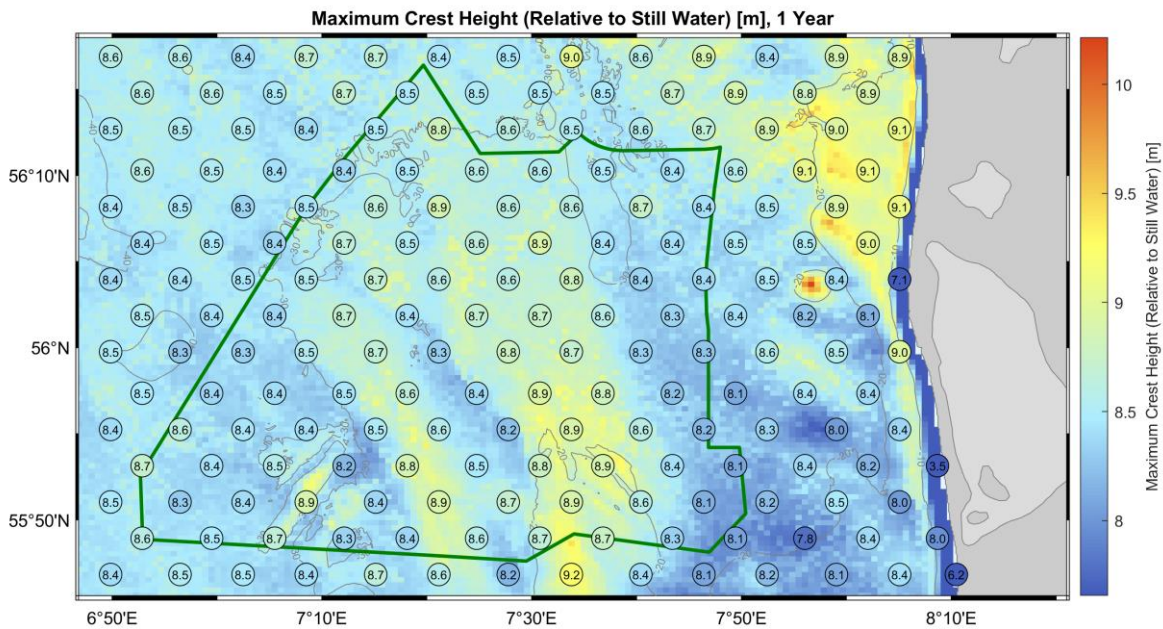
Figure 3-19: 1-year extreme values, Cmax relative to still water level.
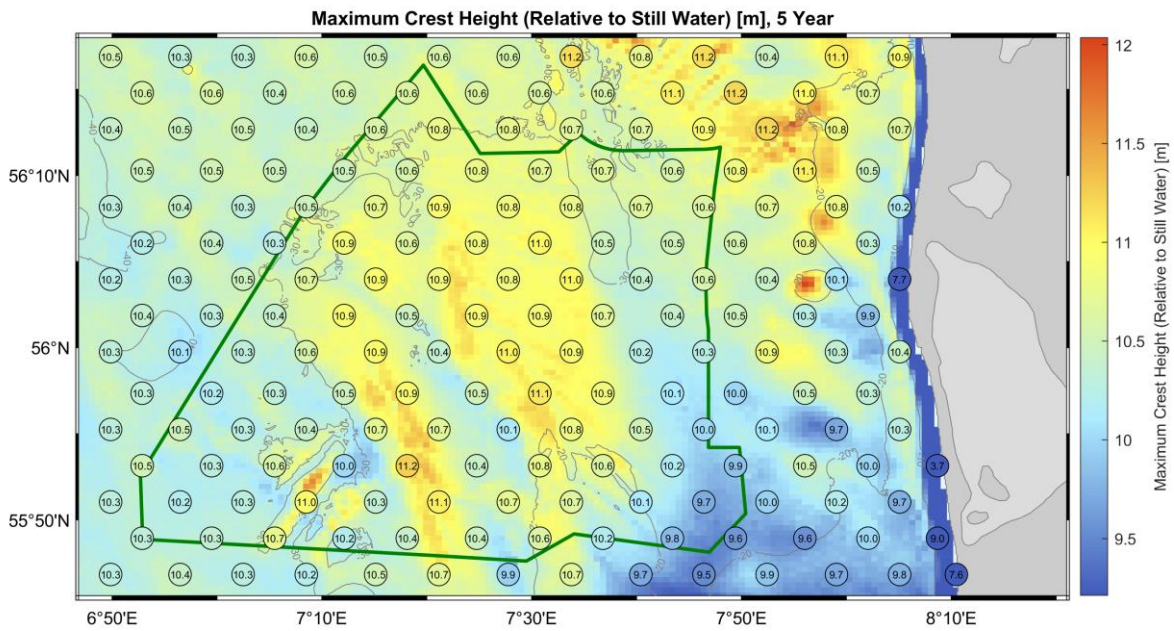
Figure 3-20: 5-year extreme values, Cmax relative to still water level.
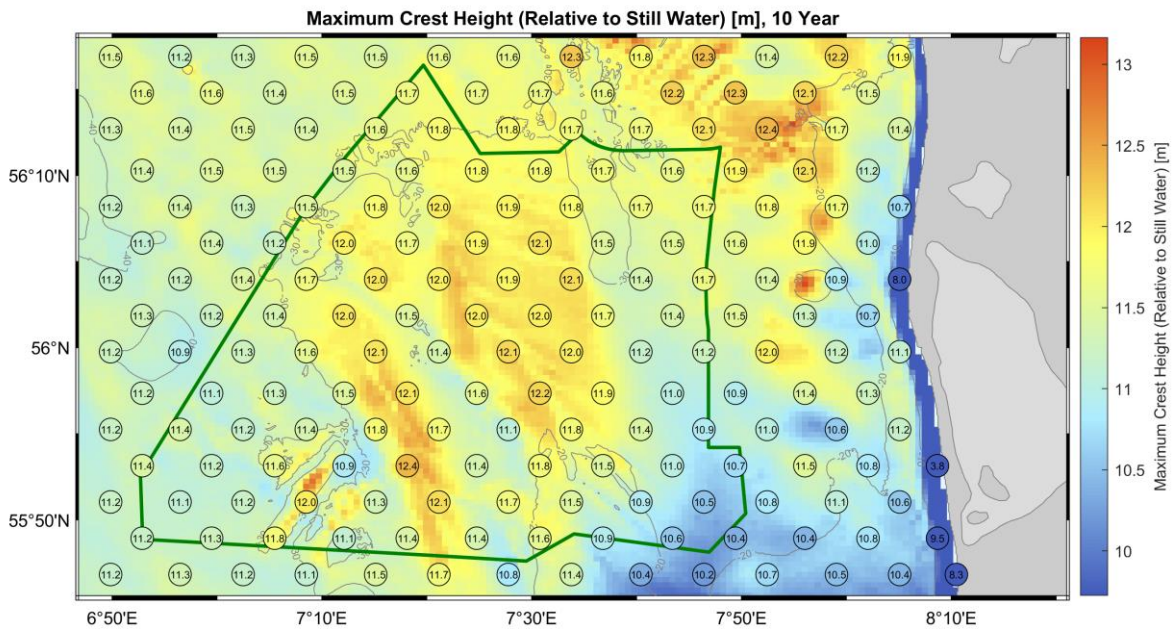
Figure 3-21: 10-year extreme values, Cmax relative to still water level.
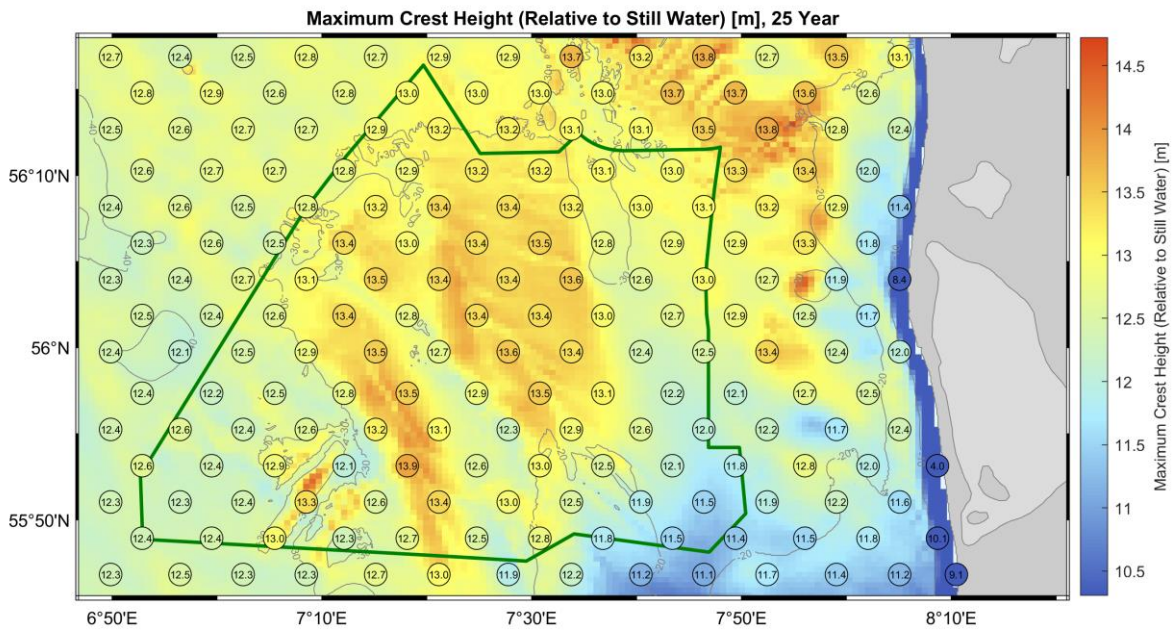
Figure 3-22: 25-year extreme values, Cmax relative to still water level.
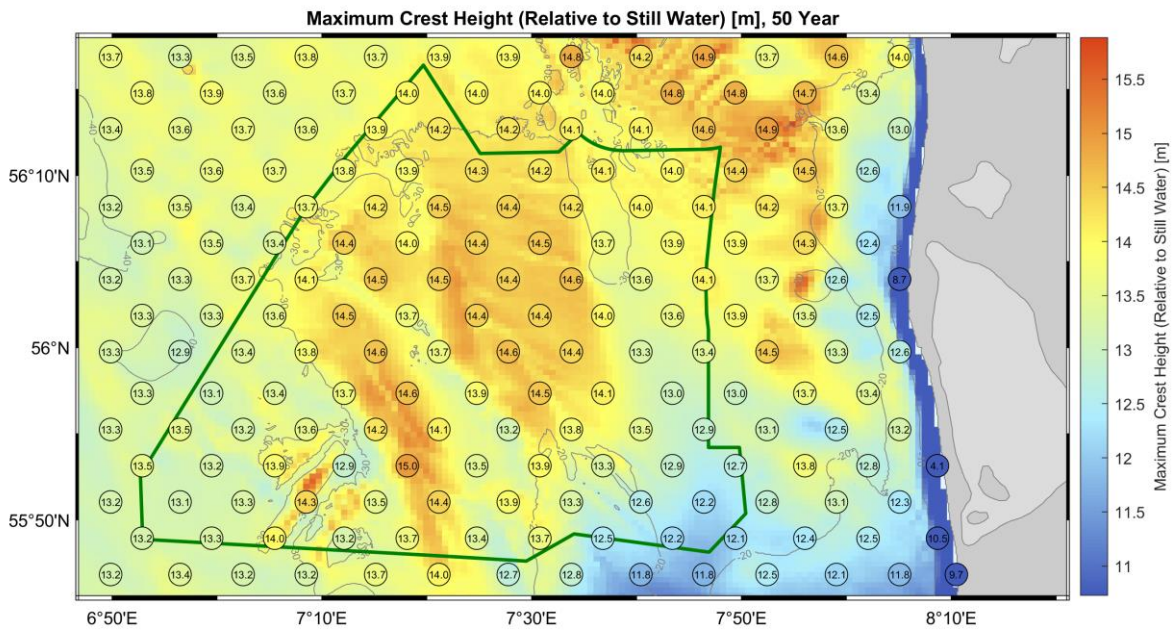
Figure 3-23: 50-year extreme values, Cmax relative to still water level.

3.3 Currents and Water Levels

3.3.1 Operational Statistics

In Figure 3-24 through Figure 3-30 the following statistics are shown for water levels and current speeds:

- **Minimum and maximum water levels** (combined tide and surge).
- **50th, 90th, 99th and 99.9^{th} percentiles** of depth-averaged current speed.
- **Maximum** of depth-averaged current speed.
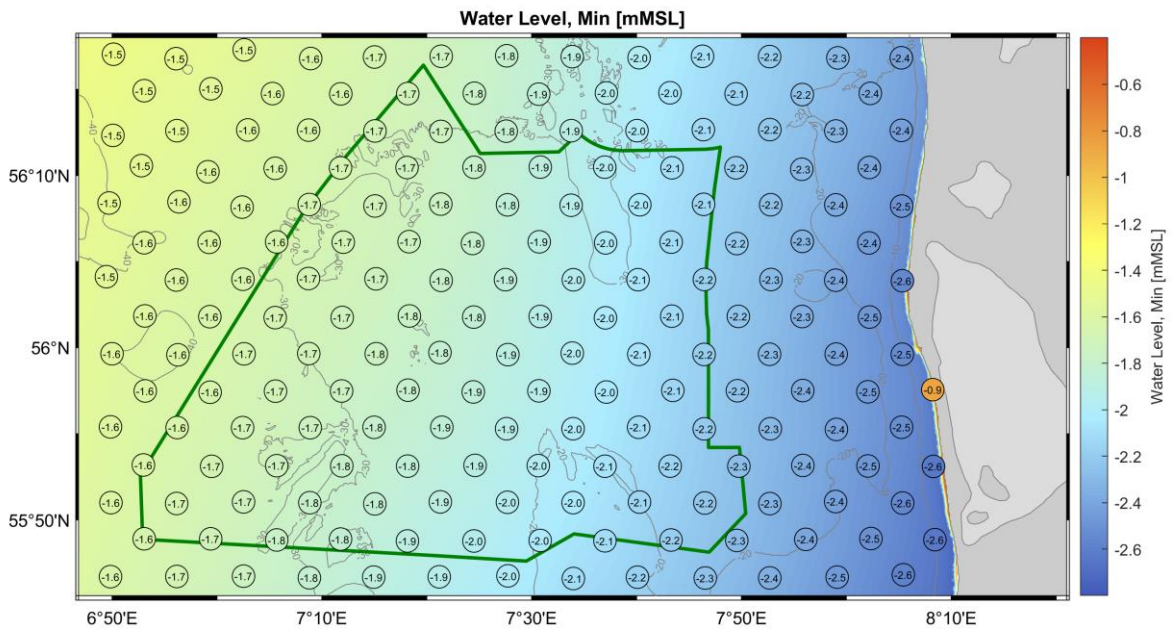
Figure 3-24: Minimum water level (tide + surge).
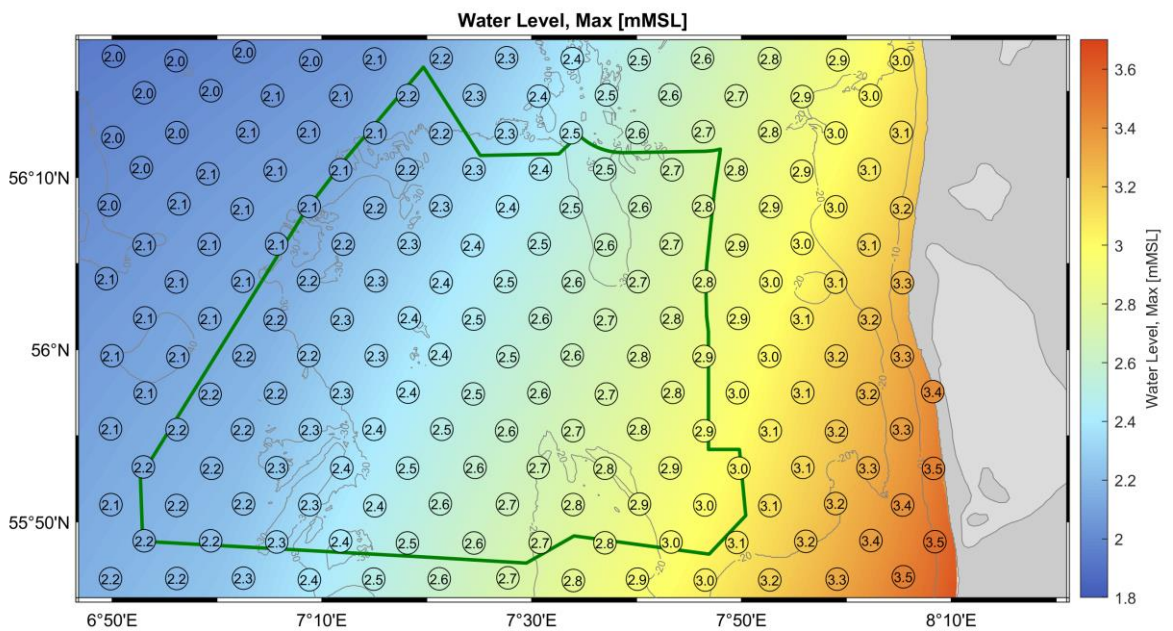
Figure 3-25: Maximum water level (tide + surge).
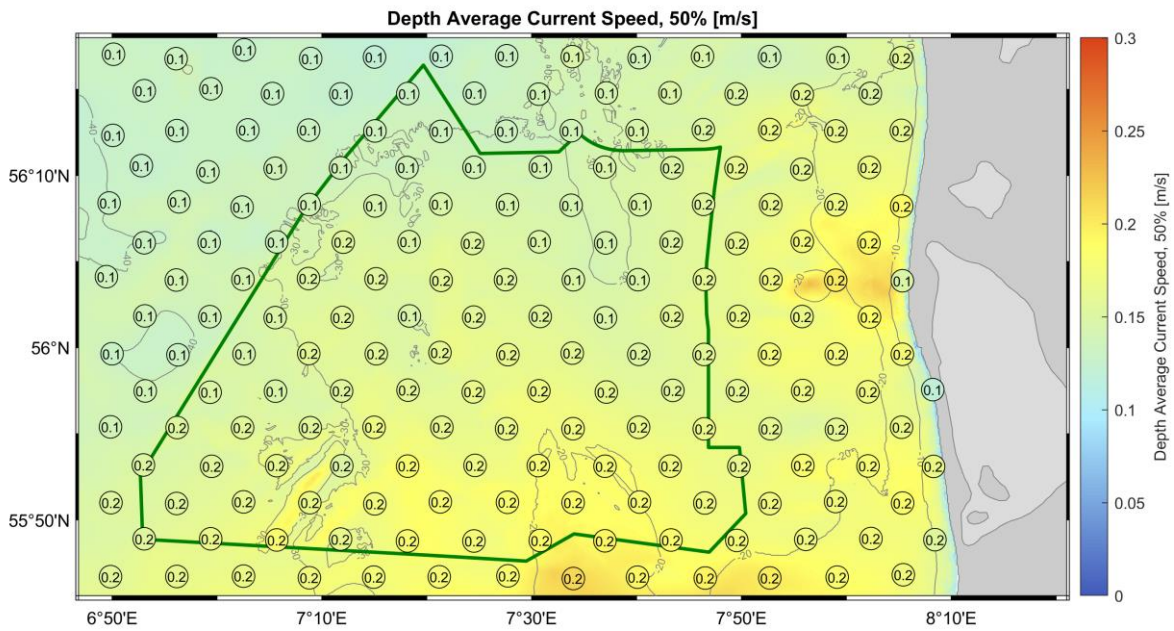
Figure 3-26: 50th percentile of depth-averaged current speed.
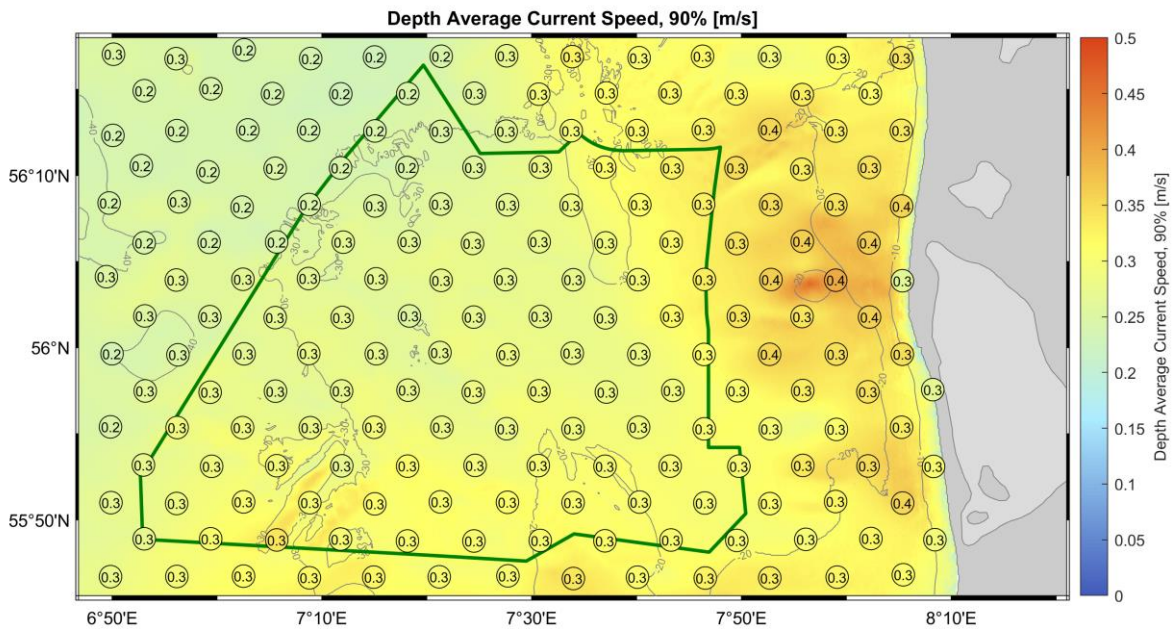
Figure 3-27: 90th percentile of depth-averaged current speed.
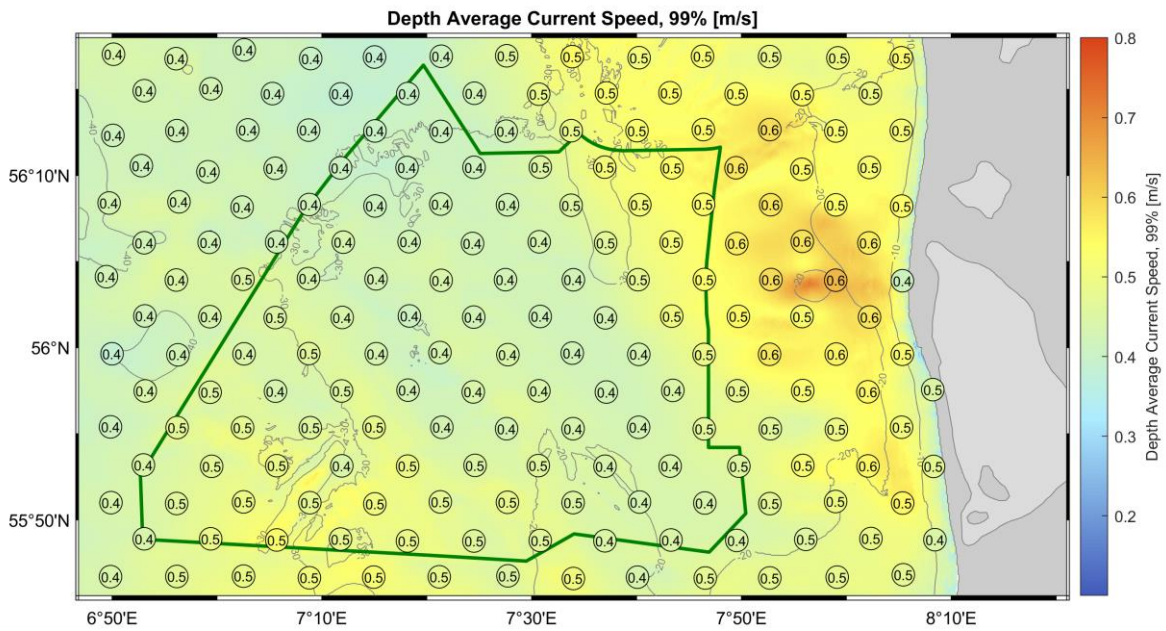
Figure 3-28: 99th percentile of depth-averaged current speed.
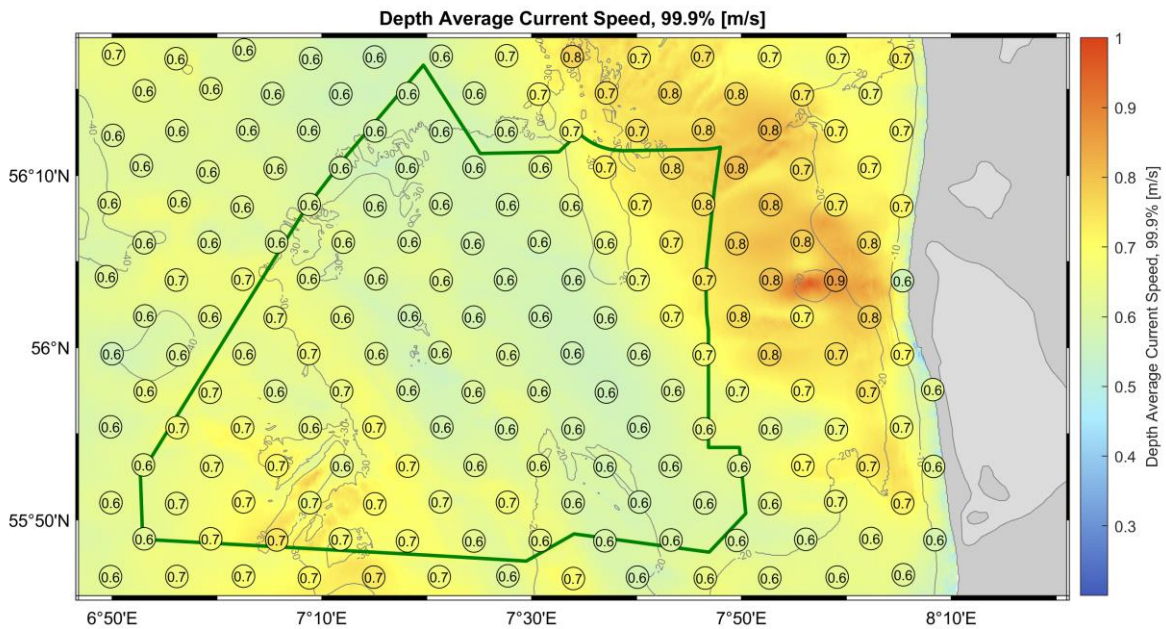
Figure 3-29: 99.9th percentile of depth-averaged current speed.
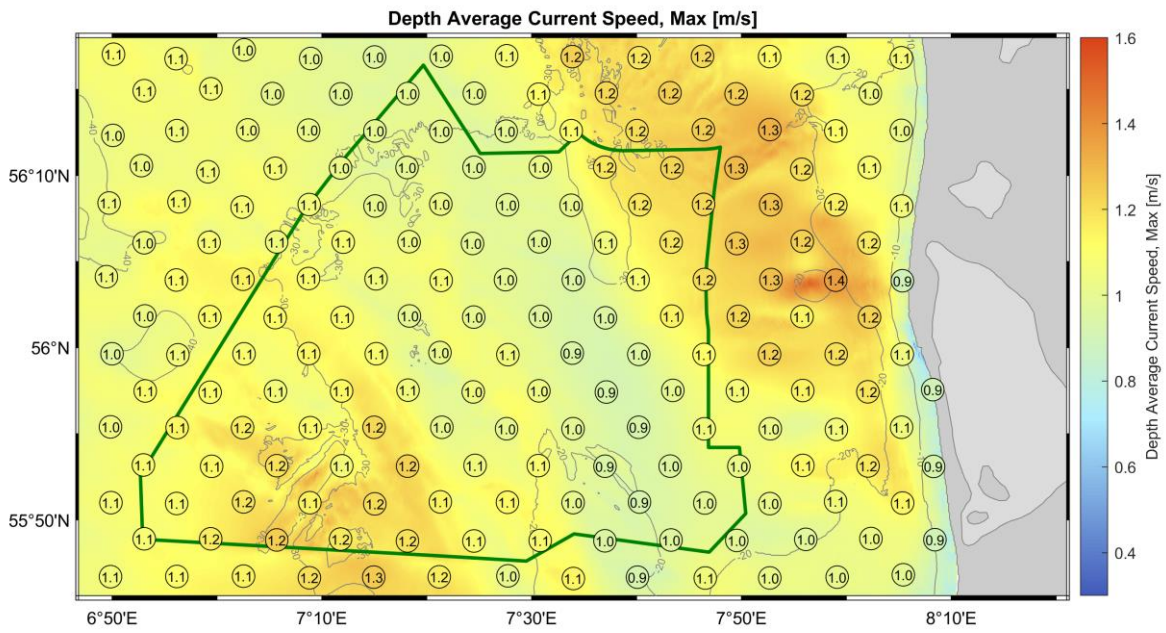
Figure 3-30: Maximum depth-averaged current speed.

3.3.2   Extreme Criteria

Maps showing extreme values associated with 1-, 5-, 10-, 25- and 50-year return periods are shown as follows:

- **Negative surge** (Figure 3-31 through Figure 3-35)

- **Positive surge** (Figure 3-36 through Figure 3-40)

- **Depth average current speed** (Figure 3-41 through Figure 3-45)

Additionally, lowest and highest astronomical tides (**LAT** and **HAT**) are shown in Figure 3-46 and Figure 3-47.
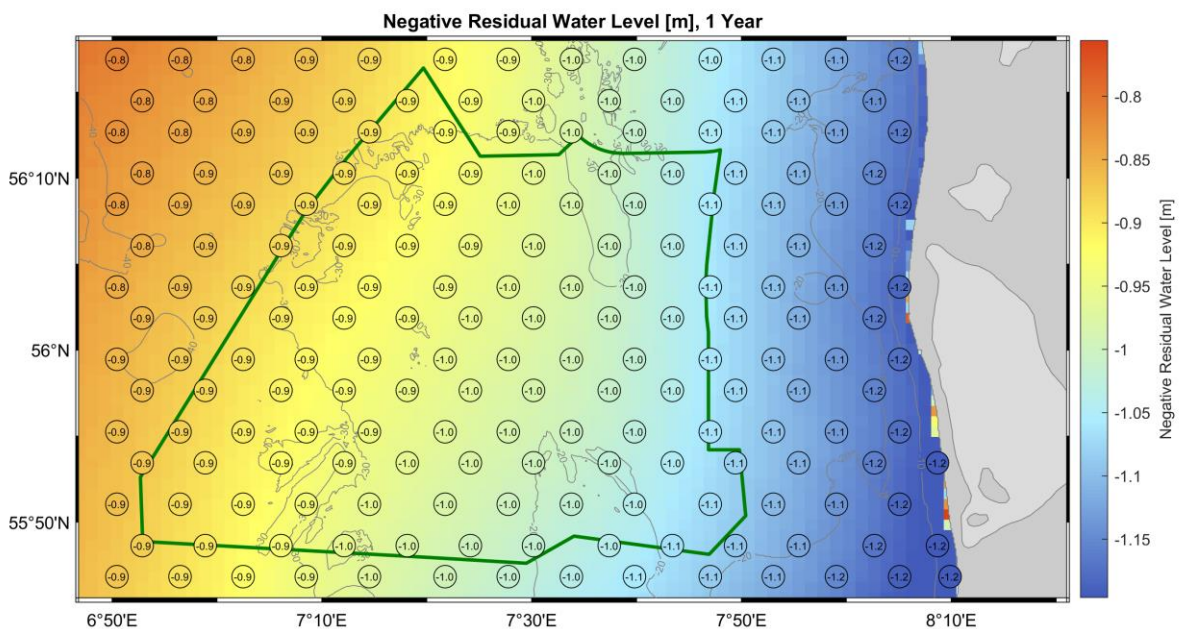
Figure 3-31: 1-year extreme values, negative surge.
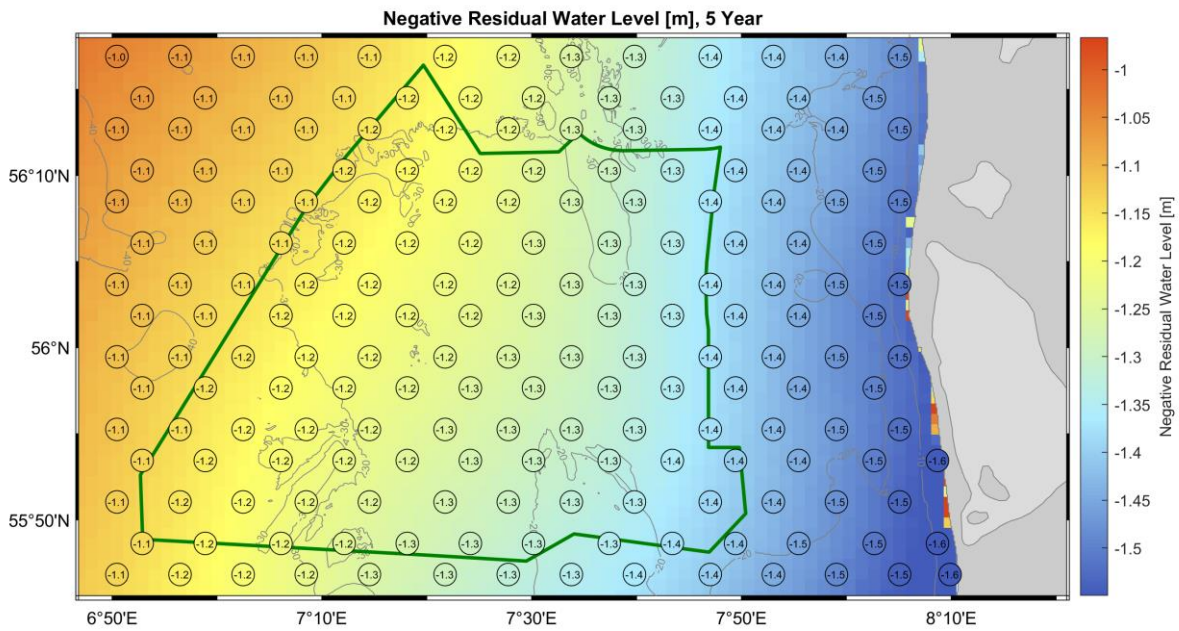
Figure 3-32: 5-year extreme values, negative surge.
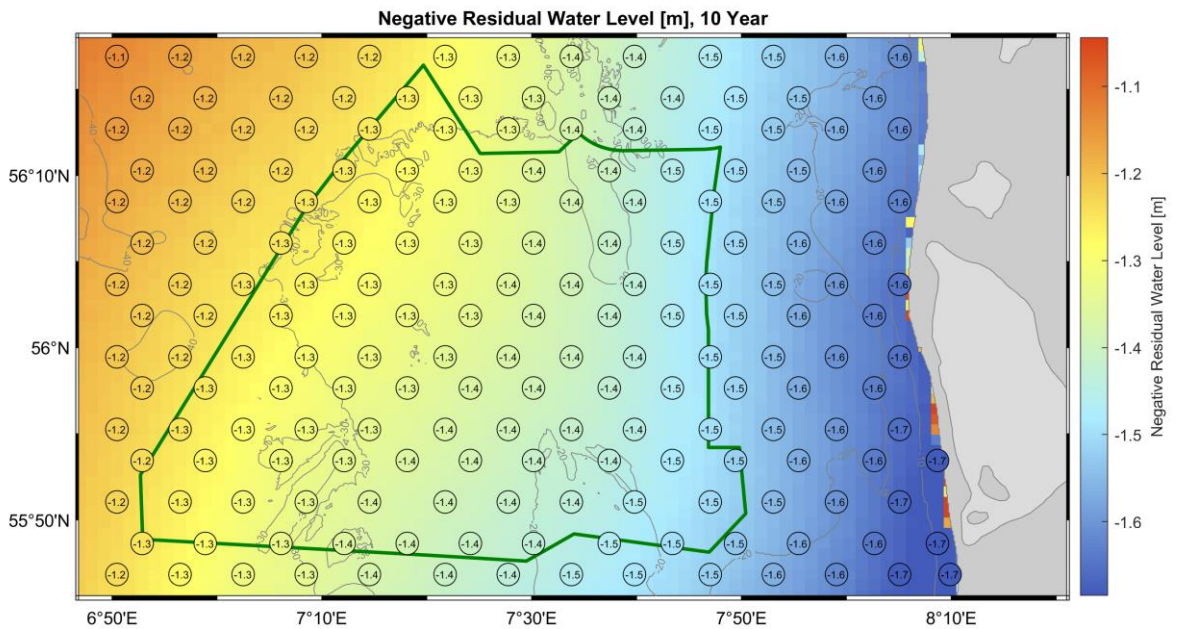
Figure 3-33: 10-year extreme values, negative surge.
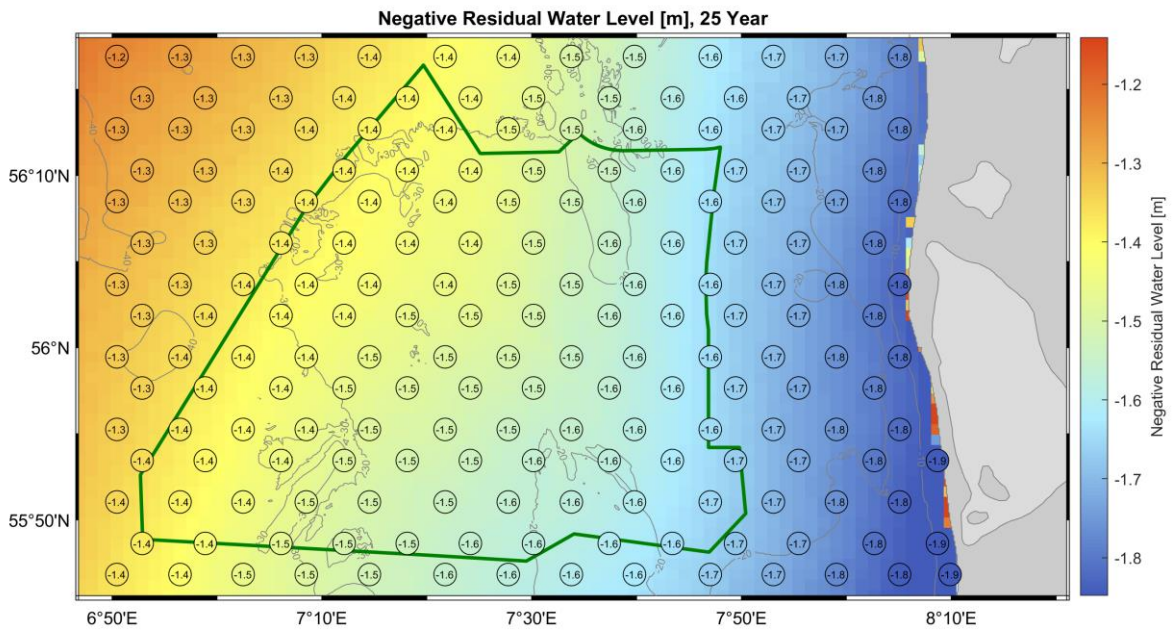
Figure 3-34: 25-year extreme values, negative surge.
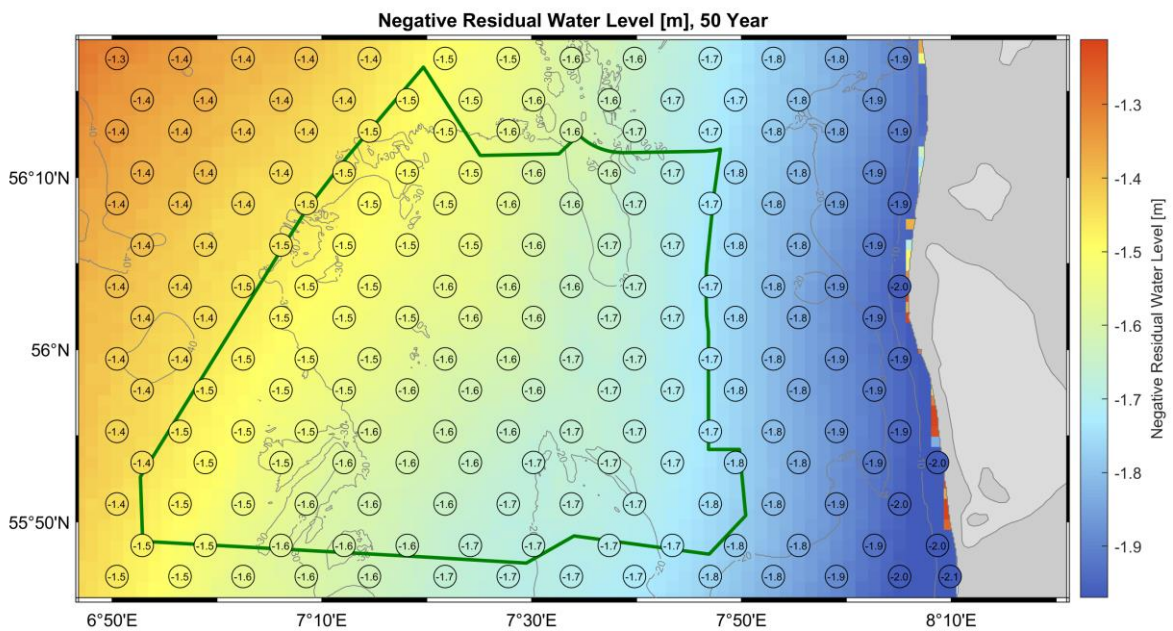
Figure 3-35: 50-year extreme values, negative surge.
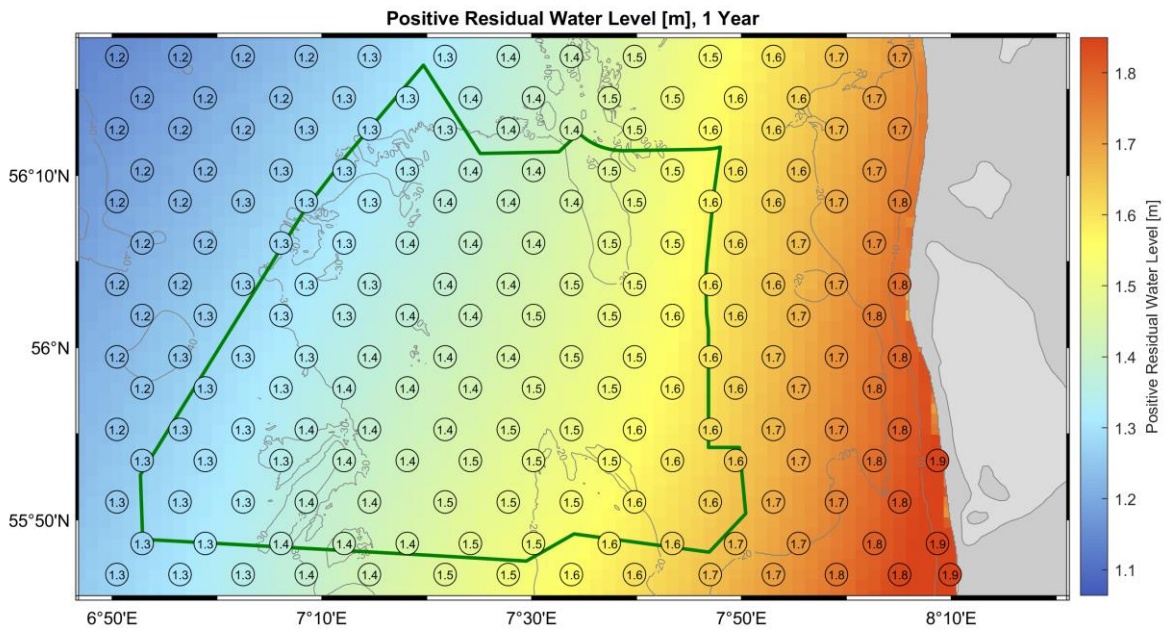
Figure 3-36: 1-year extreme values, positive surge.
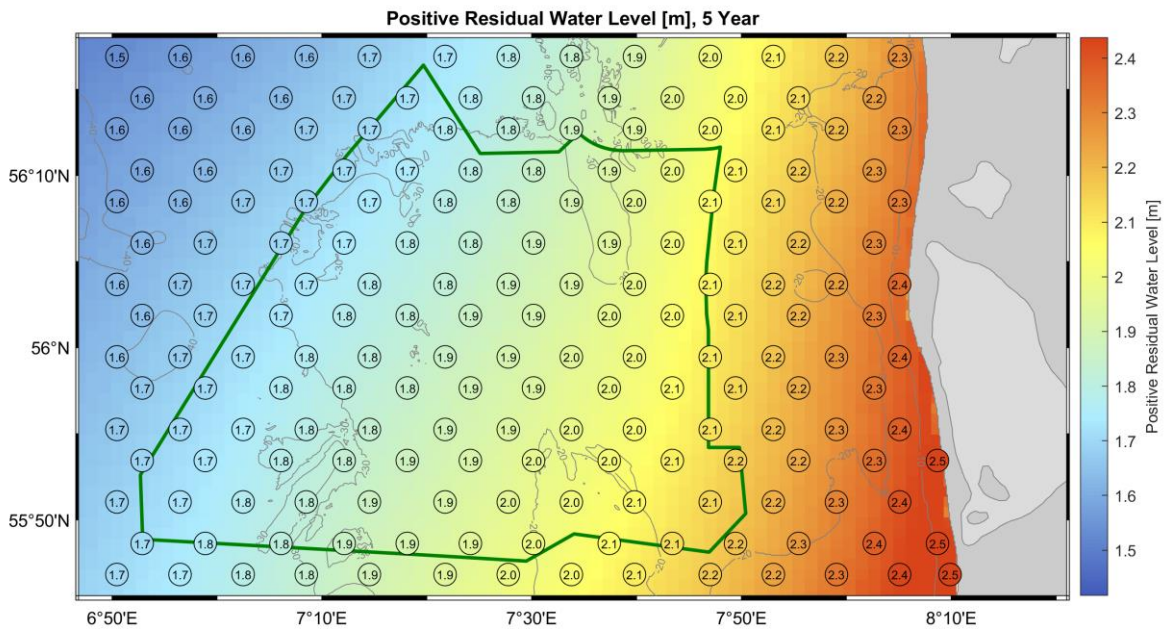
Figure 3-37: 5-year extreme values, positive surge.
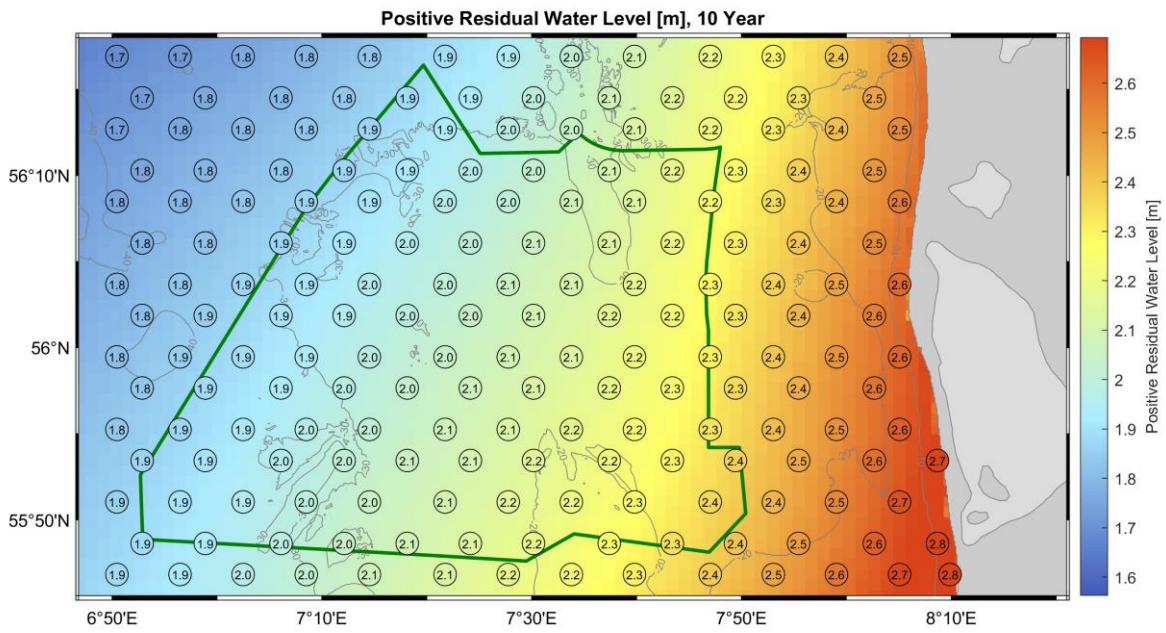
Figure 3-38: 10-year extreme values, positive surge.
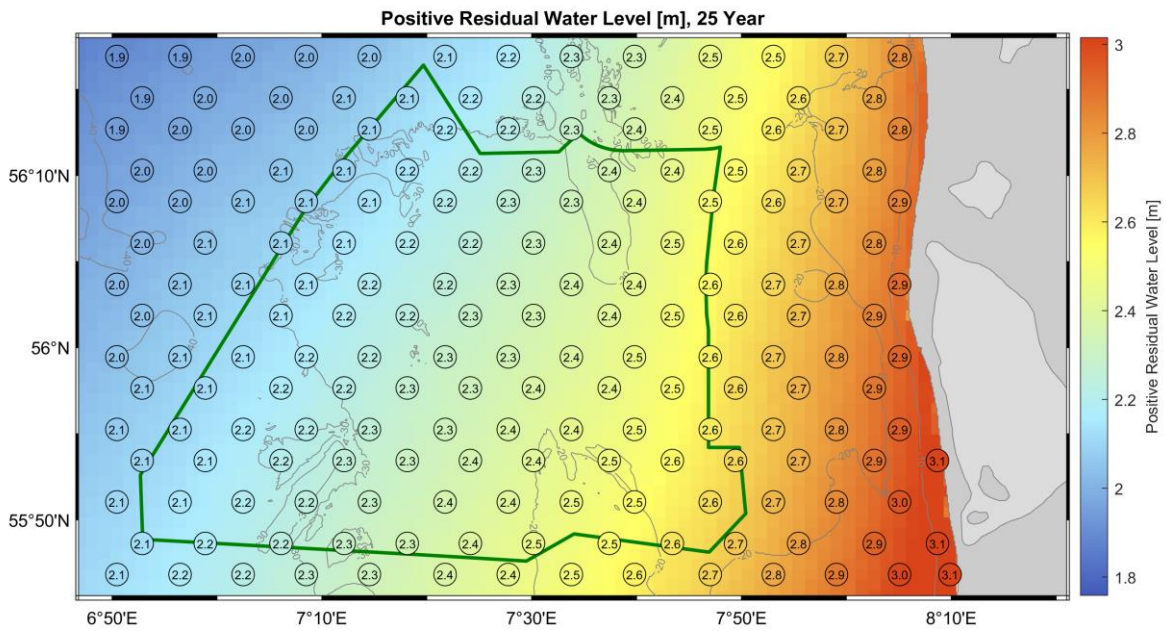
Figure 3-39: 25-year extreme values, positive surge.
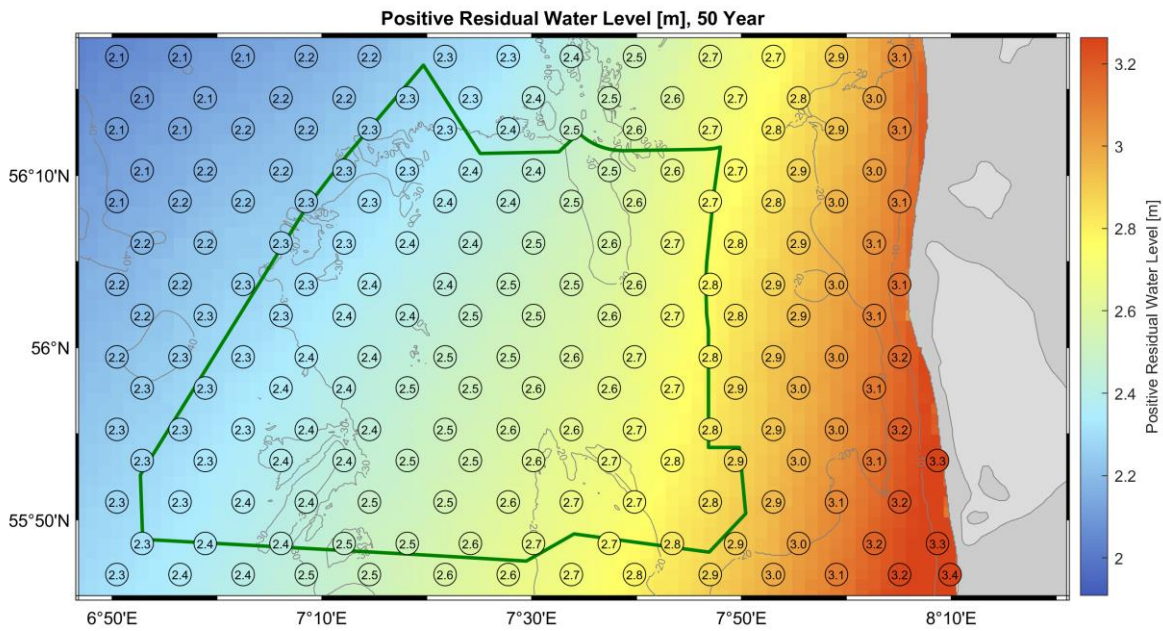
Figure 3-40: 50-year extreme values, positive surge.
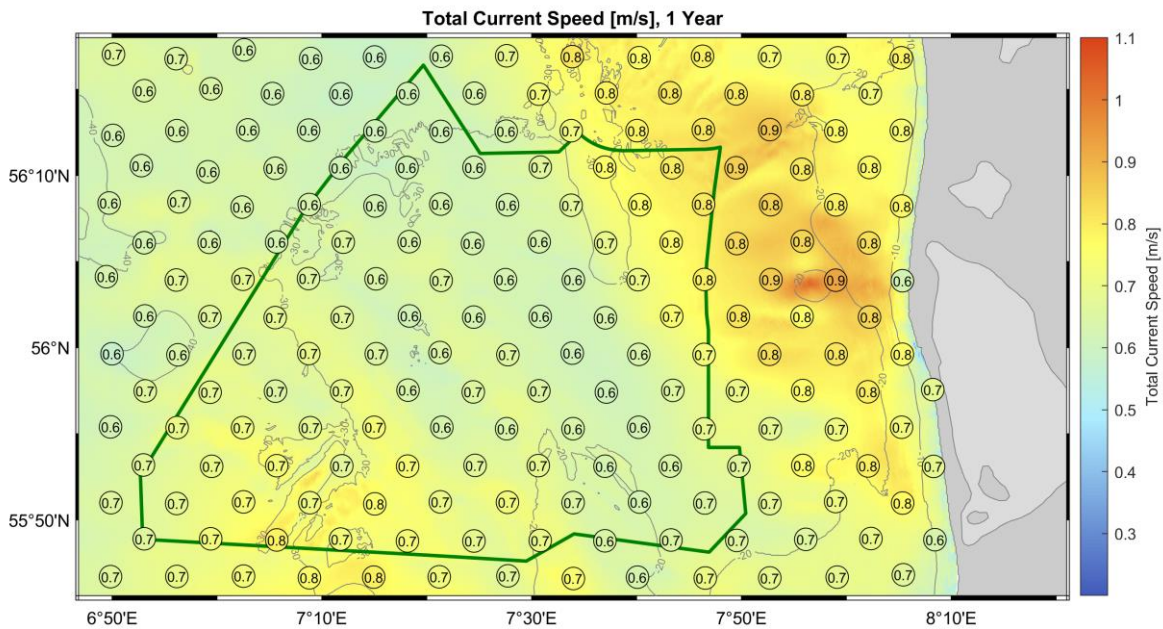
Figure 3-41: 1-year extreme values, depth-averaged current speed.
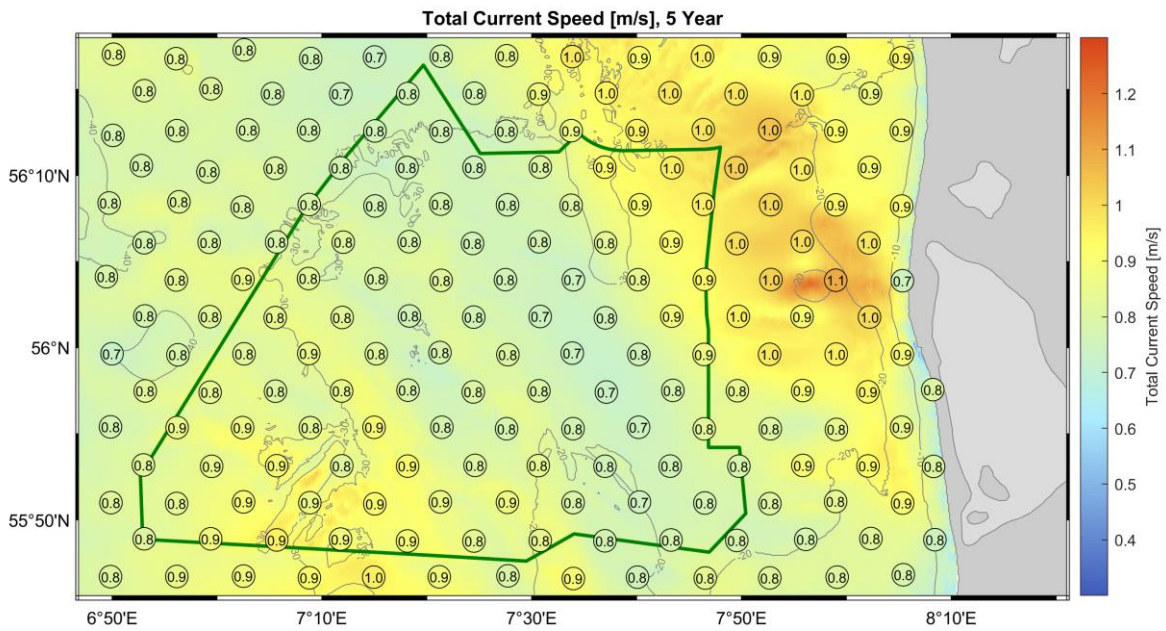
Figure 3-42: 5-year extreme values, depth-averaged current speed.
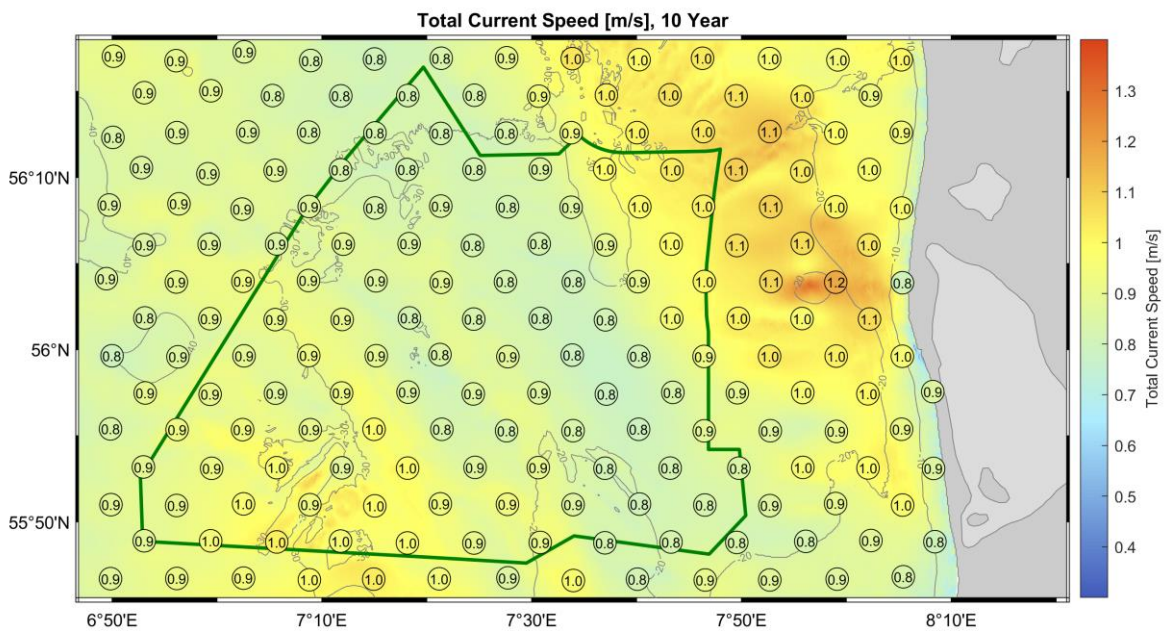
Figure 3-43: 10-year extreme values, depth-averaged current speed.
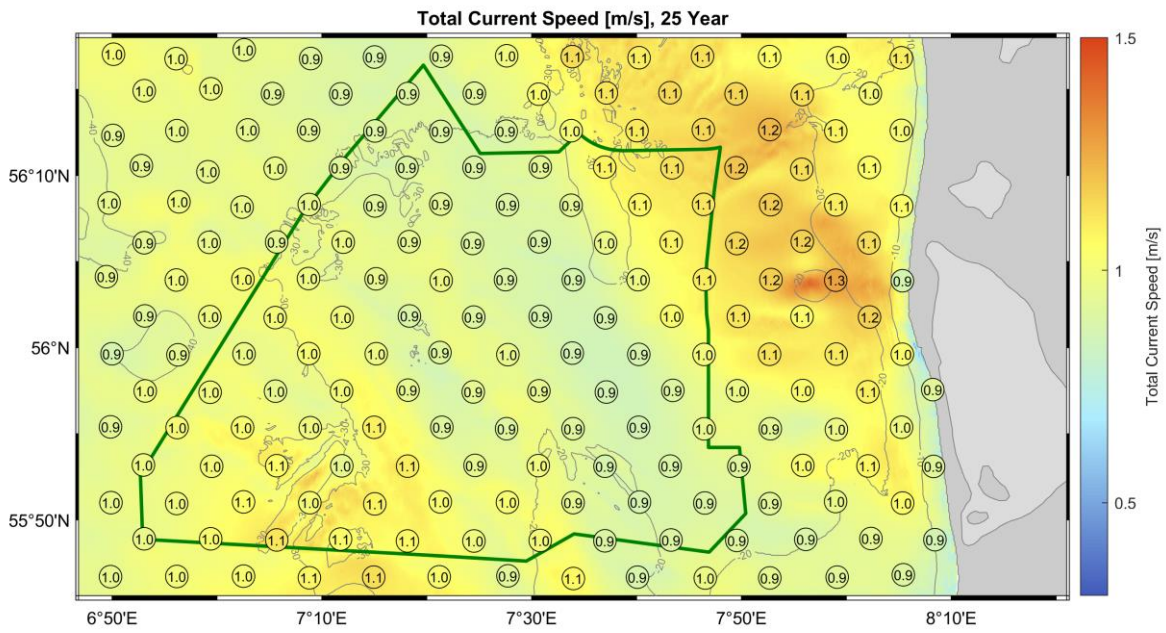
Figure 3-44: 25-year extreme values, depth-averaged current speed.
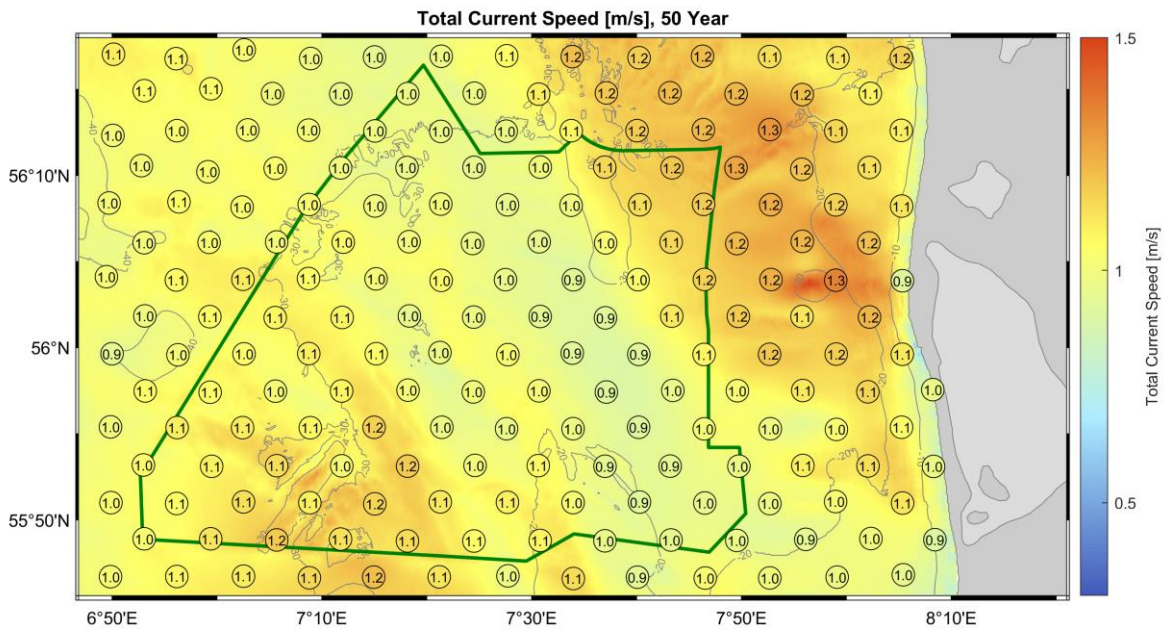
Figure 3-45: 50-year extreme values, depth-averaged current speed.
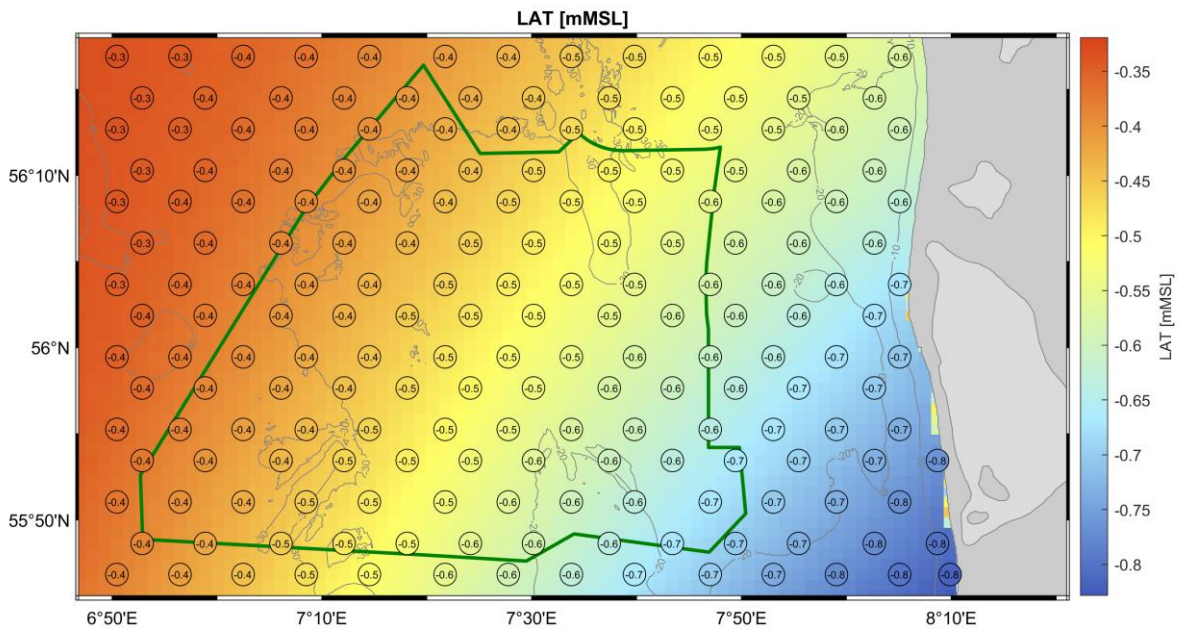
Figure 3-46: LAT.
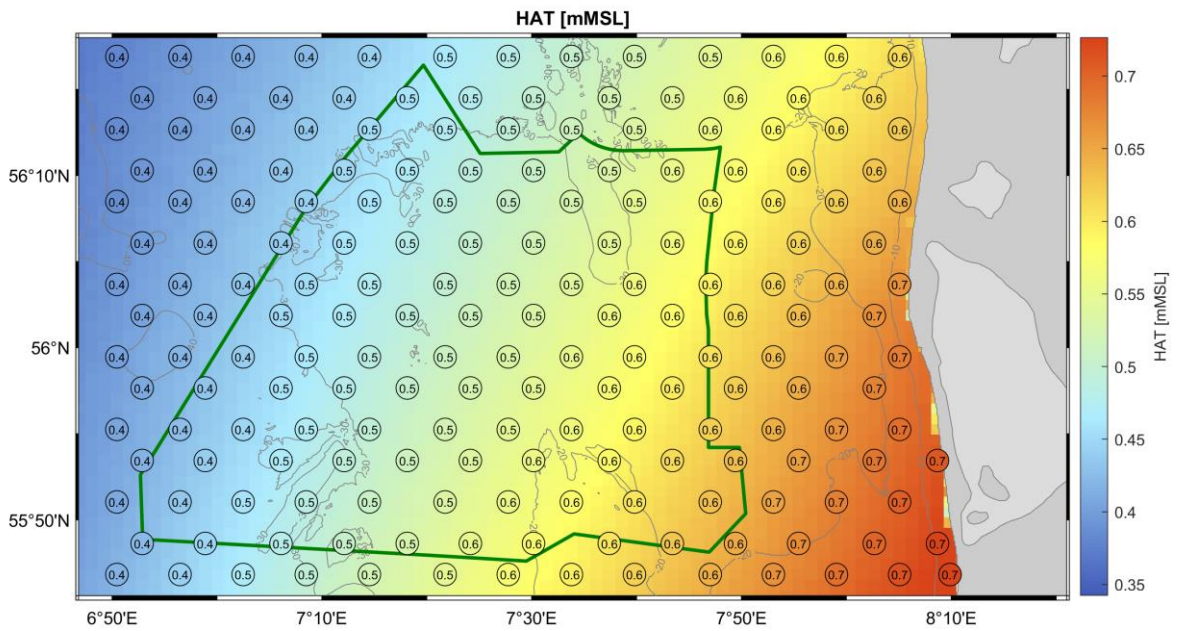
Figure 3-47: HAT.

4 Analysis Locations

Nine analysis locations were scoped into the present study with requirements such that two locations should be taken to represent each of the respective offshore wind development areas A1, A2 and A3, with 3 additional analysis locations within the remaining wider development area (described herein as A0). These locations were chosen by inspection of the spatial maps described in Section 3 and through client consultation.

The selection process followed the general principle of aiming towards representing the most onerous conditions within each of the respective areas to ensure that any engineering applications of the data would yield a conservative outcome. With at least four primary metocean phenomena to consider (wind, waves, currents and water levels) and only two (or three) representative locations available in each sub-area, some trade off in representing the absolute most onerous conditions for any single phenomenon was necessary.

In this development area there is a general tendency for waves (and winds) to be most extreme towards the north and west, whereas hydrodynamic phenomena (currents and water levels) are most extreme towards the south and east. Therefore, a natural choice in any given sub-area is a pair of representative locations positioned respectively to the west and to the east resolving the more onerous conditions for wave and hydrodynamic contexts. Since representative wind conditions have been defined independently ([1]) and are accommodated within this study using the approaches described in Section 5.5, coincidence between the analysis locations used herein and those representative wind locations was considered less of a priority.

The final locations selected are described in Table 4-1 and Figure 4-1.

Table 4-1 Analysis locations used in this study.

Site	Location	Longitude [°E]	Latitude [°N]	Notes
A1	A1W	7.3826	55.9184	Location of largest 50 yr Hm0 and Hmax
	A1E	7.8239	55.8281	Location of largest 50 yr positive water level
A2	A2W	7.2823	56.0588	Location of largest 50 yr Hmax (close to largest Hm0)
	A2E	7.7637	56.0287	Midpoint between most onerous water level and current speed
A3	A3W	7.3224	56.1791	Location of largest 50 yr Hm0 (similar Hmax value to largest Hmax)
	A3E	7.7838	56.1590	Midpoint between most onerous water level and current speed
A0	A0N	7.1820	56.1290	Coincident with wind analysis location and representative of larger end of range of wave conditions
	A0W	6.9614	55.8682	Location of largest current speeds and wave crests, an area of shallow bathymetry and representative of larger end of range of water level conditions
	A0E	7.3024	55.8682	Generic location chosen for spatial representativity in lieu of uncertainty regarding site zoning
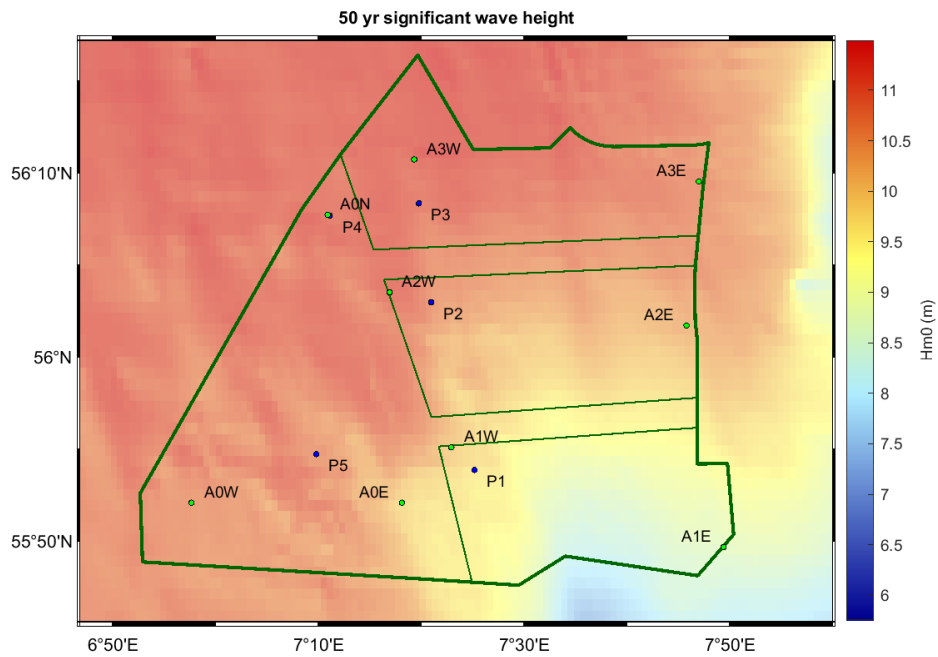
Figure 4-1 Selected analysis locations plotted in context of the spatial variation in the 50 yr extreme significant wave height. Points labelled "Px" show the representative wind locations used in the independent wind assessment [1].

5 Analysis Methods

5.1 Extreme Value Analysis

In this section, we discuss the approaches used in calculating all-year, omni-directional extreme criteria beginning with a brief overview of the procedure MetOceanWorks generally adopts. Thereafter, specific details pertinent to the derivation of extreme wave criteria in the Metocean Design Bases are given.

5.1.1 General Approach

Step 1: Data Preparation and Review

Carry out a detailed review of the model data, including calibrations against measurements.

Step 2: Method Selection

Decide whether to extrapolate from Peaks over Threshold (PoT), block maxima, or all data. Preference is given to PoT should there be sufficient data. Investigate any potential concerns with an all-year, omni-directional approach, e.g., larger waves arriving from very different directions, with potentially different extreme distributions or different driving mechanisms.

Note: For this study, a PoT approach has been used throughout, thus only relevant steps are included hereafter.

Step 3: Find peaks over threshold

a) Split data into points above and below a user specified *Threshold*.
b) Discard all points below, creating a new time-series of only values above the *Threshold*.
c) Place the first point in "Cluster 1". If the second point is temporally within a user specified *Reset Duration* of the first, it too is in Cluster 1. Otherwise, Cluster 1 is complete and this becomes the first point in Cluster 2.
d) Proceed to the third point. If it is within *Reset Duration* of the second, it is in the same cluster. Otherwise, it is the start of a new cluster.
e) Continue through the entire time-series until all data above the *Threshold* are assigned to a cluster.
f) Take the maximum of each cluster.

Essentially, the data are split into local clusters and maxima for each cluster found. Time series of the original data and selected cluster peaks are reviewed. In particular, we check high data peaks close to one another since their inclusion/exclusion may significantly affect extreme values. Adjust clustering parameters as necessary, and if highly subjective decisions affect inclusion/exclusion of high peaks, continue separate analysis on each option to review implications.

Step 4: Fit Distributions to Highest Peaks

Carry out independent fits to highest 50, 60, 70, …, 100 ,125, 150, …, 250 cluster peaks. For each, include the following fits:

- 3-Parameter Weibull (Maximum Likelihood (MLM), Method of Moments (MoM), Maximum Product of Spacings (MPS), L-Moments (Lmom)).
- Generalised Pareto (MLM, MoM, MPS, Lmom)
- Exponential (MLM, MoM, Lmom)

Step 5: Review Fits

Review each fit, including the following:

- If the fitted distribution is a bad fit to the data, discard.
- If the extreme values are not stable to changes in the number of peaks, discard (e.g., if results for a 60 peak fit are considerably different to for a 50 and 70 peak fits).

Step 6: Decide on Extreme Values

Of the remaining fits, a representative fit is selected. This is generally a fit whose 100-year extreme value is close to the median value of estimates of all remaining fits. However, some subjectivity is included to take into account the level of conservatism considered appropriate.

5.1.2 Worked Example at A3W for Extreme Significant Wave Heights

Step 1: Data Preparation and Review

These data originate from a bespoke, project specific model and have been well validated against site-specific measurements. Thus, they are deemed of a suitable quality for extreme value analysis.

Step 2: Method Selection

There is sufficient data for a PoT analysis. Since all major peaks come from the same general population, taking an all-year, omni-directional approach seems reasonable.

Step 3: Find Cluster Peaks

A threshold of 5 m and reset duration of 72 hours is used to provide in excess of 250 peaks, as shown in Figure 5.1. A little sensitivity testing is carried out around these values with little change overall to the top 200 peaks, as shown in Figure 5.2. Hence, single analysis with these peaks is considered appropriate.
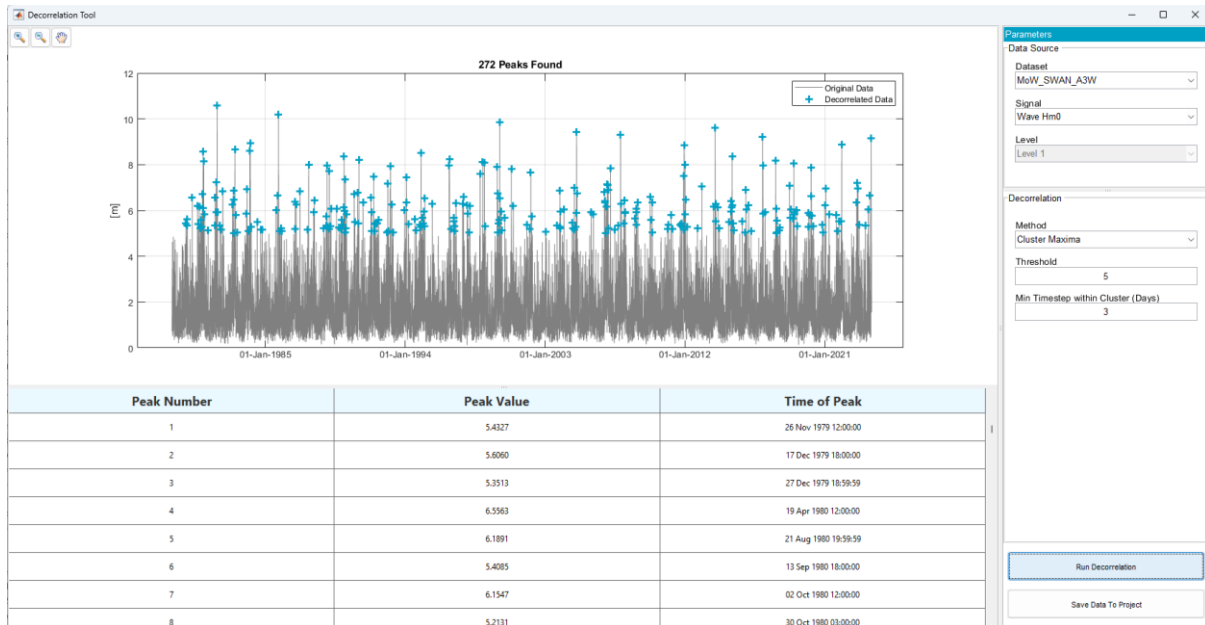
Figure 5.1: Peak selection at A3W.
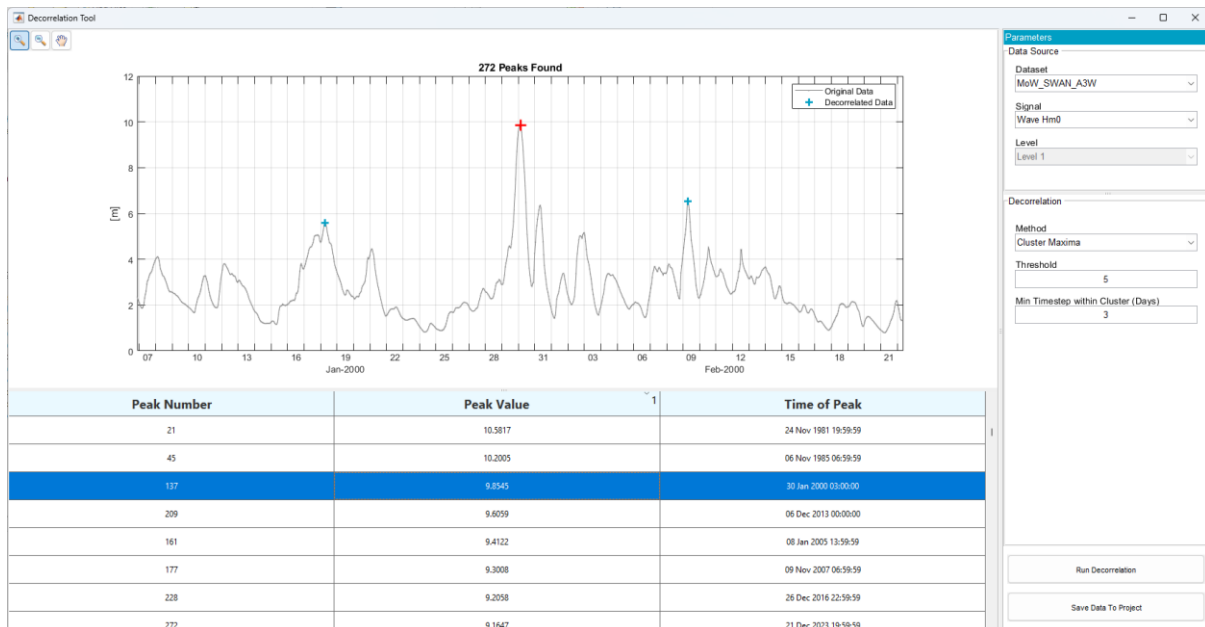
Figure 5.2: Selection of threshold and reset duration.

Step 4: Fit distributions

Select the number of peaks, distributions and fitting methods to be used.
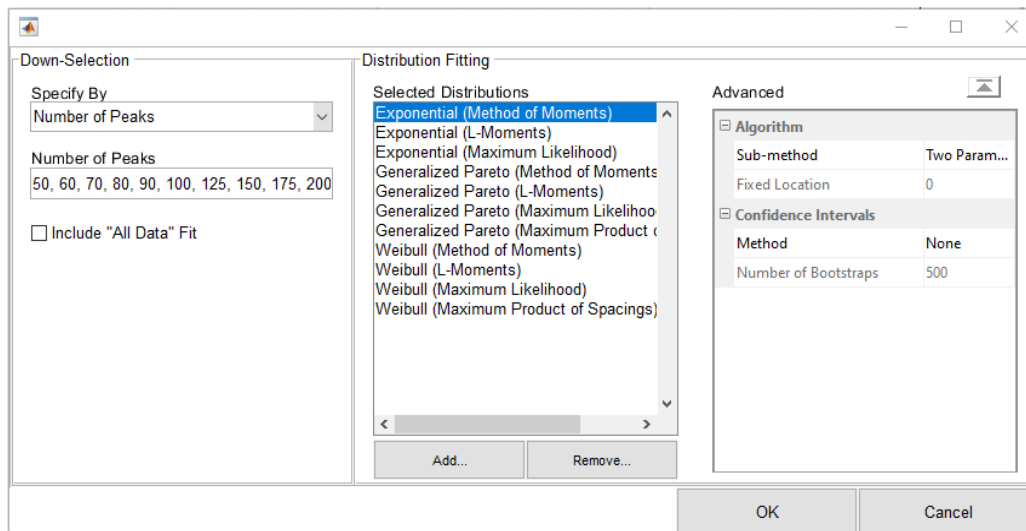
Figure 5.3: Selection of distributions and fitting methods.

Step 5: Review Fits

To give an overview of the manual review process, all of the distributions fitted to the highest 220 peaks are shown in Figure 5.4. Here, some of the Weibull fits are unbounded and curve unrealistically upwards as we approach higher values. Thus, in this instance, we only carry the selected distributions highlighted in green forward for the final selection of extreme values as shown in Figure 5.5.
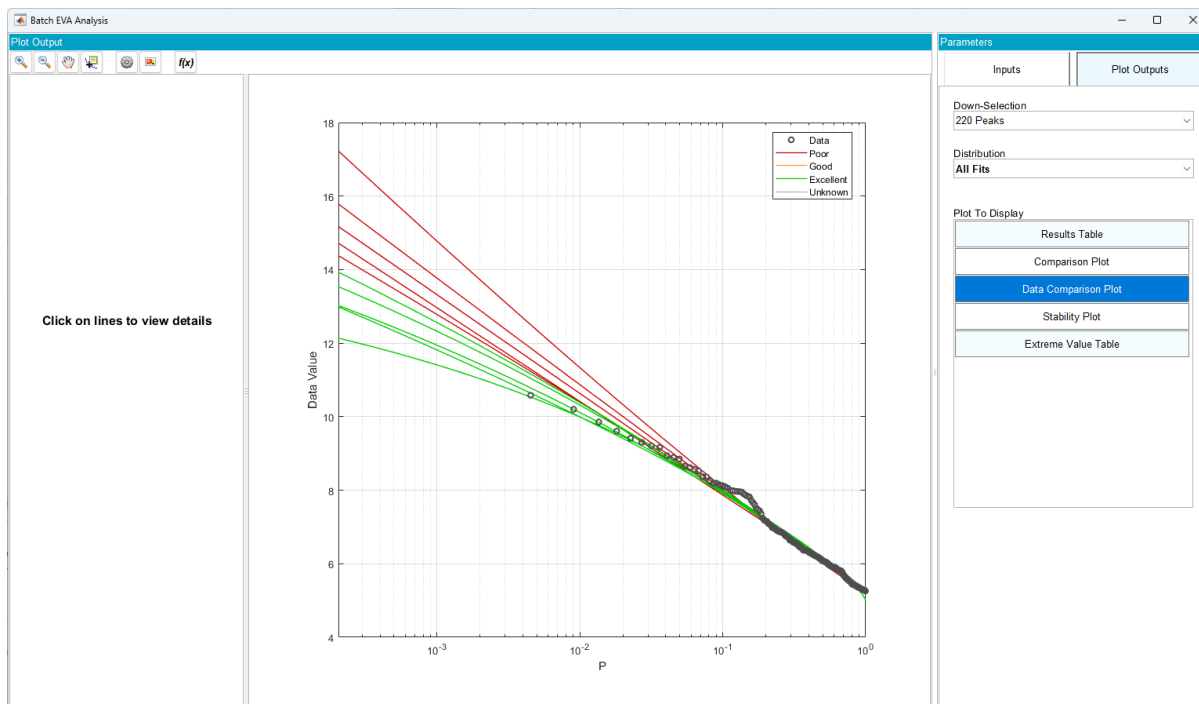
Figure 5.4: All fits for 220 peaks at A3W.
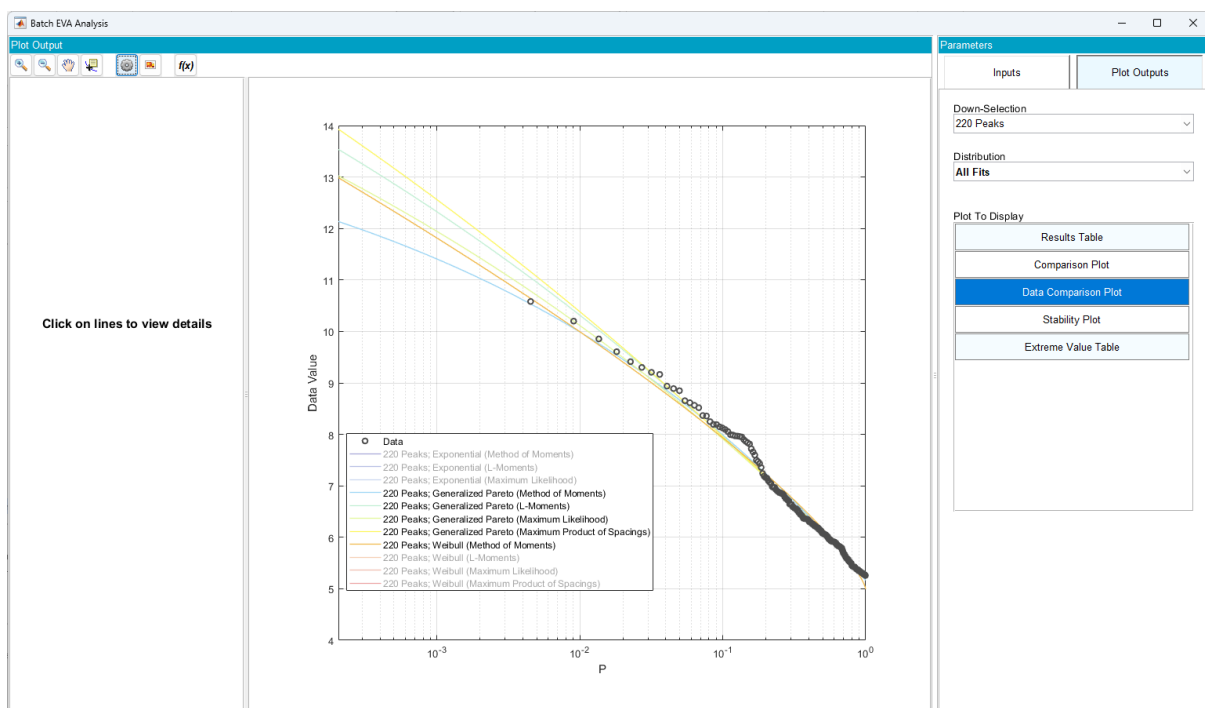
Figure 5.5: Selected fits for 220 peaks at A3W.

Step 6: Decide on Extreme Values

After reviewing all fits, those shown in red in Figure 5.6 have been discarded, with those shown in green remaining from which a single representative fit is selected, as shown in Figure 5.7 and Figure 5.8. Five hundred parametric bootstraps are then used to generate the 95% confidence intervals.
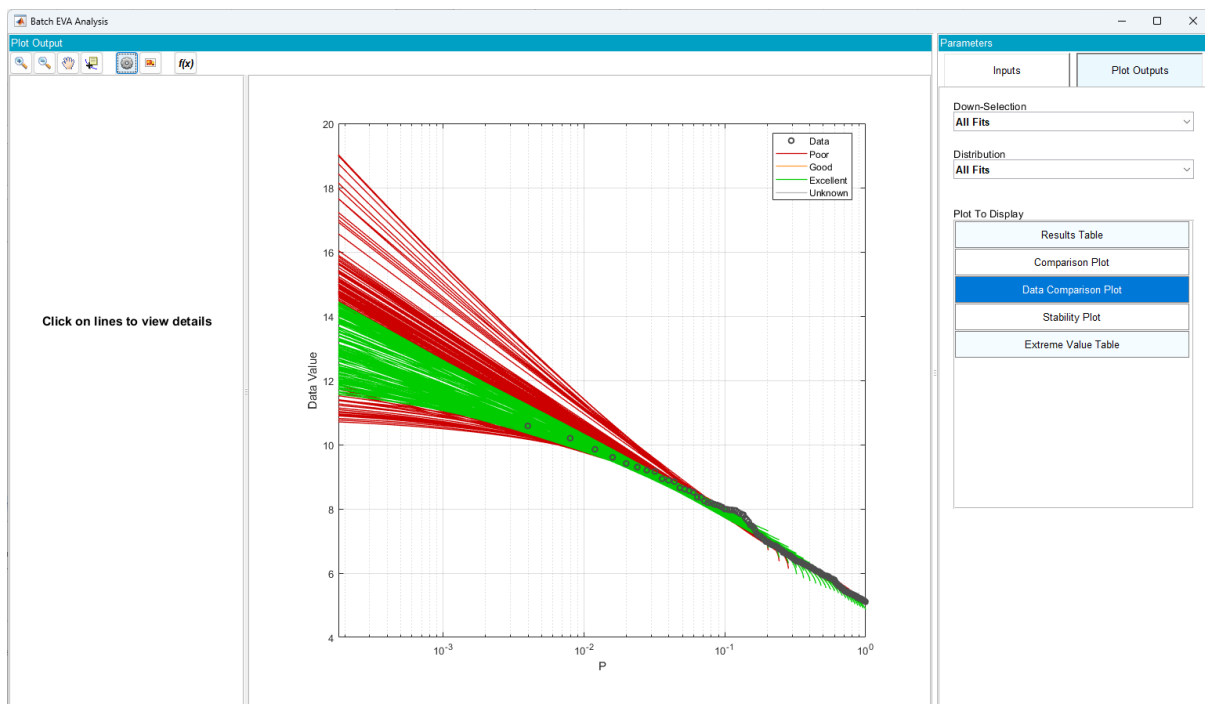
Figure 5.6: All fits for all peaks at A3W.
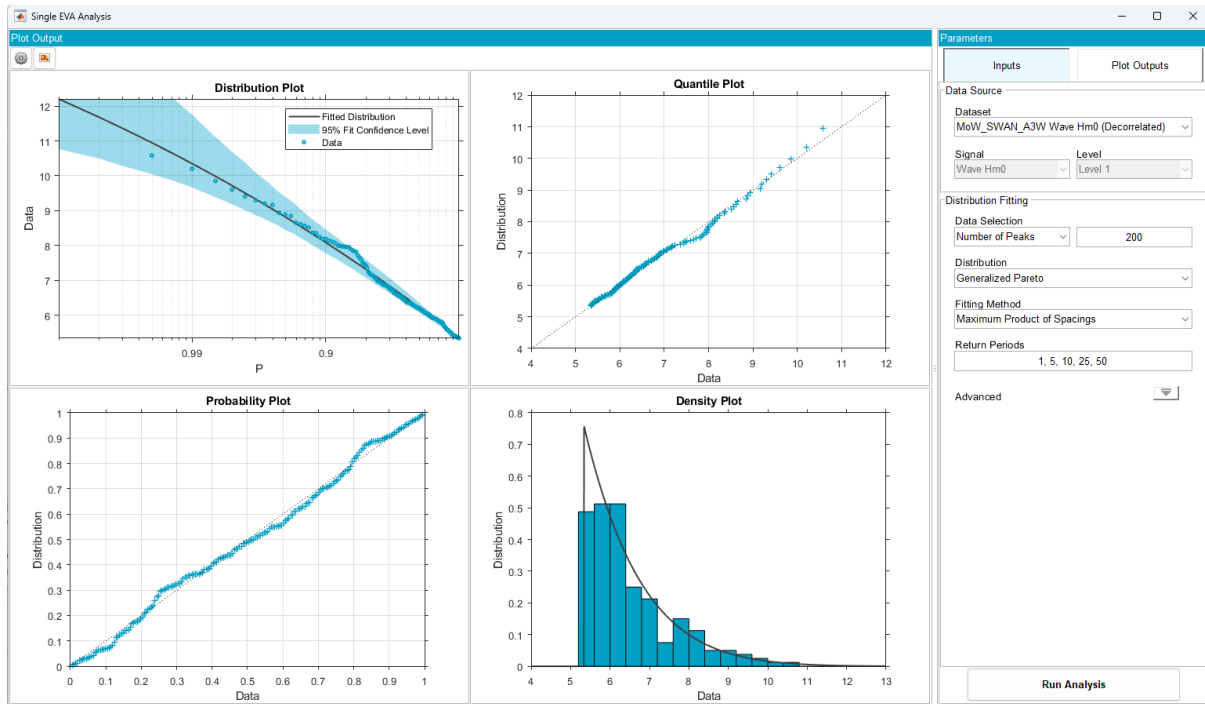
Figure 5.7: Chosen representative fit with diagnostic plots.
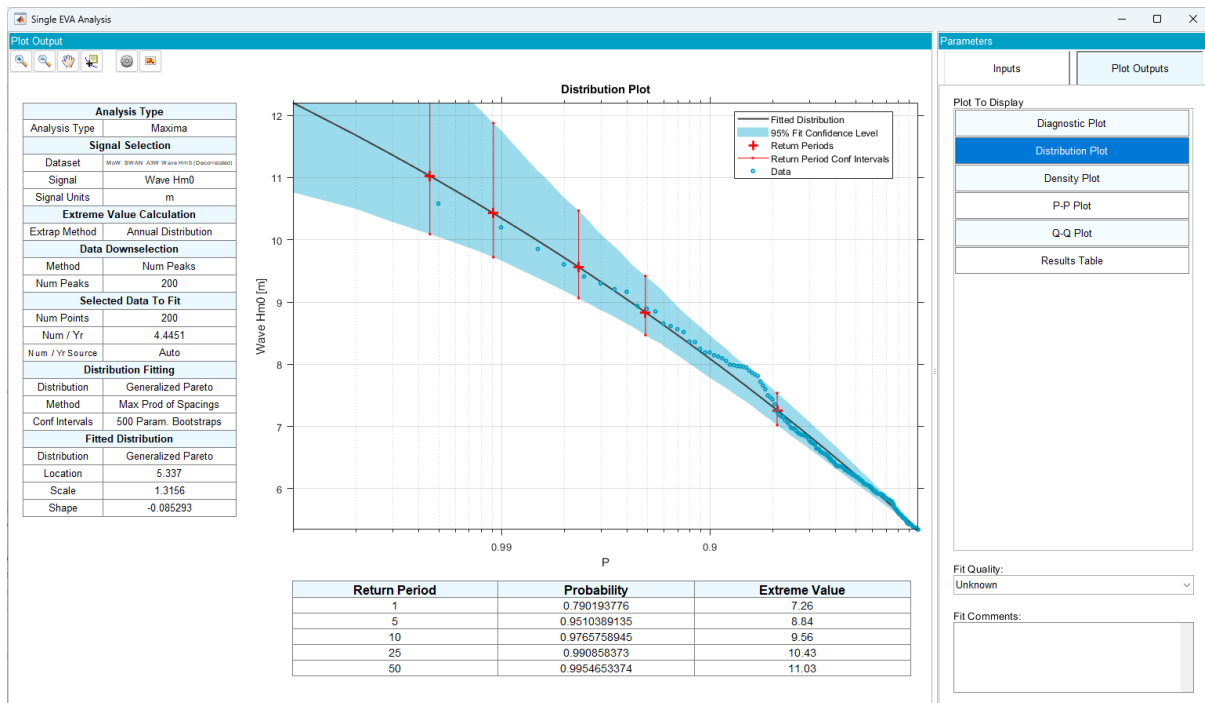
Figure 5.8: Chosen representative fit with return period estimates.

5.1.3 Directional and Monthly Extremes

Directional and monthly extremes were calculated by multiplying the omni-directional extreme values by relative severity factors (RSFs). In general, these scaling factors are determined from the relative intensity of the considered parameter at the 99.9th and 100th percentile of non-exceedance in each directional sector and in each month. In some instances, engineering judgement was applied to add a little conservatism in the presence of uncertainty.

5.2 Extreme Maximum Wave and Crest Heights

In this section we explore the derivation of maximum individual wave and crest heights using the ISO-compliant method proposed by Tromans and Vanderschuren [2].

5.2.1 General Approach

Step 1: Data Preparation and Review

Carry out of a detailed review of the model data, including calibrations against measurements.

Step 2: Method Selection

Preference is to use the storm-based approach of Tromans and Vanderschuren (TVM). For shorter datasets, all data (or higher sea-state) convolutions of Hm0 and short-term wave height/crest distributions are also considered.

Additionally, we need to select appropriate short-term wave height and crest height distributions. In deep water, we use the Forristall deep water distribution for wave height and the Forristall 3D distribution for crest height [3]. In shallow water, a number of alternatives are considered. Please see Sections 5.2.2 and for more details on these short-term distributions.

Note: For this study a TVM approach is used throughout, thus only relevant steps are included hereafter.

Step 3: Identify Storms

Split data into storms above a specified threshold. Merge storms that are temporally within a configurable reset duration.

Review time series of original data and storms. In particular, review larger storm peaks which may or may not have been merged into the same storm. Adjust parameters as necessary, and if highly subjective decisions affect merging of high peaks, continue separate analysis on each option to review implications.

Step 4: Calculate Hmp and Cmp for each storm

For each storm combine Hm0 with Tm01 or Tm02 values with the short-term distribution selected to determine the most probable extreme wave height (Hmp) or crest (Cmp) for the storm.

Step 5: Fit Distributions to Hmp/Cmp

Carry out independent fits to highest 50, 60, …, 190, 200 Hmp/Cmp values. For each, include the following fits:

- 3-Parameter Weibull (Maximum Likelihood (MLM), Method of Moments (MoM), Maximum Product of Spacings (MPS), L-Moments (Lmom))
- Generalised Pareto (MLM, MoM, MPS, Lmom)
- Exponential (MLM, MoM, Lmom)

Step 6: Convolution

For each fitted distribution, carry out a final convolution between the fitted distribution and that of individual heights/crests in a single storm given Hmp/Cmp. The individual heights/crests distribution in a storm is that given by Tromans and Vanderschuren, with N taken to be the mean number of waves per storm.

Step 7: Review Fits

Review each fit, including the following:

- If the fitted distribution is a bad fit to the data, discard.
- If the extreme values are not stable to changes in the number of peaks, discard (e.g., if results for a 60-peak fit are considerably different to for a 50- and 70-point fit).
- Consider if physical implications of extreme behaviour are realistic, e.g., unbounded fits in shallow water, fits that rapidly reach an upper bound (i.e., similar 100- and 10,000-year extremes) in deep water with long fetch. If not, discard.

Step 8: Determine Extreme Values

The previous step normally gives a large selection of options. If all cover a similar range of extreme values, then choose a representative fit, generally whose values are close to the median value of estimates. If they do not (e.g., the three different distributions may suggest three different ranges) decisions can be far more subjective, often needing more investigation, discussion with client, precedence in the region, etc. before a final decision. Of the remaining fits, a representative fit is selected.

Steps 9: Compare to Physical Limitations

In shallower waters, physical limitations are also taken into account in the following post-processing steps:

- For wave heights, the maximum wave height is limited to 0.78 times the local water depth. IEC 61400-3-1 [4] "Wind energy generation systems – Part 3-1: Design requirements for fixed offshore wind turbines" includes a section on wave breaking. In Annex B, "B.4 Breaking waves" a 78% of water depth limit is included as seen in other guidelines:

    Waves may break in different ways, depending principally on the ratio of deep-water wave steepness to sea floor slope.

    In shallow water, the empirical breaking limit of the wave height is approximately 78 % of the local water depth. The presence of a sloping sea floor (still water depth decreasing in the direction of wave propagation) can lead to breaking waves which are significantly higher than limiting height regular waves in the same local water depth (0,78d). Guidance is provided by Barltrop and Adams [see [5]].

- For crest heights:
    o If wave height has *not* been limited as per above, the results of the TVM approach is compared to a stream function methodology, with the most conservative of the two used.
    o If wave height *has* been limited, stream function results are used.

5.2.2   Short term wave height distributions

A key part of the TVM method is the selection of an appropriate distribution to describe the short-term distribution of individual wave heights within each sea-state. Various wave height distributions are suggested across the literature and relevant guidelines, with no clear consensus as to the most appropriate. Indeed, studies

comparing a selection of distributions to measured data (see, for example, Wu et al. (2016) [6] and Karmpadakis et al. (2020) [7]) generally do not conclude that any particular distribution is superior to the others, but that the "best" performing distribution differs both by location *and* conditions.

The distributions can broadly be split into "Deep Water Distributions" that do *not* account for the effects of water depth, and "Shallow Water Distributions" which do. A brief summary of those distributions included in relevant guidelines and the two reviews noted above are included in

Table 5.1 below. It should be noted that many are variations and/or improvements on others, for example with the three Glukhovskiy distributions being similarly formulised.

Table 5.1: Summary of individual wave height distributions.

Distribution	IEC 61400-3-1	DNV-RP-C205	DNV-ST-0437	IS0 19901-1	Wu et al. (2016) [6]	Karmpadakis et al. (2020) [7]
Deep Water Distributions						
Rayleigh	✓		✓	✓	✓	✓
Rayleigh / Naess	✓	✓	✓			✓
Forristall (deep water)	✓	✓		✓	✓	✓
Shallow Water Distributions						
Goda	✓					
Battjes and Groenendijk	✓		✓		✓	✓
Forristall (shallow water)					✓	
Glukhovskiy	✓		✓			
Glukhovskiy / van Vledder					✓	✓
Glukhovskiy / Klopman						✓
Mendez-Losada-Medina					✓	✓
LoWiSh II (Weibull-generalised Pareto)					✓	✓
Boccotti						✓
Boccotti / Tayfun					✓	

For this project, we used the "Glukhovskiy / Klopman" distribution, as described in Karmpadakis et al. because:

a) Much of the site is in shallow to intermediate waters, and as such, water depths should be taken into account.

b) Of the shallow water options available, only the Glukhovskiy and Battjes and Groenendijk distributions are specified in multiple guidelines.

c) The Battjes and Groenendijk distribution has a number of restrictions placed on its usage within the guidelines with regard to seabed slope, wave direction and current speeds which may not be applicable

to the site. Furthermore, in the detailed review of Karmpadakis et al. its performance is highly variable, being very good in some of the locations considered, but particularly bad in others. The Glukhovskiy distribution performs well throughout. Thus, we select the Glukhovskiy distribution.

d) Unfortunately, the guidelines are not particularly detailed with regard to a full definition of this distribution, with Annex B Section B.3.1 of IEC61400-3-1 [4] citing only a paper in Russian, whilst DNV-ST-0437 [8] offers no reference or equations at all. Equations are provided for two variants by Karmpadakis et al., with TVM analyses at the analysis location suggesting that the variant attributed to Klopman is likely to be a little more conservative. Thus, it has been used.

5.2.3   Short term crest height distribution

Similar considerations are needed for the short-term wave crest distribution, where two options – the Forristall 2D and 3D distributions – are commonly suggested. DNV-RP-C205 [9] recommends the Forristall 2D distribution for long-crested seas, and the 3D distribution for short-crested seas. Both distributions are also given in Annex B Section B.3.4 of IEC61400-3-1 [4], though the only note to differentiate between the two is to state that they are based on 2D and 3D irregular wave train simulations respectively. No particular guidance is given with regard to their usage. Annex A Section A.8.7 of ISO19901-1 [10] only specifies the 3D equation and introduces it with:

Recent research suggests that crest elevations for seas with typical directional spreading of wave energy are satisfactorily predicted by second order, random, directional wave theory.

One further point is worth consideration: Section 3.5.10 of DNV-RP-C205 [9] states that:

It should be noted that the Forristall distribution is based on second order simulations. Higher order terms may result in slightly higher crest heights. Hence extremes predicted by this distribution are likely to be slightly on the low side. To account for higher order non-linearities, it is recommended to increase the maximum crest height with a factor of 1.05.

The final sentence – specifically recommending a factor of 1.05 – is a recent addition in the 2019 revision of this recommended practice and was not present in the 2017 edition.

For this project, the Forristall 3D distribution has been used, and an uplift factor of 1.05 has been applied.

5.2.4   Worked Example at A3W

Step 1: Data Preparation and Review

Here we are using the same dataset from the bespoke, project wave specific model. These data have been validated against measurements and are deemed of a suitable quality for extreme value analysis.

Step 2: Method Selection

Sufficient data is available for a TVM approach. The Glukhovskiy wave height and Forristall 3D crest height distributions are used.

Step 3: Identify Storms

The same parameters were used as for deriving Hm0 extreme values. Please see Section 5.1.2 for details.

Steps 4-6: Calculate Hmp/Cmp, Fit Hmp/Cmp, Convolution

Nothing unusual to note.

Steps 7 & 8: Review Fits and Select Determine Values

Fits are reviewed, and representative fits for Hmp and Cmp are chosen in an analogous manner to those for Hm0 extreme values. Please see Section 5.1.2 for details. It should also be noted that the selected fits are not necessarily the "best" fits to the data in their own right, but chosen to best represent all selected fits.

The final fit for Hmp at the A3W is shown in Figure 5.9 with the final fit for Cmp shown in Figure 5.10. These show the Hmp/Cmp data (blue circles) and the selected fit to them (solid black line) alongside the distribution for individual height/crests resulting from the TVM convolution in Step 6 (dashed red line) from which extreme values are taken.

Step 9: Compare to Physical Limitations

As might be expected, physical limitations are dependent on location. At the A3W location (water depth 30.2 m), the extreme wave heights do not become depth limited, but stream function does provide more conservative crests at the 5-year return period and above. In summary, the Forristall 3D distribution has been used, and an uplift factor of 1.05 applied. These values were then compared to those determined by stream function using the maximum wave height and associated wave period, with the most conservative of the two methods used. In the case of A3W, stream function values are used for return periods of 5-years and longer, where it yields more conservative results.

Signal Selection	
HmO Dataset	MoW_SWAN_A3W:Wave HmO (Storms)
HmO Signal	Wave HmO
HmO Signal Units	m
Tm01 Dataset	MoW_SWAN_A3W:Wave HmO (Storms)
Tm01 Signal	Wave Tm01
Tm02 Dataset	MoW_SWAN_A3W:Wave HmO (Storms)
Tm02 Signal	Wave Tm02
Water Depth (Manual)	30.2
Offset from MSL Dataset	MIKE21_56p180N_7p323W_30m
Offset from MSL Signal	Waterlevel
Short Term Distribution	
Short Dist. Type	Wave Height
Distribution	Gluhovski
Method	KlopmanB
HmO To Hrms Method	Rayleigh
Data Downselection	
Method	Num Peaks
Num Peaks	250
Selected Data To Fit	
Num Points	250
Num / Yr	5.5563
Num / Yr Source	Auto
Distribution Fitting	
Distribution	Generalized Pareto
Method	Max Prod of Spacings
Fitted Distribution	
Distribution	Generalized Pareto
Location	9.9127
Scale	1.8326
Shape	-0.049957
Hmp Extreme Values	
Extrap Method	Annual Distribution
1 Year	12.9956
5 Year	15.3867
10 Year	16.5193
25 Year	17.9024
50 Year	18.8906

Return Period	Probability	Extreme Value
1	0.8262492949	13.60
5	0.9606354955	16.22
10	0.9812164038	17.47
25	0.9926799882	19.01
50	0.9963706219	20.14

Figure 5.9: Final fit, Hmp, A3W.

Signal Selection	
HmO Dataset	MoW_SWAN_A3W:Wave HmO (Storms)
HmO Signal	Wave HmO
HmO Signal Units	m
Tm01 Dataset	MoW_SWAN_A3W:Wave HmO (Storms)
Tm01 Signal	Wave Tm01
Tm02 Dataset	MoW_SWAN_A3W:Wave HmO (Storms)
Tm02 Signal	Wave Tm02
Water Depth (Manual)	30.2
Offset from MSL Dataset	MIKE21_56p180N_7p323W_30m
Offset from MSL Signal	Waterlevel
Short Term Distribution	
Short Dist. Type	Crest Height
Distribution	Forristall Shallow 3D
Data Downselection	
Method	Num Peaks
Num Peaks	180
Selected Data To Fit	
Num Points	180
Num / Yr	4.0006
Num / Yr Source	Auto
Distribution Fitting	
Distribution	Generalized Pareto
Method	Max Prod of Spacings
Fitted Distribution	
Distribution	Generalized Pareto
Location	6.31
Scale	1.3492
Shape	-0.015314
Cmp Extreme Values	
Extrap Method	Annual Distribution
1 Year	8.1762
5 Year	10.1554
10 Year	11.0995
25 Year	12.2904
50 Year	13.167

Return Period	Probability	Extreme Value
1	0.7569947874	8.56
5	0.9457489651	10.65
10	0.9740073235	11.67
25	0.9898478092	12.96
50	0.994962757	13.92

Figure 5.10: Final fit, Cmp, A3W.

5.3 Periods associated with Hm0

Relationships between significant wave height (Hm0) and wave periods (Tm02 or Tp) are determined by applying a conditional modelling approach (CMA) as follows:

a) Data is binned according to Hm0, for example into bins of 0.25 m width.

b) To the associated wave period data in each bin, a lognormal distribution is fitted. Each such lognormal distribution has two parameters, the mean of the logarithm of the periods (hereafter μ) and the standard deviation of the logarithm of the periods (hereafter σ).

c) Parametric forms are fitted to the collections of μ and σ for all bins to describe how they change in relation to Hm0. Throughout this project, the following equations (originating from Haver & Nyhus [11]) are used:

$$\mu = p_1 + p_2 \log(H_s + p_3)$$
$$\sigma^2 = q_1 + q_2 \exp(q_3 H_s^{q_4})$$

Where p_1, p_2, p_3, and q_1, q_2, q_3, q_4 are fitted independently for each relationship considered.

d) Central, upper and lower estimates are generated for a given Hm0 and are determined by first calculating the corresponding lognormal distribution according to the relationships fitted in c) and then finding the 5th, 50th and 95th percentiles (lower, central and upper estimates respectively).

These relationships have been examined directionally and sectors with similar fetch and steepness characteristics have been grouped together, see Figure 5.11 below. This results in five custom sectors as well as the omni-directional case and these are applied in any directional analysis to the appropriate sector.
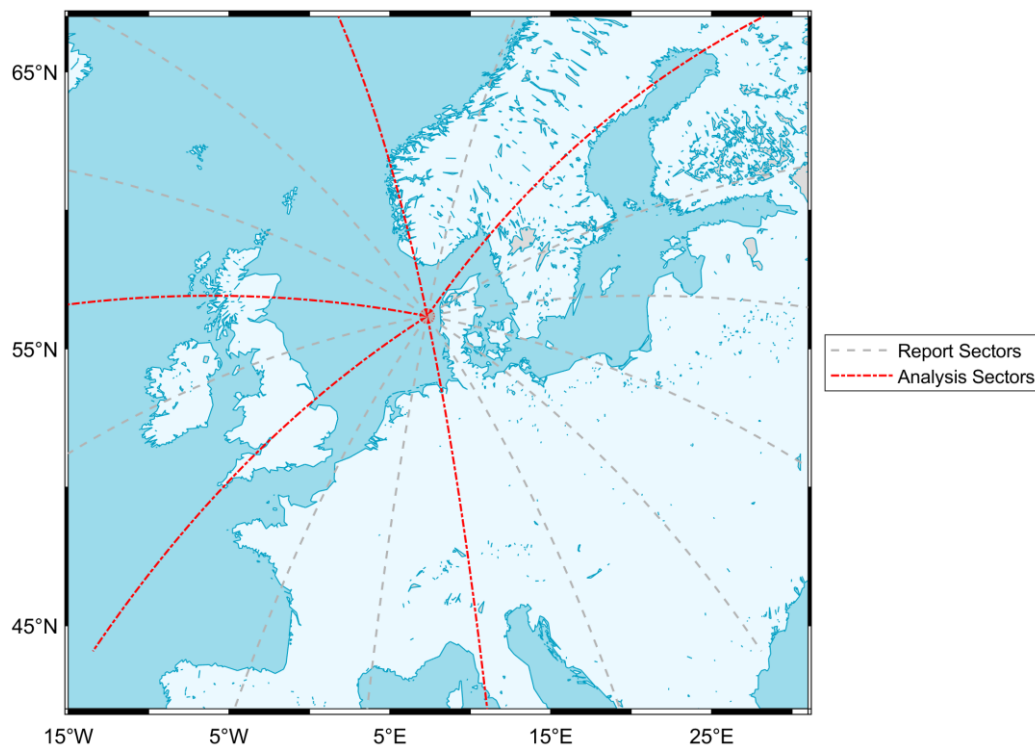
Figure 5.11: Directional sector grouping for significant wave height and wave period relationships.

5.3.1 Periods associated with Hmax (Tass)

The lower, central and upper estimates of the period associated with the maximum wave height, *Tass*, are taken to be 0.9 times the lower, central and upper estimates of the peak wave period (Tp) for the corresponding return period. ISO [10] recommends a Tass/Tp ratio between 0.8 and 1.0, whilst research from Haring et. al. [12] suggest Tass = Tp*0.9.

5.4 Wave Spectral Partitioning

Wave spectra were partitioned into wind-sea and swell components using XWaves 5.7, a GUI-driven ocean surface wave spectrum analysis and display tool, developed by WaveForce Technologies.

Wave spectral partitioning provides an efficient approach to characterise energy levels of individual wind-sea and swell wave components in directional wave spectra. Here a 'wave component' is defined as a specific wind-sea or swell that can be attributed to a region of enhanced energy in the directional wave spectrum. The time evolution of a series of related wave components forms a 'wave system' that can be traced to a specific generation region on the ocean surface.

The first step of spectral partitioning is to isolate spectral regions associated with individual energy peaks. This is accomplished by efficient image processing routines that were designed for making watershed delineations in topographic imagery. Treating the spectrum as an inverse topographic domain, an 8-point connected smoothing transform removes fine-scale noise in the spectrum. A watershed delineation transform then identifies the boundaries forming the minima between remaining spectral peaks. Spectral regions surrounded by such boundaries become individual partitions.

The resulting wave components are sorted into wind-sea or swell. To be classified as wind-sea, a spectral peak must be forced by a component of the existing wind. A wave-age criterion is used to identify and combine the 2D wind-sea partitions. All remaining peaks are labelled as swell. In cases where there are more than one swell component, we have combined them into a single partition. As a final step in producing consistent results with minimal noise, any wind-sea or swell component that falls below a significant wave height threshold of 0.1 m is removed from analysis and labelled as miscellaneous energy.

Further details on the methodology can be found in Appendix G of the Metocean Data Overview.

5.5 Hub height wind speed for NSS and SSS

Both Normal Sea State (NSS) and Severe Sea State (SSS) analyses involve the development of representative environmental conditions describing the interrelationship of hub height winds with waves. The most coherent basis for these joint analyses is to combine output from a wave model with hub height wind conditions which have been derived from the same wind model that was used to force it. This ensures that correspondence between the timing and magnitude of wind and wave events is maximised, meaning that their joint occurrence can be described most accurately. A complication to this approach is found when other parts of a design basis make use of different datasets, perhaps sampled from different representative locations or from different data sources entirely. This may introduce inconsistencies in the statistical representation of some phenomena, particularly when used in Integrated Loads Analyses for WTG tower and foundation design.

In the present case, wind conditions have been developed independently of this study [1], with representative locations that are different from those identified as being optimal for the description of wave conditions. In order to ensure consistency between the independent wind- and the joint wind-wave conditions, adjustments

have been made to the hub height wind data used in the development of NSS and SSS. Specifically, this involves using hub height wind data extracted at the wave analysis locations from the same calibrated ERA5 dataset used to force the wave model, but with an adjustment made to the wind speeds in order that their statistical distribution matches that defined in the wind assessment. This is advantageous in that it provides both tight coherency of the wind and wave phenomena and consistency with independent wind criteria.

Locations used in the development of representative wind conditions are shown in Table 5-2. For each of these locations, Weibull parameters are defined [1] describing the statistical distribution of hub height wind speeds, and a mapping to the locations used in this study is described.

Table 5-2: Locations used to define representative wind conditions.

Site	Location	WGS84	A [m/s]	k	Mean wind speed [m/s]	Mapping to locations in present study
A1	P1	55.8983°N, 7.4227°E	11.85	2.25	10.50	A1W, A1E
A2	P2	56.0487°N, 7.3425°E	11.90	2.26	10.54	A2W, A2E
A3	P3	56.139°N, 7.3224°E	11.94	2.26	10.58	A3W, A3E
A0[*]	P4	56.129°N, 7.182°E	12.01	2.27	10.64	A0N
A0[*]	P5	55.9084°N, 7.1619°E	11.98	2.27	10.61	A0W, A0E

[*] This area is described by the label A4 in [1].

The following method is used to derive hub height wind conditions for NSS and SSS:

a) As a starting point, hub height wind speed and direction timeseries are extracted from the MetOceanWorks calibrated ERA5 model (described in section 4.5 of the Metocean Data Overview document) at each of the analysis locations used in this study.

b) For each location, a two-parameter Weibull distribution is fitted to the omni-directional wind speed data. Hereafter, we denote the scale parameter of this fitted distribution $A_{hindcast}$ and the shape parameter $k_{hindcast}$.

c) For each location, a mapping is made to a counterpart location for representative wind conditions (Table 5-2) based upon their mutual inclusion within designated offshore wind development areas (A1, A2, etc.). Weibull parameters for the representative wind conditions are denoted $A_{adjusted}$ and $k_{adjusted}$ as these describe the target distributions towards which adjustments are made.

d) For each location, the following transformation is applied independently to each wind speed value in the MetOceanWorks calibrated ERA5 data, denoted $WS_{hindcast}(t)$:

$$WS_{adjusted}(t) = A_{adjusted} \cdot \left(\frac{WS_{hindcast}(t)}{A_{hindcast}}\right)^{\frac{k_{hindcast}}{k_{adjusted}}}$$

If the MetOceanWorks calibrated ERA5 data is exactly described by a Weibull distribution, this procedure would serve to transform from $WS_{hindcast}(t)$, with Weibull distribution given by {$A_{hindcast}$, $k_{hindcast}$}, to $WS_{adjusted}(t)$, which would also be Weibull distributed with parameters {$A_{adjusted}$, $k_{adjusted}$}.

e) The timeseries given by $WS_{adjusted}(t)$ is subsequently used to represent wind speed at hub height throughout NSS and SSS analyses.

f) Wind *directions* at hub height are taken to be those of the nearest ERA5 level to this elevation, and in particular, no further modifications are included.

Further details on this transformation can be found in Appendix B of this document.

5.6 Normal Sea States

Full details of the steps used to create Normal Sea State (NSS) criteria can be found in Appendix C.

5.7 Severe Sea States

Full details of the steps used to create Severe Sea State (SSS) criteria can be found in Appendix D.

5.8 Extreme Currents

Extreme current speeds were calculated from the analysis of modelled current data using the method outlined in Section 5.1.

5.9 Current Profile

ISO guidelines (ISO 19901-1, [10]) state that:

Typically, shallow water current profiles in which tides are dominant can often be characterized by simple power laws of velocity versus depth, whereas deep-water profiles are more complex and can even show reversals of the current direction with depth.

In this context, the sites of interest would generally be considered *"shallow water"* and tides contribute significantly to the overall flow regime. For such locations, the guidelines go on to specify that:

The power law current profile [as given below] can be used where appropriate (e.g. in areas dominated by tidal currents in relatively shallow water)

With an equation as follows:

$$v_c(z) = v_c(0) \left(\frac{d+z}{d} \right)^{\alpha}$$

Where:

       z = the distance from still water level, positive *upwards*
       $v_c(z)$ = the current speed at z
       d = the water depth to still water level (taken positive)
       α = the exponent, which the ISO guidelines state is "typically 1/7".

Through the analysis of relevant regional measurements, presented in Appendix D of the Metocean Data Overview, we recommend a power law profile with exponent α of 1/8 is used to describe current speeds in the vertical throughout this project.

5.10 Extreme Water Levels

5.10.1 Extreme Total Water Levels

Direct summation of the wave crest, tide and surge value does not make any allowance for the joint probability of occurrence of these three components. This issue has been recognised by both the metocean and structural communities, and a realistic approach for deriving extreme total water levels (ETWL) is contained in ISO 19902 [13]. The guidance in this standard presents two equations for the combination of the three components, depending on the degree of association between the surge and the wave crest in the extreme storm.

If surge is not expected to occur at the same time as the wave crest, Equation (1) applies:

$$H1 = \sqrt{(a^2 + s^2 + t^2)} + f \tag{1}$$

If surge is expected to occur at the same time as the wave crest, Equation (2) applies:

$$H2 = \sqrt{((a+s)^2 + t^2)} + f \tag{2}$$

Where:

        a = extreme wave crest height;

        s = extreme surge;

        t = maximum elevation of the tide relative to mean sea level (MSL);

        f = the expected sum of subsidence, settlement and sea level rise over the design service life of the structure.

The difference in results when using Equations (1) or (2) can be considerable, with the latter being more conservative. Scatter plots of simultaneous significant wave heights and water levels produced for this project suggest that extreme waves and water levels are likely to occur at the same time. They are presented in the section describing Water Level Criteria of the accompanying Metocean Design Criteria reports. As a result, the more conservative Equation (2) is used throughout.

5.11 Tidal Analysis

Harmonic analysis has been carried out on the modelled hydrodynamic data using the MATLAB based UTide package [14]. This has been used to separate meteorologically induced water-levels and currents from those arising from astronomical tide-producing forces.

6 Additional Parameters

6.1 Marine Growth

Any hard structure submerged in the sea will eventually host a community of marine organisms growing on and associated with its surface. This marine growth, or biofouling, is comprised of a variety of species depending on the location, depth and configuration of the structure.

Biofouling is a complex process that involves colonization by microfouling organisms, such as viruses, bacteria, cyanobacteria, fungi, protozoa and microalgae, and larger macrofouling organisms, including macroinvertebrates and macroalgae. Macrofouling comprises calcareous hard-fouling organisms such as barnacles, mussels and tubeworms and soft-fouling organisms such as non-calcareous algae (seaweeds and kelps), sponges, anemones, tunicates and hydroids. The colonization process is often broadly described as a succession of four main stages which are summarised by Vinagre et al [15]:

1. Within minutes to hours of submersion, the substrata adsorb a biochemical conditioning biofilm, consisting of organic material such as glycoproteins, proteoglycans and polysaccharides naturally dissolved in the seawater.
2. Within hours, primary colonisers, assemblages of unicellular organisms that secrete extracellular polymeric substances (EPS) adhere to the substrata. Together, the microorganisms and EPS facilitate the settlement of macrofoulers.
3. Within days to weeks, secondary colonizers consisting of sessile macrofoulers, including soft and hard-foulers, develop and overgrow the microfouling. As they grow and age, macrofoulers provide "micro-habitats" that attract further settlements.
4. Within weeks to months, the substrata are fouled by tertiary colonizers which typically reside within the sessile biofouling. The biofouling communities reach maturity within a few years, accompanied by an increase in species diversity and richness. The communities are characterised by a variety of sessile and mobile benthic and epibenthic organisms.

Whilst marine organisms generally colonise a structure soon after installation, the growth generally tapers off after a few years. An anti-fouling coating can delay the process, but significant marine growth is likely within two to four years. The growth rate and type of colonisation may vary seasonally and on an inter-annual basis due to natural processes and ecological cycles.

The amount and type of marine assemblages which develop on structures varies with time, latitude, depth of water and distance from the coast. Different types of marine growth occur at different positions in the water column and so thickness will depend on the location of the structural component relative to the sea surface. Other factors that will have an impact include orientation relative to the sea surface and relative to the dominant current, the age of the component and its maintenance strategy. Marine growth also depends on additional environmental conditions such as salinity, oxygen content, pH value and temperature.

Marine growth is likely to extend from the splash zone to the sea bed, with the greatest thicknesses between the sea surface and a depth of 40 m. The paucity of publicly available data has not allowed for a site-specific assessment of marine growth terminal thicknesses and the best estimates are likely from inspection records of any existing marine infrastructure close to the proposed developments (i.e., adjacent wind farms). The closest in-situ observations that we have identified are approximately 34 km and 200 km to the south of the proposed

development site, see Figure 6-1. The details of these observations were obtained from the European Biofouling Database[1].
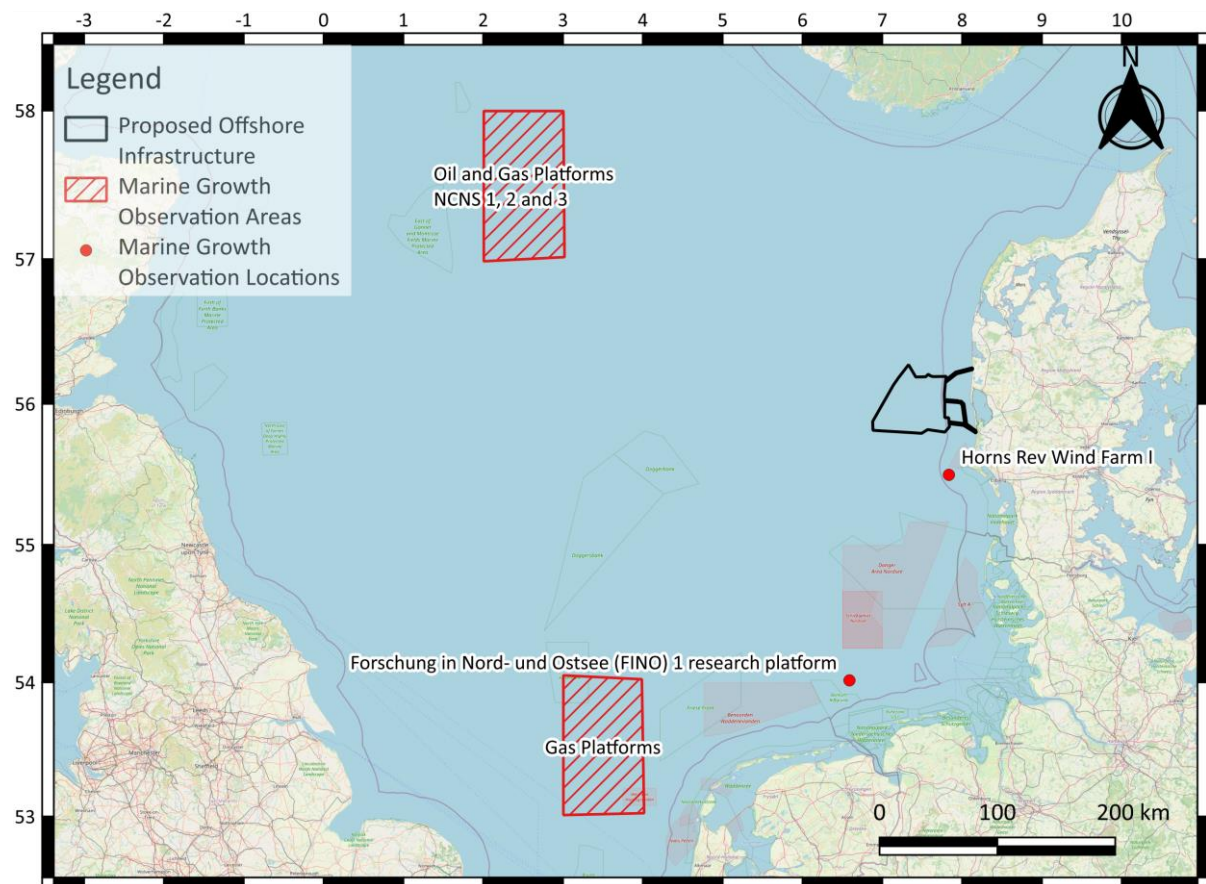
Figure 6-1. Locations of observations of marine growth.

This database draws on previous work by Vattenfall [16], Krone et al. [17], and Theophanatos [18] about growth on various structures in the marine environment.

Vattenfall [16] provides details of biofouling on monopile structures at the Horns Rev wind farm. Over periods of 12 to 42 months, sample weights of up to 3.02kg/m² fresh weight (FW) were noted, mostly consisting of common and blue mussels at depths of up to 10 m.

Krone et al. [17] noted that, for fouling periods of between two and four years, in temperatures ranging between 5 and 16°C, maximum thicknesses of up to 400 mm were attained for hard-foulers at the FINO1 observation location shown in Figure 6-1.

Theophanatos [18] studied the growth of marine foulers on offshore oil and gas platforms over periods of between 10 and 15 years. Whilst these sites are geographically distant from the project site, the long fouling period studied here provides a useful insight into long-term biofouling on offshore structures in the North Sea. For these sites, maximum thicknesses of up to 120 mm were obtained for hard foulers.

Table 6-1 shows the species observed at various depths from all three studies.

---

[1] For more information, please see: https://oceanic-project.eu/biofouling-database/

Table 6-1: Species observed at various depths.

Region	Depth [m]	Species	Common Name
North Sea	Intertidal	Magallana gigas (NNS)	Pacific oyster
	0-10	Mytilus edulis, Balanus crenatus, Balanus balanus	Common mussel/Blue mussel, Acorn barnacle, Northern ribbed barnacle
	2-10	Alcyonidium sp., Spirobranchus triqueter	"Seafarer" (from the Dutch "Zeevinger"), Keelworm
	4-10	Ostrea edulis	European flat oyster, Edible oyster, Common oyster
	0-25	Laminaria digitata, L. hyperborea, Saccharina latissima	Kelp
	0-28	Mytilus edulis, Bryozoa	Common mussel/Blue mussel, Bryozoa

Idealised descriptions of marine growth type, distribution and thickness are also available within the ISO and DNV guidelines. They are based on observations made on structures in several regions across the world and therefore include for a wider range of environmental conditions, and in some cases, longer periods for marine growth to establish. According to Section 2.4.11 of DNV-ST-0437 [19], marine growth for geographical coordinates between 56°N and 59°N in UK waters may be taken to have a terminal thickness of 100 mm from 2 m above MSL and down to 40 m below MSL. DNV-ST-0437 notes that somewhat higher values, up to 150 mm between mean sea level and LAT –10 m, may be seen in the Southern North Sea. In the absence of site-specific empirical data from inspection records of any existing adjacent offshore structures, and/or a mitigation strategy, we recommend consideration of the values recommended by DNV alongside the observed thicknesses from the FINO1 platform, described above.

DNV-ST-0437 suggests that the density of the marine growth may be set equal to 1,325 Kg/m³ unless more accurate data are available. In the absence of site-specific empirical data from inspection records of any existing adjacent offshore structures, and/or a mitigation strategy, we recommend use of this value.

6.2 Snow and Icing

Accumulation of ice on the surface of the structure should be considered, both with respect to added mass, and with respect to influence on load coefficients for wind and waves. Values to be applied for design are provided in Table 6-2, which is:

- For ice caused by sea-spray a reproduction of parts of Table A.3 of NORSOK N-003 [20] for geographical coordinates between 56 °N and 68 °N and application for Ultimate Limit State (ULS) with a 100-year return period, and thus conservatively applicable for the site.
- For ice caused by rain/snow, following Section 6.7.3 of NORSOK N-003 for sites south of 70 ° Northern latitude, and a return period of 100 years.

Table 6-2: Parameters for accumulated ice. The thickness and density-height-intervals for the ice created from sea spray should be linearly interpolated between heights.

Height ASL [m]	Ice caused by sea-spray		Ice caused by rain/snow	
	Thickness [mm]	Density [kg/m³]	Thickness [mm]	Density [kg/m³]
0 - 5	0 - 80	900	0	N/A
5 - 10	80	900	10	900
10 - 25	80 – 3	900		
25 - 60	3	900		
Above 60	0	N/A		

6.3   Sea Ice and Icebergs

No significant sea ice or icebergs are expected, as stated in Sections 6.8.2 and 6.9.2 of NORSOK N-003.

7 Climate Change

Here we examine the possible changes to the metocean climate at the site as a result of climate change. Specifically, we look at the following parameters:

- Mean Sea Level
- Water temperature
- Winds
- Waves
- Currents

Our assessment of climate change is based upon the projections provided in the Intergovernmental Panel on Climate Change (IPCC) Sixth Assessment Report (AR6) [21].

The IPCC Fifth Assessment Report projections use Representative Concentration Pathways (RCPs) to describe four different 21st century scenarios of Greenhouse gas emissions and atmospheric concentrations, air pollutant emissions and land use. The RCPs include a stringent mitigation scenario (RCP2.6), two intermediate scenarios (RCP4.5 and RCP6.0) and one scenario with very high greenhouse gas emissions (RCP8.5). RCP2.6 is representative of a scenario that aims to keep global warming less than 2°C above pre-industrial temperatures. Scenarios without additional efforts to constrain emissions ('baseline scenarios') lead to pathways ranging between RCP6.0 and RCP8.5. The IPCC Sixth Assessment Report projections use both RCPs and Shared Socioeconomic Pathways (SSPs). SSP-based scenarios are referred to as SSPx-y, where 'SSPx' refers to the Shared Socioeconomic Pathway describing the socioeconomic trends underlying the scenarios, and 'y' refers to the level of radiative forcing (in watts per square meter, or W m-2) resulting from the scenario in the year 2100. The SSPs are SSP1-1.9, SSP1-2.6, SSP2-4.5, SSP3-7.0 and SSP5-8.5.

Climate change projections, and therefore, the response of metocean parameters to changes in the climate, are associated with considerable uncertainty, and so the details provided herein should be treated with appropriate caution if they are to be applied to engineering design. Users of this information are advised to consult the relevant literature to supplement their understanding of any uncertainties, if important decisions are to be made based upon this assessment.

7.1 Mean Sea Level

Global mean sea level (GMSL) rise is caused by thermal expansion of seawater, and by the input of water to the ocean from the loss of land-based ice and water. Regional sea level and spatial changes can occur due to changes in land-based ice and water storage and the resulting impact on Earth's gravity field. Local changes in seawater density and ocean circulation also give rise to spatial differences.

The IPCC Sixth Assessment Report states with medium confidence that GMSL will rise between 0.40 m (likely range 0.26 to 0.56) (RCP2.6) and 0.81 m (likely range 0.58 to 1.07 m) (RCP8.5) by 2100, relative to 1995 to 2014.

Figure 7-1 shows likely global mean sea level change for SSP scenarios resulting from processes in whose projection there is medium confidence. Projections and likely ranges by 2150 are shown on the right. Lightly shaded ranges and thinner lightly shaded ranges on the right show the 17th–83rd and 5th–95th percentile ranges for projections including low confidence processes for SSP1-2.6 and SSP5-8.5 only, derived from structured expert judgement and marine ice-cliff instability projections. The black line shows historical GMSL change, and

thick solid and dash-dotted black lines show the mean and likely range extrapolating the 1993 to 2018 satellite altimeter trend and acceleration.
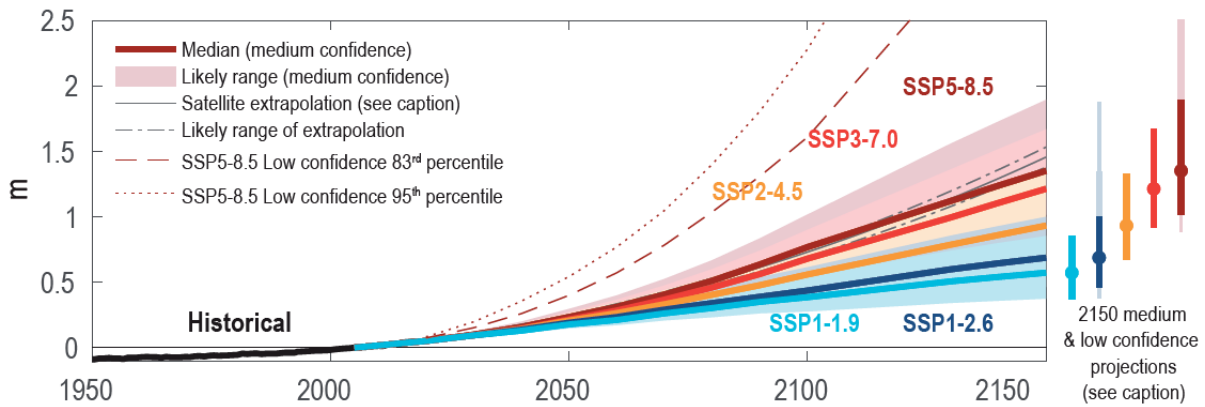
Figure 7-1: Global mean sea level rise under different SSP scenarios.

Around Europe, from 1900 to 2018, a new tide gauge-based reconstruction finds a regional mean relative sea level rise (RSLR) change of 1.08 mm/year (likely range 0.79 to 1.38 mm/year) in the subpolar North Atlantic [22], compared to a GMSL change of around 1.7 mm/year. For the period 1993 to 2018, the RSLR rates, based on satellite altimetry, increased to 2.17 mm/year (likely range 1.66 to 2.66 mm/year) [22], compared to a GMSL change of 3.25 mm/year. Regional mean RSLR projections for the oceans around Europe range from 0.4 to 0.5 m under SSP1-2.6 to 0.7 to 0.8 m under SSP5-8.5 for 2081 to 2100 relative to 1995 to 2014 (median values), which means there are locally large deviations from the projected GMSL change. These RSLR projections may, however, be underestimated due to potential partial representation of land subsidence in their assessment. The signal is strongest for the North Sea and Atlantic coasts.

7.2   Water Temperature

The IPCC Sixth Assessment Report assessed that it is very likely that global mean SST changed by 0.88 [0.68 to 1.01] °C from 1850–1900 to 2011–2020, and 0.60 [0.44 to 0.74] °C from 1980 to 2020. An assessment of the global mean SST modern history and modelled projections to 2100 from the IPCC Sixth Assessment Report is presented in Figure 7-2.
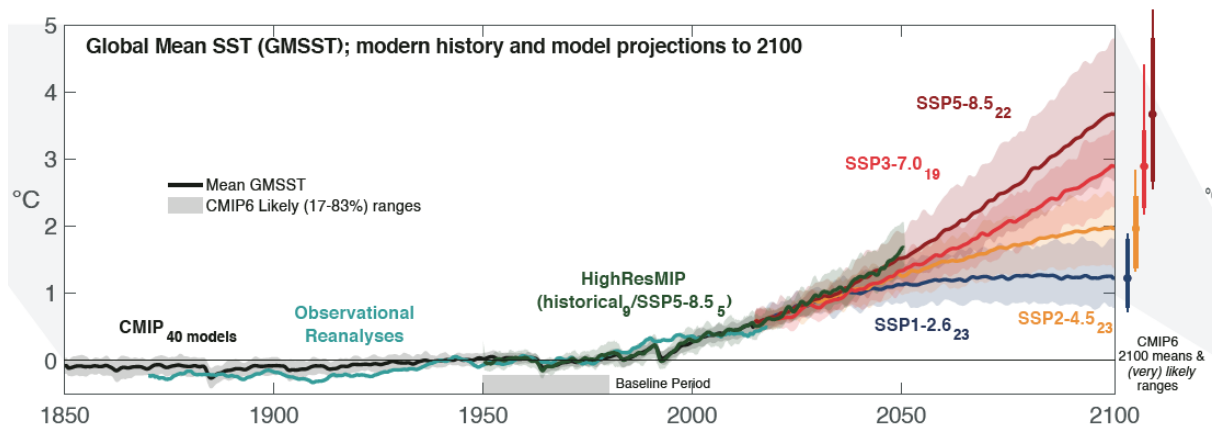
Figure 7-2: Time series of global mean SST anomaly relative to 1950–1980 climatology.

Regions vary in the rate of SST warming, with slight cooling in some regions. Based on this observation, for the SSP5-8.5 scenario over the period 2005-2100, the western Danish seaboard is predicted to warm at a rate of approximately 0.4 °C/decade to 2100, meaning that between the expected installation time and the intended decommissioning date, an SST increase of 1.2 °C can be expected under the SSP5-8.5 scenario.

Marine heatwaves (MHW) are periods of extreme high sea temperature relative to the long-term mean seasonal cycle. The mean SST of the Atlantic Ocean has increased between 0.25 °C and 1 °C since 1982–1998. This mean ocean surface warming is correlated to more frequent, larger magnitude and longer duration marine heatwaves in the region [23].

Over the period 1982 to 2016, the coastlines of Europe experienced on average more than 2.0 MHW/year. The average duration was between 10 and 15 days. Changes over the 20th century, derived from MHW proxies, show an increase in frequency of between 1.0 and 2.0 MHWs per decade in Europe (although the trend is not statistically significant), with an increase in intensity per event in the North Atlantic. Therefore, between the expected installation time and the intended decommissioning date, an increase in MHW frequency of around four to five extra MHWs per year is predicted.

7.3   Winds

Direct investigation of past changes in wind climatology has been hampered by the sparseness of long-term, high-quality wind measurements from terrestrial anemometers, arising from the influence of changes in instrumentation, station location, and surrounding land use.

Early marine observations of wind speed were based on ship speed through the water, sails carried, or on visual estimates of sea state converted to wind speed using the Beaufort scale. Anemometer measurements were introduced starting in the 1950s, with mean anemometer height increasing over time. Surface winds have been measured from space using various microwave range instruments since the late 1970s.

The lack of a single source of longer-term reliable measurements of winds, along with the high level of variability at different temporal scales, has meant that separating long-term climate trends in wind speed from background variability is difficult. This inhibits robust calibration and validation of climate models against suitable observed data. Therefore, climate projections for wind tend to focus on qualitative predictions of changes in the track of regional weather systems, and on predictions of the intensity and frequency of extreme weather events.

7.3.1   Mean wind speeds

Figure 7-3 shows average changes in mean wind speeds from a 31-member ensemble of Global Climate Models from the IPCC's Sixth Assessment Report for a future where 2 °C warming is realised, relative to a baseline period of 1850-1900. Black hatching indicates areas where there is low model agreement.

The images suggest increases in mean wind speeds of up to 0.9 % over the project site for winter, and decreases of approximately 2.3 % during the summer months, noting that model agreement is consistently poor over the project site.

The IPCC ascribes medium confidence in the projections of changes in winds discussed above.

7.3.2   Extreme winds

Extratropical storms can propagate to the study site, producing extreme wind events. The IPCC's Sixth Assessment Report assesses that it is likely that extratropical storm tracks have shifted poleward in both the Northern and Southern Hemispheres. In Europe, extreme near-surface winds have been decreasing in the past decades ([24] [25] [26]) according to near-surface observations.

Strong winds and extratropical storms are projected to have a slightly increasing frequency and amplitude in the future, in northern, western and central Europe ([27] [28] [29] [30] [31] [26]) under RCP8.5 by the end of the century (medium confidence). This is the case off the European coasts as well ([32]) due to the increase in intensity of extratropical storms at a 2 °C or above global warming scenario ([33]).
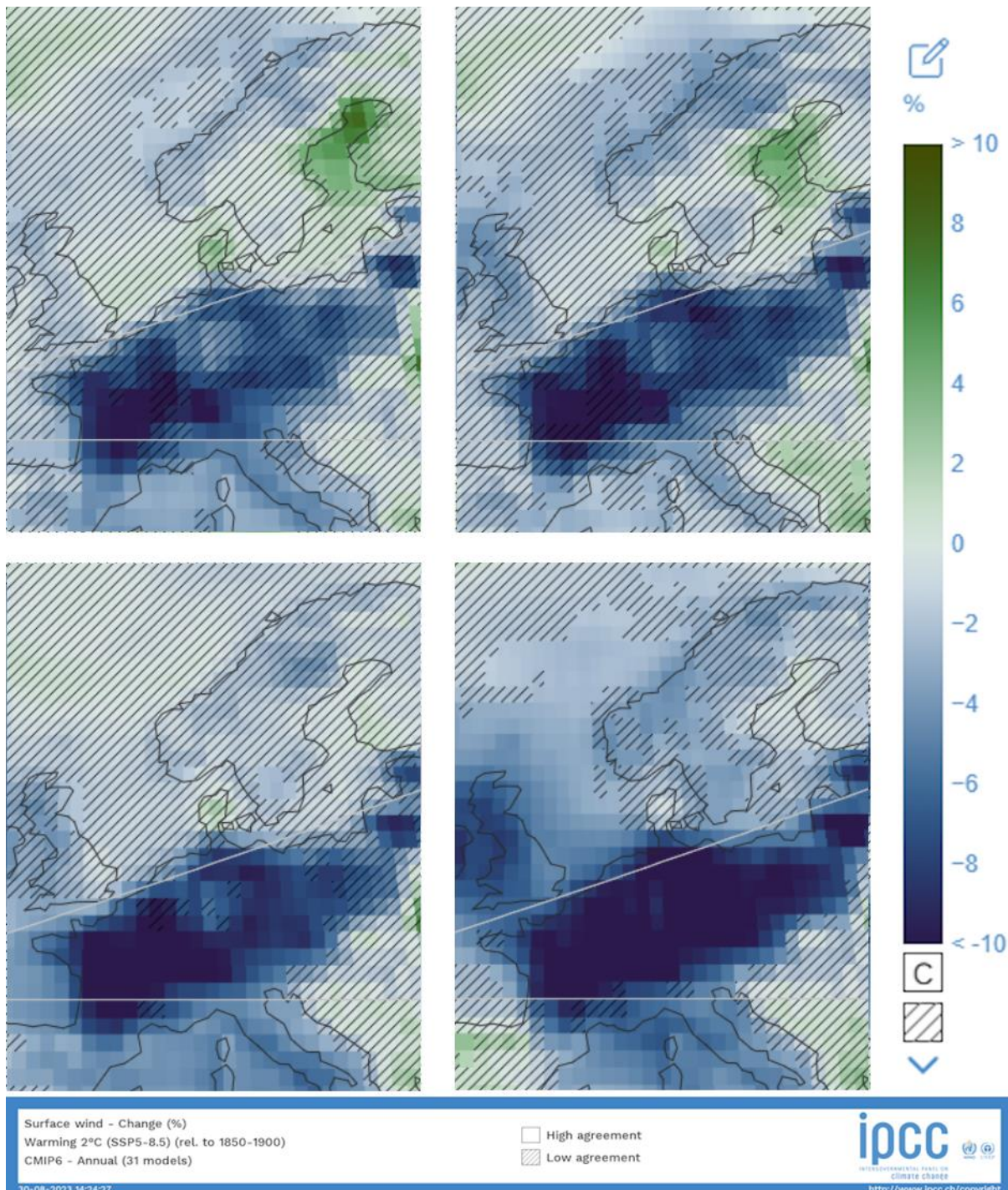
Figure 7-3: Modelled % changes in seasonal mean wind speeds. Clockwise from top left, December to February, March to May, June to August and September to November. Adapted from https://interactive-atlas.ipcc.ch/.

7.4 Waves

The Intergovernmental Panel on Climate Change (IPCC) Sixth Assessment Report does not generally provide analysis or predictions of changes in wave regimes, owing to similar challenges as those described for winds (Section 7.3). Nonetheless, since the wave regime is directly driven by wind processes, we can apply similar conclusions, i.e., medium confidence in a decrease in mean wave energy, and low confidence in any projected changes in extreme wave events. Due to the low confidence in the projections, we would recommend adopting an assumption of 'no change' for waves in the future.

7.5 Surge and Extreme Total Water Levels

The present-day 1-in-100-year extreme total water level (ETWL) is between 2.5 and 5 m along North Sea coasts ([34]). There is high confidence that ETWL magnitude and occurrence frequency will increase throughout Europe.

Across the region, by 2050, the 5–95th percentile range of the 1-in-100-year ETWL is projected to increase (relative to 1980 to 2014) ([35] [34]):

- By 4 to 40 cm under RCP4.5, and
- By 6 to 47 cm under RCP8.5

Furthermore, under RCP4.5, the present day 1-in-100-year ETWL is mostly projected to have median return periods of between1-in-20-years and 1-in-50-years by 2050 ([35]).

7.6 Currents

Marine currents at the project site are primarily driven by tides. A relatively smaller contribution is made (in either the positive or negative direction) by non-tidal effects, e.g., surges.

Since climate change is not predicted to affect tidal processes, we can conclude here that marine currents are unlikely to substantially change as a direct result of climate change.

References

[1]   C2Wind, "Lot 3 (North Sea I) – Wind Assessment, 23072-04-06, Rev.2," 3 September 2024.

[2]   P. S. Tromans and L. Vanderschuren, "Response based design conditions in the North Sea: application of a new method," *Proc. 27th Offshore Technology Conference, OTC 7683,* 1995.

[3]   G. Forristall, "On the statistical distribution of wave heights in a storm," *J. Geophys. Res. ,* no. 83, pp. 2353- 2358, 1978.

[4]   IEC (International Electrotechnical Commission), "IEC 61400-3-1: Wind energy generation systems – Part 3-1: Design requirements for fixed offshore wind turbines," IEC, 2019.

[5]   N. D. P. Barltrop and A. J. Adams, Dynamics of Fixed Marine Structures, Butterworth Heinemann.

[6]   Y. Wu, D. Randell, M. Christou, K. Ewans and P. Jonathan, "On the distribution of wave height in shallow water," *Coastal Engineering,* vol. 111, pp. 39-49, 2016.

[7]   I. Karmpadakis, C. Swan and M. Christou, "Assessment of wave height distributions using an extensive field database," *Coastal Engineering,* vol. 157, 2020.

[8]   DNV, "DNV-ST-0437. Standard - Loads and conditions for wind turbines.," DNV, Edition 2016-11 - Amended 2021-11.

[9]   DNV, "DNV-RP-C205. Recommended Practice – Environmental conditions and environmental loads.," DNV, Edition 2019-09 - Amended 2021-09.

[10] ISO, "ISO 19901-1:2015 Petroleum and natural gas industries – Specific requirements for offshore structures – Part 1: Metocean design and operating considerations. Second Edition.," ISO, 2015.

[11] S. Haver and K. A. Nyhus, "A Wave Climate Description for Long Term Response Calculations," *OMAE,* 1986.

[12] R. Haring, A. Osborne and L. Spencer, "Extreme Wave Parameters Based on Continental Shelf Storm Wave Records," *Coastal Engineering,* pp. 151-170, 1976.

[13] ISO, "ISO-19902: Petroleum and natural gas industries — Fixed steel offshore structures," ISO, 2020-11.

[14] D. Codiga, "UTide Unified Tidal Analysis and Prediction Functions (https://www.mathworks.com/matlabcentral/fileexchange/46523-utide-unified-tidal-analysis-and-prediction-functions)," *MATLAB Central File Exchange,* Retrieved July 9, 2020.

[15] P. A. Vinagre, T. Simas, E. Cruz, E. Pinori and J. Svenson, "Marine Biofouling: A European Database for the Marine Renewable Energy Sector.," *Journal of Marine Science and Engineering,* p. 495, 2020.

[16] BioConsult and Vattenfall, "Benthic communities at Horns Rev before, during and after construction of Horns Rev Offshore Wind farm: Final Report," Vattenfall, 2006.

[17] R. Krone, L. Gutow, T. Joschko and A. Schröder, "Epifauna dynamics at an offshore foundation –
Implications of future wind power farming in the North Sea," *Marine Environmental Research,* vol. 85,
pp. 1-12, 2013.

[18] T. A., "Marine growth and the hydrodynamic loading of offshore structures. PhD Thesis," University of
Strathclyde, Glasgow, UK, 1988.

[19] DNV, "DNV-ST-0437. Standard - Loads and conditions for wind turbines.," DNVGL, Edition 2016-11 -
Amended 2021-11.

[20] NORSOK, "NORSOK STANDARD N-003: Actions and action effects. Edition 3. Standards Norway,"
including Corrigendum NORSOK N-003:2017/AC2018., 2017-01-20.

[21] T. Stocker, D. Qin, G.-K. Plattner, M. Tignor, S. Allen, J. Boschung, A. Nauels, Y. Xia, V. Bex and P. Midgley,
"Climate Change 2013: The Physical Science Basis. Contribution of Working Group I to the Fifth
Assessment Report of the Intergovernmental Panel on Climate Change," Intergovernmental Panel on
Climate Change, Cambridge, United Kingdom and New York, NY, USA, 2013.

[22] Frederikse, T. et al, "Antarctic Ice Sheet and emission scenario controls on 21st-century extreme sea-
level changes," *Nature Communications,* vol. 1, no. 11, p. 390, 2020.

[23] Oliver, E.C.J. et al., "Longer and more frequent marine heatwaves over the past century," *Nature
Communications,* vol. 9, no. 1, p. 1324, 2018.

[24] A. Smits, A. Klein Tank and G. Können, "Trends in storminess over the Netherlands, 1962-2002,"
International Journal of Climatology, vol. 10, no. 25, pp. 1331-1344, 2005.

[25] Q. Tian, G. Huang, K. Hu and D. Niyogi, "Observed and global climate model based changes in wind
power potential over the Northern Hemisphere during 1979–2016," *Energy,* no. 167, p. 1224–1235,
2019.

[26] Vautard, R. et al., "Human influence on European winter wind storms such as those of January 2018,"
Earth System Dynamics, vol. 2, no. 10, pp. 271-286, 2019.

[27] S. Outten and I. Esau, "Extreme winds over Europe in the ENSEMBLES regional climate models,"
Atmospheric Chemistry and Physics, vol. 10, no. 13, pp. 5163-5172, 2013.

[28] Feser, F. et al., "Storminess over the North Atlantic and northwestern Europe - A review," *Quarterly
Journal of the Royal Meteorological Society,* vol. 687, no. 141, pp. 350-382, 2015.

[29] Forzieri, G. et al., "Multi-hazard assessment in Europe under climate change," *Climatic Change,* Vols. 1-2,
no. 137, pp. 105-119, 2016.

[30] T. Mölter, D. Schindler, A. Albrecht and U. Kohnle, "Review on the Projections of Future Storminess over
the North Atlantic European Region," *Atmosphere,* vol. 4, no. 7, p. 60, 2016.

[31] K. Ruosteenoja, T. Vihma and A. Venäläinen, "Projected Changes in European and North Atlantic
Seasonal Wind Climate Derived from CMIP5 Simulations," *Journal of Climate,* vol. 19, no. 32, pp. 6467-
6490, 2019.

[32] Martínez-Alvarado, O. et al., "Increased wind risk from sting-jet windstorms with climate change," *Environmental Research Letters,* vol. 4, no. 13, 2018.

[33] G. Zappa, L. Shaffrey, K. Hodges, P. Sansom and D. Stephenson, "A Multimodel Assessment of Future Projections of North Atlantic and European Extratropical Cyclones in the CMIP5 Climate Models," *Journal of Climate,* vol. 16, no. 26, pp. 5846-5862, 2013.

[34] Kirezci, E. et al., "Projections of global-scale extreme sea levels and resulting episodic coastal flooding over the 21st Century," *Scientific Reports,* vol. 1, no. 10, p. 11629, 2020.

[35] Vousdoukas, M.I. et al., "Global probabilistic projections of extreme sea levels show intensification of coastal flood hazard," *Nature Communications,* vol. 1, no. 9, p. 2360, 2018.

[36] DNV, "DNV-RP-C205. Recommended Practice – Environmental conditions and environmental loads.," DNV, Edition 2019-09 - Amended 2021-09.

Appendix A. Extreme Value Maps Methodology

A.1 Introduction

This Appendix outlines the methods used to calculate the extreme value wave maps shown in Section 3. Whilst the principles follow those that we would normally use to determine extreme values for design criteria at a single location, the need to process thousands of grid points means that it is not feasible for all fits to be assessed by an analyst. Instead, the assessment is automated. Whilst this approach allows extreme values to be estimated across the entire region of interest, less scrutiny is applied to each location than is necessary for detailed design criteria. As such, the maps should be used for general guidance only. Furthermore, parameters have been optimised based on locations within the lease area, and as such a little more caution should be applied to values further from this region.

In order to describe the process of creating the extreme value maps, this Appendix proceeds as follows:

- In Section A.2, the standard steps we would use for estimation of extreme values of a single parameter, such as significant wave height (Hm0), current speed or positive/negative surge, at a *single* location with *manual* review are summarized.
- In Section A.3, the modifications included to *automate* the process are discussed.
- In Section A.4, additional steps used in creating maximum wave and crest heights (Hmax and Cmax) are described.

A.2 General Approach, Single Location

Here we briefly outline those steps which we would generally carry out in determining extreme values of Hm0, current speed and positive/negative surge for each *individual* location considered in a set of design criteria. Please see Section 5.1 for more detail, including a worked example.

Step 1: Data Preparation and Review

Carry out of a detailed review of the model data, including calibrations against measurements.

Step 2: Method Selection

Decide whether to extrapolate from Peaks over Threshold (PoT), block maxima, or all data. Preference is given to PoT should there be sufficient data. Investigate any potential concerns with an all-year, omni-directional approach, e.g. larger waves arriving from very different directions, with potentially different extreme distributions or different driving mechanisms.

Note: For this study, a PoT approach has been used throughout, thus only relevant steps are included hereafter.

Step 3: Find Peaks over Threshold

a) Split data into points above and below a user specified *Threshold*.
b) Discard all points below, creating a new time-series of only values above the *Threshold*.
c) Place the first point in "Cluster 1". If the second point is temporally within a user specified *Reset Duration* of the first, it too is in Cluster 1. Otherwise, Cluster 1 is complete and this becomes the first point in Cluster 2.
d) Proceed to the third point. If it is within *Reset Duration* of the second, it is in the same cluster. Otherwise, it is the start of a new cluster.
e) Continue through the entire time-series until all data above the *Threshold* are assigned to a cluster.

f) Take the maximum of each cluster.

Review time series of original data and selected cluster peaks. In particular, check high data peaks close to one another since their inclusion/exclusion may significantly affect extreme values. Adjust clustering parameters as necessary, and if highly subjective decisions affect inclusion/exclusion of high peaks, continue separate analysis on each option to review implications.

Step 4: Fit Distributions to Highest Peaks

Carry out independent fits to highest 50, 60, 70, …, 100 ,125, 150, …, 250 cluster peaks. For each, include the following fits:

- 3-Parameter Weibull (Maximum Likelihood (MLM), Method of Moments (MoM), Maximum Product of Spacings (MPS), L-Moments (Lmom)).
- Generalized Pareto (MLM, MoM, MPS, Lmom)
- Exponential (MLM, MoM, Lmom)

Step 5: Review Fits

Review each fit, including the following:

- If the fitted distribution is a bad fit to the data, discard.
- If the extreme values are not stable to changes in the number of peaks, discard (e.g. if results for a 60 peak fit are considerably different to for a 50 and 70 peak fits).

Step 6: Decide on Extreme Values

Of the remaining fits, a representative fit is selected. This is generally a fit whose 100-year extreme value is slightly conservative and is within the 50th – 70th percentile of estimates of all remaining fits. However, some subjectivity is included to take into account the level of conservatism considered appropriate.

A.3   Automated Fit Assessment

The steps outlined in the previous section allow for subjective input from an analyst throughout - in determining storm thresholds; in deciding which fits are and are not representative of extremal behaviour; in determining the appropriate percentile for the final prediction. For design criteria at a small selection of locations, these decisions can be made by the analyst manually reviewing a number of diagnostics. For the generation of maps, more automated steps are necessary, and are described in the subsections which follow.

A.3.1   Storm Peaks

Based on previous experience of extreme value analysis of wave heights in European waters, and corroborated by review of time-series data at a selection of sites across the region, for each grid point, the storm threshold for Hm0 was set to be 45% of the maximum significant wave height at the location. A minimum reset duration of three days was required between storms. The same reset duration was used for hydrodynamic parameters, though with the threshold set to a value that gives approximately 300 peaks for each location.

A.3.2   Distribution Fitting

Fits were carried out to the highest 50 storm peaks, then 60 peaks, increasing in steps of 10 peaks to a maximum of 250. For each collection, the following fits were used:

- Exponential distribution (maximum likelihood, method of moments, L-moments)

- 3-Parameter Weibull distribution (maximum likelihood, method of moments, L-moments, maximum product of spacings)
- Generalized pareto distribution (maximum likelihood, method of moments, L-moments, maximum product of spacings)

A.3.3   Fit Assessment

To outline the process used to assess each collection of fits, let us first consider fits to the highest 100 Hm0 peaks at a single example location[2], shown in Figure A.1.
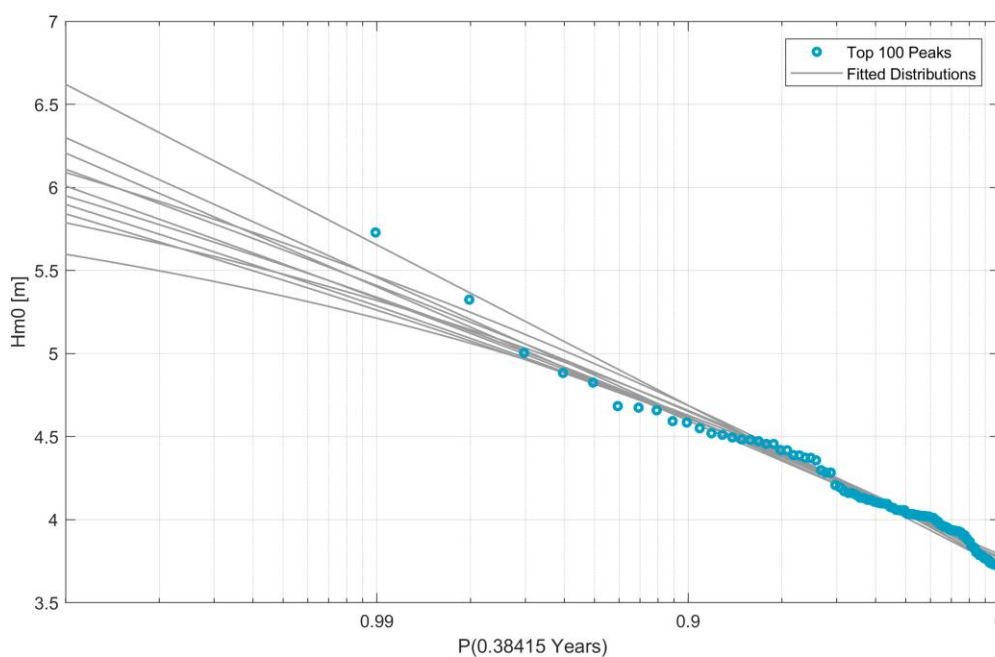
Figure A.1: Example fits, 100 peaks.

Firstly, bounds are placed around each data point independently to allow for a certain percentage of error in the value predicted by the fit. For this example, we use the range from a 3% underprediction to a 5% overprediction, though more detail on the values used in creating the final maps can be found in Section A.3.5. The resulting ranges are shown in Figure A.2. Here, and for all ranges considered, slightly more margin is allowed towards overprediction for the sake of conservatism.

---

[2] The location is not specific to this project, simply a useful example to illustrate the overall methodology.
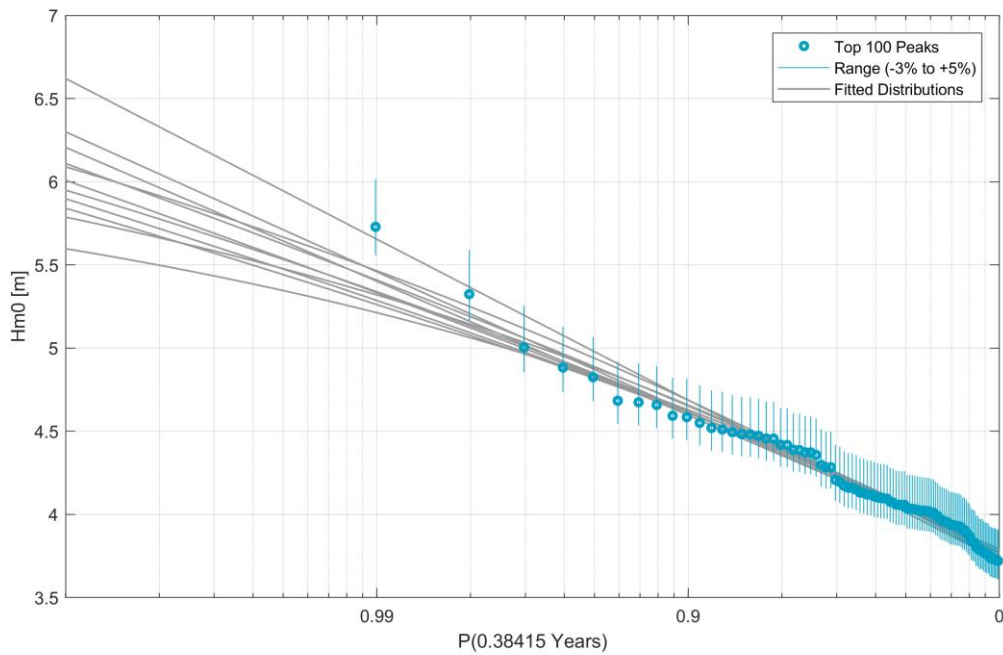
Figure A.2: Example fits, with over/underprediction ranges, 100 peaks.

Next, for each fit, we determine if it passes through this range for *all* data points, all data points *except* one, all data points *except* two, etc. In our example, we will consider a fit "reasonable" if it misses at most one range, under which criterion all reasonable fits are highlighted in green in Figure A.3.
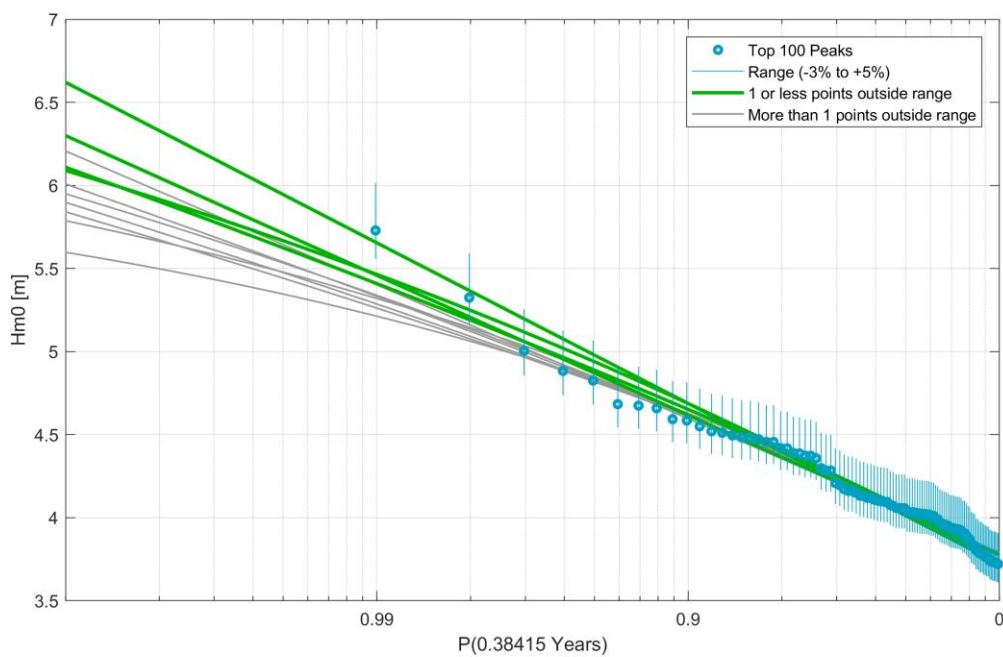
Figure A.3: Example fits, with automated assessment, 100 peaks.

This process is subsequently repeated across *all* collections of peaks, i.e. 50 peaks, 60 peaks, …, 240 peaks, 250 peaks. The result is a larger collection of selected fits, as shown for our example location in Figure A.4.
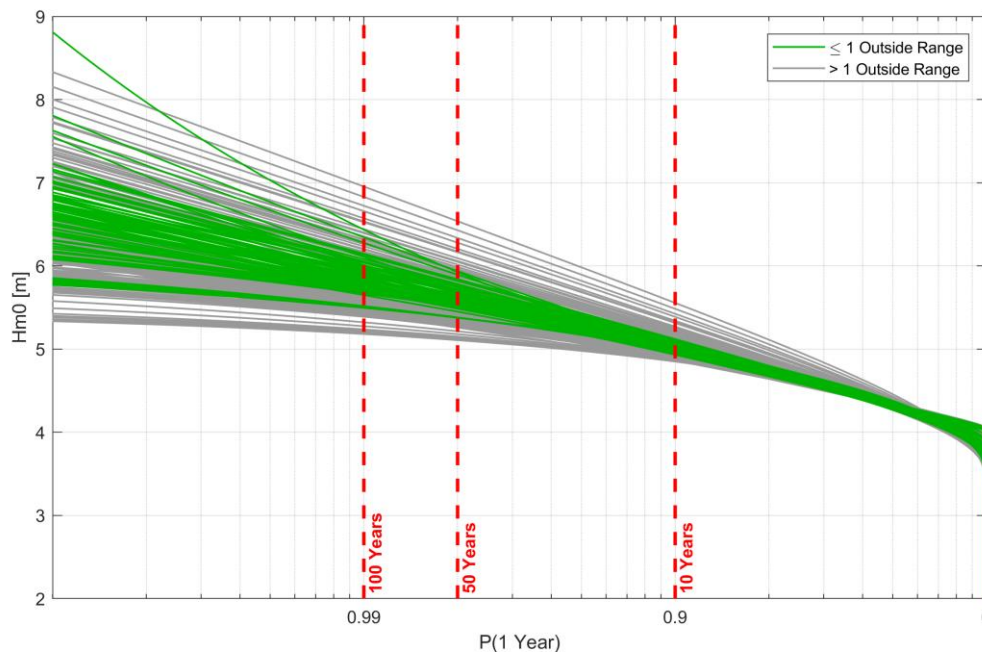
Figure A.4: Example fits, with automated assessment, all peak collections.

A.3.4   Extreme Value Selection

The collection of selected fits leads to a range of potential extreme values, as shown for this example in Figure A.5. From this range, the final extreme value shown in the maps is taken to be the 70th percentile of extreme values for all selected fits, with the percentile determined by comparisons between automated and more detailed manual analyses. Note that if less than 20 fits (of over 230 considered) are considered reasonable for a given location, no extreme value is given: the map will have missing data at these locations.
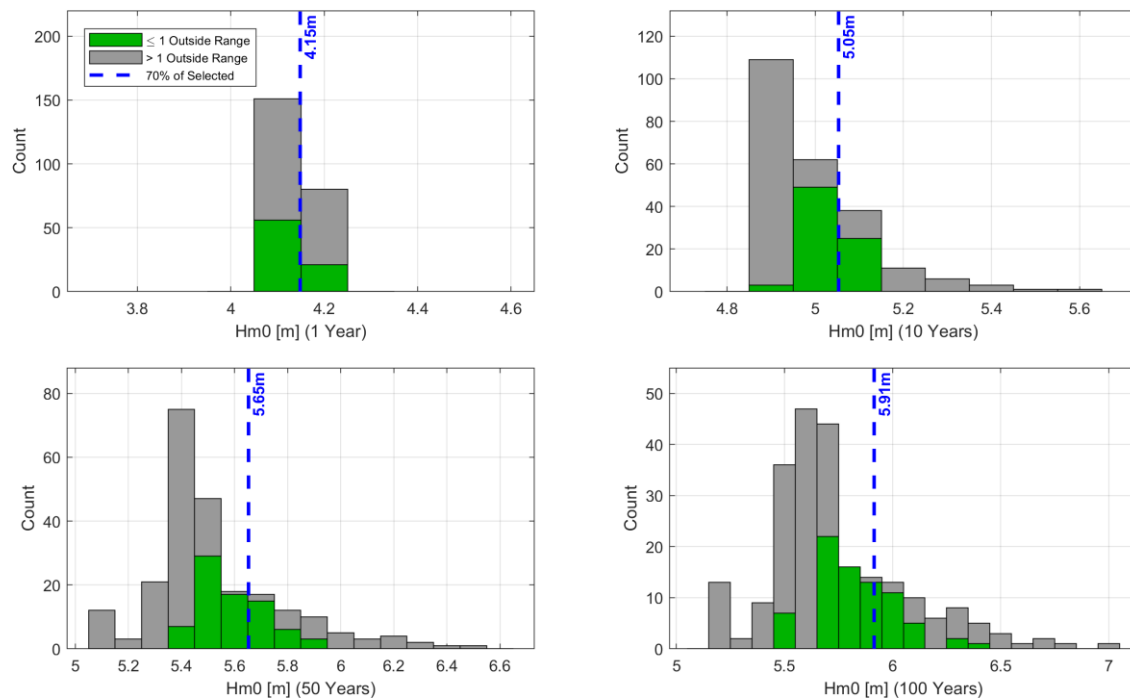
Figure A.5: Example extreme values, with automated assessment.

A.3.5 Parameter Settings

Through the previous examples, fits have been considered representative if based on:

- A prediction range between -3% and +5% for each data value.
- Falling outside this range for *at most* one data value.

Various alternate options are also considered, comprising each combination of:

- Prediction ranges: -3% to 5%; -5% to 7.5%; -7.5% to 10%.; -10% to 10%.
- 0, 1, 2 or 3 data points falling outside the prediction range.

Fits are reviewed at a selection of locations under each option, with maps as a whole also compared. The final set of parameters selected after this review for all wave and hydrodynamic parameters were:

- A prediction range between -7.5% to +10% for each data value.
- No values falling outside this range, *except* for positive and negative surge where at most one data value is allowed outside this range.

A.4   Hmax and Cmax

A.4.1   Methodology, Single Location

In line with ISO guidelines, all maximum wave height (Hmax) and maximum crest height extreme values are calculated using the method of Tromans and Vanderschuren [2]. Again, we begin by considering those steps which we would take for determining design criteria for a *single* location (see Section 5.2 for more details) which proceed as follows:

Step 1: Data Preparation and Review

Carry out of a detailed review of the model data, including calibrations against measurements.

Step 2: Method Selection

Preference is to use the storm-based approach of Tromans and Vanderschuren (TVM). For shorter datasets, all data (or higher sea-state) convolutions of Hm0 and short-term wave height/crest distributions are also considered.

Also, we need to select appropriate short-term wave height and crest height distributions. In deep water, we use Forristall deep water distribution for wave height and Forristall 3D distribution for crest height [3]. In shallow water, a number of alternatives are considered.

Note: For this study a TVM approach is used throughout, thus only relevant steps are included hereafter.

Step 3: Identify Storms

Split data into storms above a specified threshold. Merge storms that are temporally within a configurable reset duration.

Review time series of original data and storms. In particular, review larger storm peaks which may or may not have been merged into the same storm. Adjust parameters as necessary, and if highly subjective decisions affect merging of high peaks, continue separate analysis on each option to review implications.

Step 4: Calculate Hmp and Cmp for each storm

For each storm combine Hm0 with Tm01 or Tm02 values with the short-term distribution selected to determine the most probable extreme wave height (Hmp) or crest (Cmp) for the storm.

Step 5: Fit Distributions to Hmp/Cmp

Carry out independent fits to highest 50, 60, 70, …, 190, 200 Hmp/Cmp values. For each, include the following fits:

- 3-Parameter Weibull (Maximum Likelihood (MLM), Method of Moments (MoM), Maximum Product of Spacings (MPS), L-Moments (Lmom)).
- Generalized Pareto (MLM, MoM, MPS, Lmom)
- Exponential (MLM, MoM, Lmom)

Step 6: Convolution

For each fitted distribution, carry out a final convolution between the fitted distribution and that of individual heights/crests in a single storm given Hmp/Cmp. The individual heights/crests in a storm are those given by Tromans and Vanderschuren, with N taken to be the mean number of waves per storm.

Step 7: Review Fits

Review each fit, including the following:

- If the fitted distribution is a bad fit to the data, discard.
- If the extreme values are not stable to changes in the number of peaks, discard (e.g. if results for a 60-peak fit are considerably different to for a 50- and 70-point fit).
- Consider if physical implications of extreme behaviour are realistic, e.g. unbounded fits in shallow water, fits that rapidly reach an upper bound (i.e. similar 100- and 10,000-year extremes) in deep water with long fetch. If not, discard.

Step 8: Determine Extreme Values

The previous step normally gives a large selection of options. If all cover a similar range of extreme values, then choose a representative fit, generally slightly conservative in the 50th – 70th percentile of estimates. If they do not (e.g. the three different distributions may suggest three different ranges) decision can be far more subjective, often needing more investigation, discussion with client, precedence in the region, etc. before a final decision.

A.4.2 Automated Fitting

Though more complex than the steps used for Hm0 outlined previously, very similar adjustments are needed to again automate the process when fitting at all locations across the model domain. In particular:

- In STEP 3, as was the case with derivations of Hm0, a value of 0.45 times the maximum Hmp value is used as a storm threshold.
- In STEP 7 all fits are assessed using the same steps described in Section A.3.2.
- In STEP 8 extreme values are again taken as the 70th percentile of all predictions considered appropriate.

Unfortunately, though not restrictive for a single dataset, the computational time for the convolution of STEP 6 becomes somewhat time-consuming when applied to upwards of 50 applicable fits at each of the many thousand data points. As such, the decision of STEP 8 is actually taken earlier – a single distribution is selected after STEP 5 whose 50- and 100- year extreme values are closest to the 70th percentile of all selected distributions. The convolution is then carried out only once per location, rather than on all selected fits. This reduces run-time from a number of days per map to a few hours. We do not expect a significant impact, except perhaps at the 1-year level, where more variation may be seen.

Appendix B. Weibull Transformation

B.1 Introduction

As outlined in Section 5.5, wind speeds at hub height are determined by applying a transformation to ERA5 hindcast to ensure that it matches the required Weibull distribution specified in [1]. This Appendix provides a little more detail on the transformation, with the mathematical basis given in Section B.2 and details of its application for location A3W included in Section B.3 for illustrative purposes.

B.2 Transformation

The foundation for the transformation used is the "Probability Integral Transform" which states that, for a random variable, X, with a continuous distribution whose cumulative distribution function (CDF) is denoted F(X), the random variable, Y, defined by:

$$Y = F(X)$$

has a *standard uniform distribution*[3]. In our case, if we assume that the ERA5 data follows a two-parameter Weibull distribution with shape parameter $A_{hindcast}$ and scale parameter $k_{hindcast}$, its own CDF is given by:

$$F_{hindcast}(x) = 1 - e^{-\left(\frac{x}{A_{hindcast}}\right)^{k_{hindcast}}}$$

Similarly, the CDF for the *adjusted* data, with scale parameter $A_{adjusted}$ and shape parameter $k_{adjusted}$ is given by:

$$F_{adjusted}(x) = 1 - e^{-\left(\frac{x}{A_{adjusted}}\right)^{k_{adjusted}}}$$

If we then apply the probability integral transform, we see that the distributions of both:

$$U_{hindcast} = 1 - e^{-\left(\frac{WS_{hindcast}(t)}{A_{hindcast}}\right)^{k_{hindcast}}} \tag{1}$$

and:

$$U_{adjusted} = 1 - e^{-\left(\frac{WS_{adjusted}(t)}{A_{adjusted}}\right)^{k_{adjusted}}} \tag{2}$$

are standard uniform distributions, i.e. they are the same distribution. Thus, to transform from one distribution to the other, we set $U_{hindcast} = U_{adjusted}$ and solve for $WS_{adjusted}$, which after a little rearrangement gives:

$$WS_{adjusted}(t) = A_{adjusted} \cdot \left(\frac{WS_{hindcast}(t)}{A_{hindcast}}\right)^{\frac{k_{hindcast}}{k_{adjusted}}}$$

It is also perhaps worth noting that although the aim of the above is a change in *distribution*, the transformations have the important property that the *order* of data does not change. That is, if $WS_{hindcast}(t_1) < WS_{hindcast}(t_2)$ then $WS_{adjusted}(t_1) < WS_{adjusted}(t_2)$ for any pair of timestamps t_1 and t_2. Thus, as we shall see for our example location shortly, the transformation serves to change the distribution as a whole, whilst maintaining relationships between parameters for individual timestamps.

---

[3] The standard uniform distribution is a distribution where there is an equal probability of any value in the interval [0, 1] and zero probability for values outside this range. In this derivation, though, its precise form is less important than noting that under this transformation, both the hindcast and the adjusted data transform to the *same* continuous distribution.

B.3   Application at A3W

As specified in [1], the Weibull distribution of the representative hub height wind speed has parameters:

$A_{adjusted}$ = 11.94 m/s

$k_{adjusted}$ = 2.26

These parameters represent the target towards which the hub height wind data at the counterpart wave analysis location (Table 5-2) is adjusted.

A Method-of-Moments[4] fit to the MetOceanWorks calibrated ERA5 data at 150 mMSL gives hindcast parameters:

$A_{hindcast}$ = 11.93 m/s

$k_{hindcast}$ = 2.27

These distributions are compared in Figure B-1. As can be seen, the distributions of the MetOceanWorks calibrated ERA5 data and the representative wind conditions are reassuringly close though not identical. The impact of the subsequent Weibull transformation is illustrated in Figure B-2, wherein it can be seen that the changes are minor in scale, being limited to less than 1% over the majority of the range.
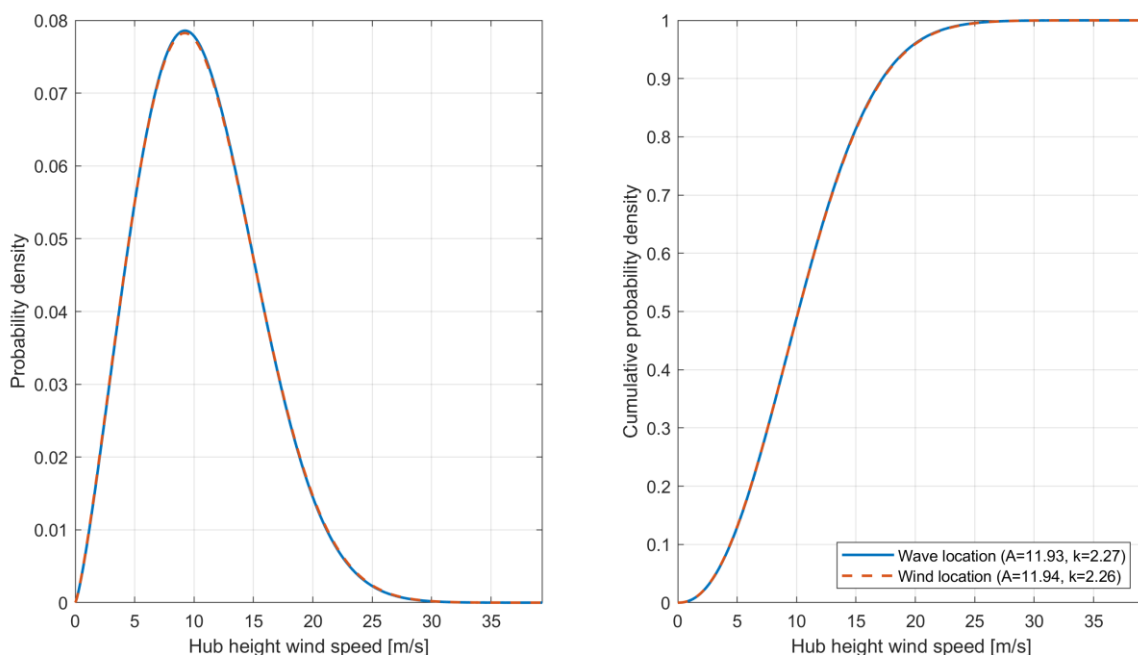

Figure B-1: Wind speed Weibull distributions for location A3W and the A3 representative wind location (P3, see [1]).

---

[4] Four fitting algorithms were used to fit Weibull distributions to hub height wind speeds: L-Moments, Method-of-Moments, Maximum Likelihood and Maximum Product of Spacings. All gave virtually identical fitting parameters.
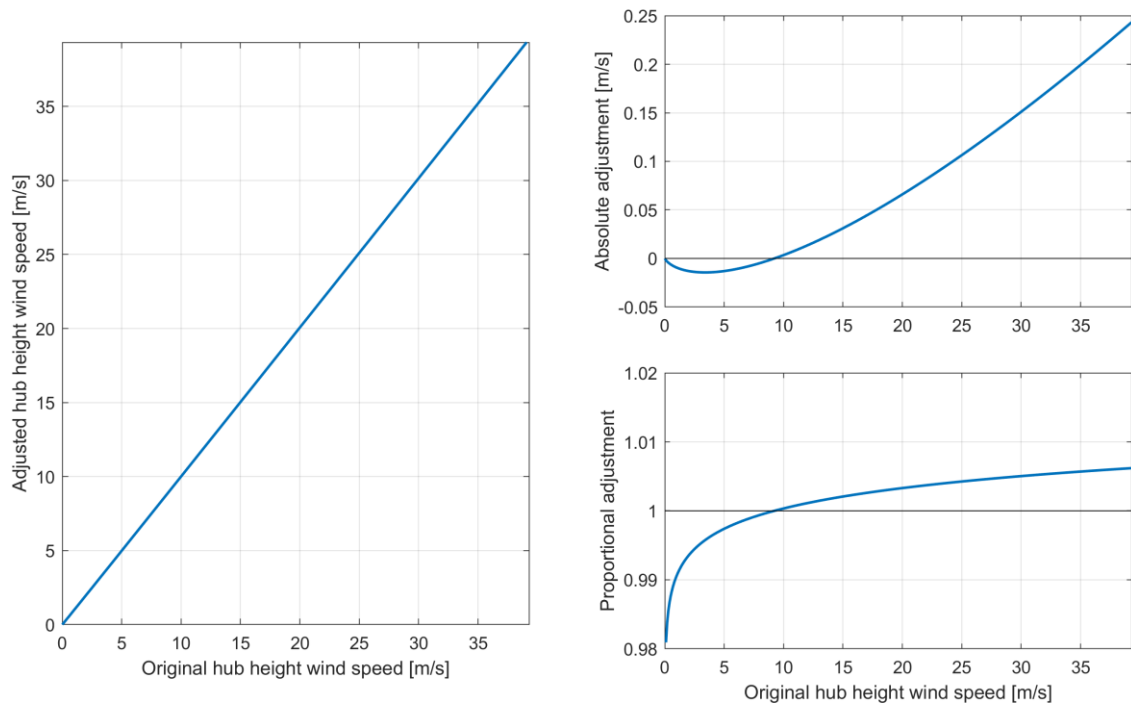
Figure B-2: Weibull adjustment of hub height wind speeds at location A3W.

Appendix C. Normal Sea States

C.1 Introduction

This Appendix provides further details on the derivation of Normal Sea State (NSS) criteria as follows:

- In Section C.2, the data sources used in deriving the NSS are outlined.
- In Section C.3, derivation of significant wave height (Hm0) for each hub height wind speed and direction bin is considered.
- In Section C.4, derivation of wave periods associated with each Hm0 is discussed.

Throughout, a worked example is provided for the A3W location using a hub height of 150 m.

C.2 Data Sources

Full details on the data sources used for this analysis, as well as validations against modelled datasets in the region can be found in the Metocean Data Overview. By way of summary:

- Wave parameters originate from a bespoke SWAN model, to produce a 45-year wave hindcast between 1979 and 2023, inclusive.
- Modelled wind data originate from ECMWF ERA5 and were subjected to bespoke adjustment by MetOceanWorks at the hub height elevation of 150 m as well as the Weibull transformations described in Appendix B.

C.3 Hm0

Significant wave height (Hm0) statistics for NSS are determined as follows:

a) Data are binned according to wind speed and direction at hub height. Wind speed bins are 2 m/s in width[5]; wind direction bins are 22.5° in width, with the first centred on 0° N.

For each combination of hub height wind speed bin and hub height wind direction bin, independently:

b) All Hm0 values are found at timestamps where wind speed and direction fall within the appropriate bin ranges.

c) The 2nd power mean of these Hm0 values is calculated and included in the NSS criteria for the appropriate wind speed and direction ranges. This 2nd power mean, $\langle H_{m0} \rangle_{(2)}$, is given by:

$$\langle H_{m0} \rangle_{(2)} = \left[\frac{1}{N} \sum_{n=1}^{N} \left(H_{m0,n} \right)^2 \right]^{1/2}$$

Where $H_{m0,n}$ is the significant wave height at timestamp n, and the sum is taken over all N timestamps for the wind speed and direction bin under consideration.

Omni-directional NSS Hm0 values are taken to be the *maximum* Hm0 for each wind speed bin, taken across all directional sectors.

The results of applying these steps for the A3W location are shown in Figure C.1.

---

[5] Note that statistics enumerated across both 1 m/s and 2 m/s wide wind speed bins are made available in the accompanying spreadsheets.
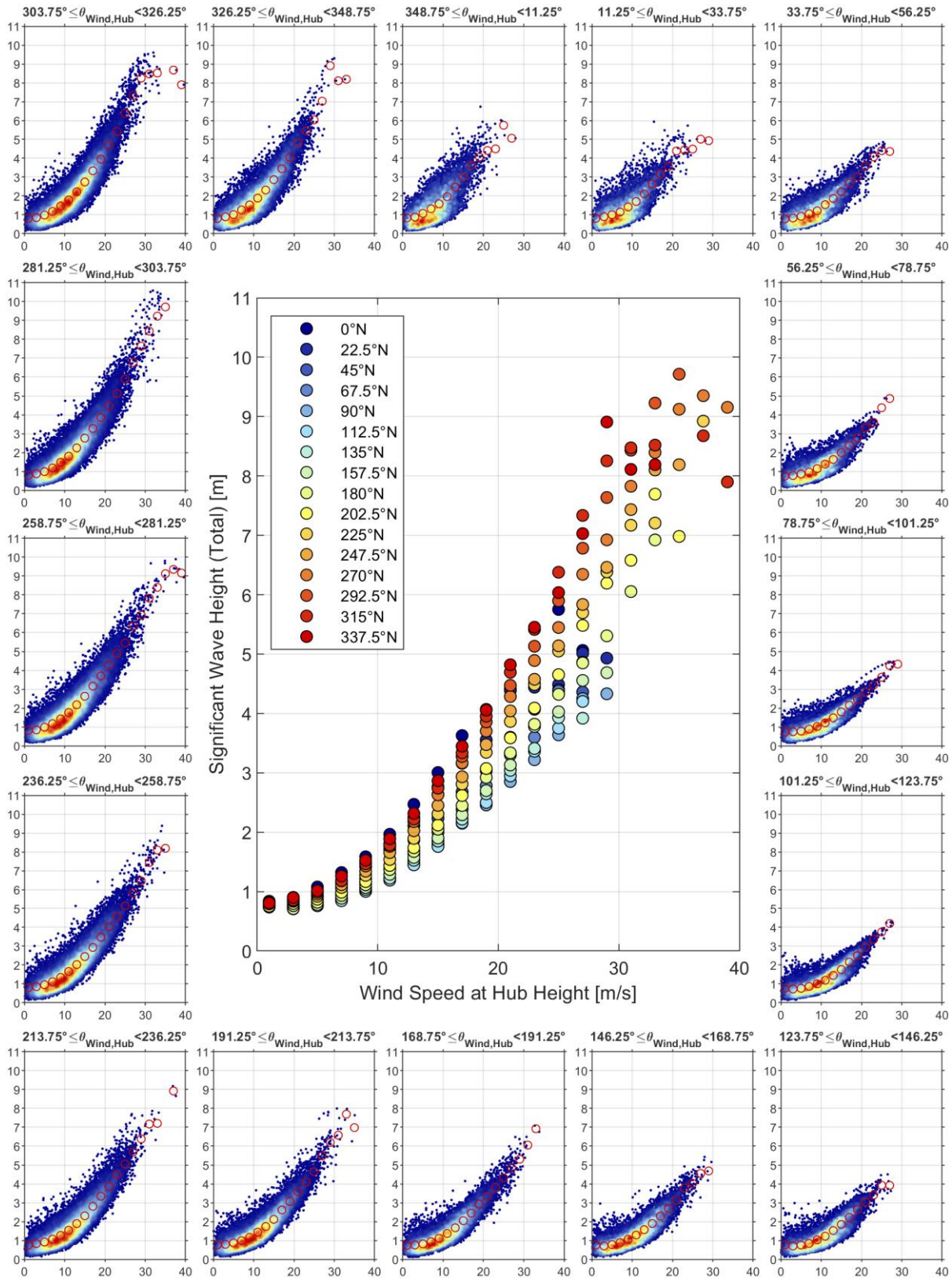
Figure C.1. Hm0 NSS statistics, A3W.

Use of the 2nd power mean is worth review here: it produces Hm0 corresponding to the mean energy spectrum rather than the mean of Hm0 itself. In practise, the resulting difference between the 2nd power mean and the mean of Hm0 itself is generally small, as shown for the A3W location in Figure C.2. As the 2nd power mean is the more conservative of the two, it has been adopted in the NSS statistics.
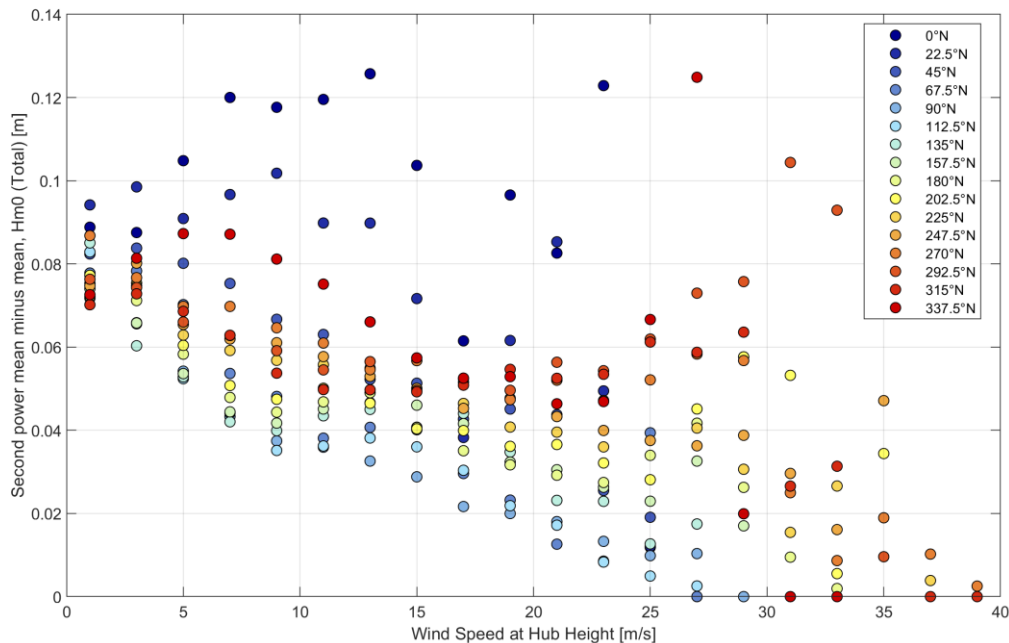

Figure C.2. Differences between second power mean and mean, A3W.

C.4 Associated Wave Periods

In order to determine associated peak wave periods (Tp) in the NSS statistics, the following steps are used:

a) For each wind direction bin, a separate fit is carried out, each using Hm0 and Tp values from timestamps where hub height wind direction falls within the appropriate bin range.

b) The data for the fit are further split into Hm0 bins that are 0.25 m in width.

c) For each bin, representative values, $Hm0_b$ and Tp_b are determined whereby:
   a. $Hm0_b$ is taken to be the centre of the 0.25 m bin.
   b. Tp_b is taken to be the mean of the Tp values for data within the 0.25 m bin.

d) A third-order polynomial is fitted to the collection of representative values found for each bin in Step c), relating Tp_b to the *square root* of $Hm0_b$. Care is taken to ensure the polynomial is not unduly influenced by sudden variations in Tp_b caused by more complex relationships seen in the data.

e) This polynomial is subsequently used in conjunction to the NSS Hm0 values to give associated Tp values.

Omni-directional values for Tp are taken to be those from the sector with the highest Hm0, i.e., that from which the omni-directional Hm0 was taken.

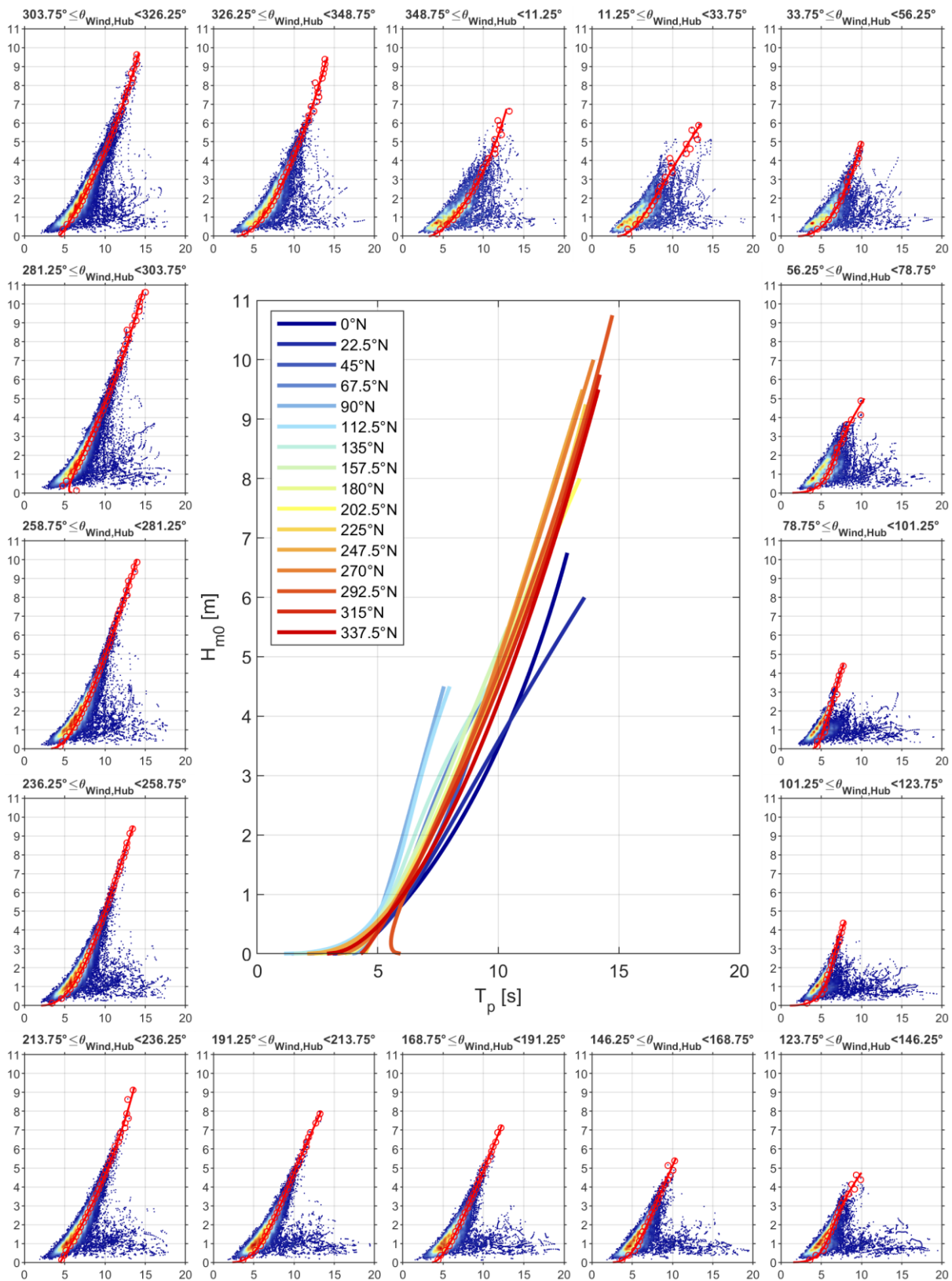Fits determined for the A3W location are shown in Figure C.3.

Figure C.3. NSS associated Tp relationships, A3W.

Appendix D. Severe Sea States

D.1 Introduction

Further details on the derivation of Severe Sea State (SSS) criteria are provided as follows:

- In Section D.2, the data sources used in deriving the SSS are outlined.
- In Section D.3, contours describing the 50-year significant wave height (Hm0) conditional on wind speed at hub height (U_{hub}) are determined based on the methods described in IEC 61400-3-1:2019 [4] (Annex F), and reviewed against the modelled data.
- In Section D.4, additional parameters such as peak wave periods and maximum wave heights to associate with the contour are considered.

Throughout, a worked example is provided for the A3W location using a hub height of 150 m.

D.2 Data Sources

Full details on the data sources used for this analysis, as well as validations against modelled datasets in the region can be found in the Metocean Data Overview. By way of summary:

- Wave parameters originate from a bespoke SWAN model, to produce a 45-year wave hindcast between 1979 and 2023, inclusive.
- Modelled wind data originate from ECMWF ERA5 and were subjected to bespoke adjustment by MetOceanWorks at the hub height elevation of 150 m as well as the Weibull transformations described in Appendix B.

D.3 50-Year Hm0 Conditional on Hub Height Wind Speed (IEC 61400-3-1)

D.3.1 Overview

For our analyses, guidance for the calculation of the SSS is taken from IEC 61400-3-1:2019 whereby:

- The severe sea state model associates a severe sea state with each wind speed in the range corresponding to power production.
- The significant wave height for each severe sea state is determined such that the combination of the significant wave height (Hm0) and the hub height wind speed (U_{hub}) has a recurrence period of 50 years.
- A joint distribution should be fitted to U_{hub} and Hm0 such that U_{hub} is fitted independently, and Hm0 fitted conditionally on U_{hub}. Conditional lognormal or normal distributions are recommended for Hm0.
- The Inverse First Order Reliability Method (IFORM) is recommended for the extrapolation of the joint distribution.
- For higher levels of U_{hub}, both log-normal and normal conditional distributions can have trouble accounting for any upper limitations in Hm0. Thus, to avoid unnecessarily large Hm0 estimates, the unconditional 50-year Hm0 extreme value may be used as an upper limit throughout.

Whilst IEC 61400-3-1:2019 (and in particular Annex F) provides much detail on the overall approach necessary, there are still a number of gaps which need consideration, for example:

1. No distribution for wind speed is explicitly specified.

2. No preference is stated between lognormal and normal Hm0 distributions, though it is noted that *"the lognormal model is conservative compared to the normal model given the same dataset".*

3. No specific guidance is given to determining sea state parameters *other* than Hm0.

D.3.2   Wind Speed Distribution

We begin by considering the distribution of wind speed. As noted above, IEC 61400-3-1:2019 does not explicitly state the distribution that should be used to describe wind speeds in the SSS contours. Other guidelines, such as DNV-RP-205 [36], suggest use of a Weibull distribution. In practise though, SSS statistics are *not* required within the upper tail of the wind speed distribution, and as such the empirical distribution of the data itself can be, and has been, used in this work.

D.3.3   Conditional Normal and Lognormal Hm0 Distributions

IEC methodology suggests that either the normal or lognormal distributions could be used to model Hm0 conditional on U_{hub}. Such contours are shown for A3W in Figure D-1. In keeping with MetOceanWorks' previous experience in using these distributions, the lognormal distribution leads to an overly conservative contour whilst the normal distribution under predicts.

In both cases:

- The empirical distribution outlined in Section D.3.2 is used to model wind speeds at hub height.
- Normal and lognormal Hm0 distributions are fitted to each 1 m/s wide wind speed bin independently.
- A 3-hour sea-state duration is used.
- The contour for each wind speed bin is taken to be the *largest* Hm0 predicted across the bin according to the IFORM method.
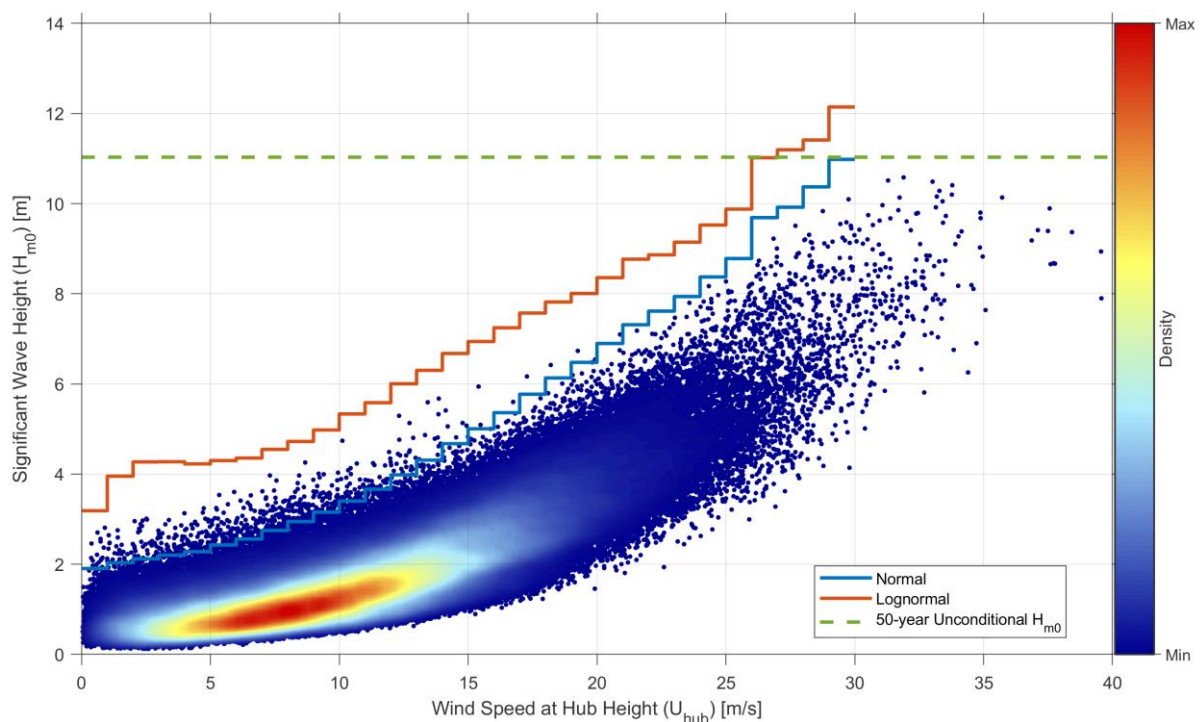

Figure D-1: IFORM contours with normal and lognormal conditional Hm0 distributions, A3W.

Also overlaid is the *unconditional* 50-year Hm0 extreme value, as provided in design criteria for each location. IEC 61400-3-1:2019 states that the 50-year unconditional Hm0 extreme value can be used as "a conservative value" for any wind speed. Thus, any final contour will ultimately be limited by this value.

D.3.4   Automated Fitting to only Highest Hm0

Given the poor performance of the lognormal and normal distributions, an alternate approach is sought to determine the more appropriate Hm0 values along the contour. For this work, we adopt an automated approach in line with that used for unconditional extreme value analysis, as described in Appendix A.

Independently for each 1 m/s wind speed bin, this proceeds as follows:

1) The top 25% of Hm0 values in the bin are found.

2) Weibull, generalized Pareto and exponential distributions are fitted to the data using a selection of methods, yielding a total of ten possible fits.

3) Composite "all data" distributions are created in each case, using an empirical distribution for the lower 75% of Hm0 values and the fitted distribution for the top 25%.

4) Steps 1) to 3) are repeated for the top 24%, 23%, …, 11% and 10% of the data.

5) The quality of each fit is assessed. For a single fit, consider the plot of data (grey circles) and fit (purple line) shown below. For each data point, we determine whether the fit *at the same probability of exceedance* is within the range of 97% to 105% of the data value. If the fit satisfies these criteria for *all* data points, it is retained, otherwise it is discarded. Note that, by definition, the lower (empirical) part of each composite distribution satisfies this condition, hence the assessment is only influenced by the fitted upper tail.
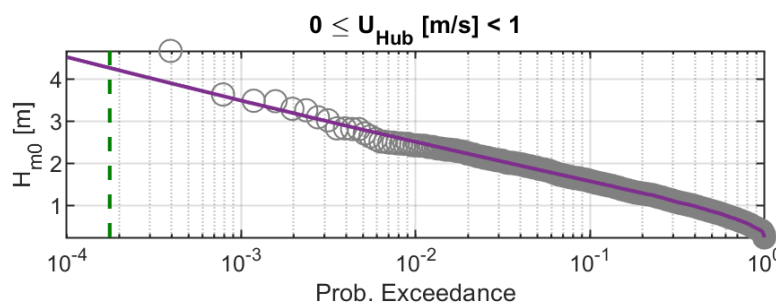
6) *If* this leaves 20 or more retained fits, we proceed to step 6). If not, the criteria for retention is extended, either by widening the range, e.g., to 95% to 107.5%, or allowing the fit for *one* data point to lie outside the permitted range. Again, if this gives 20 or more retained fits, we move to step 6), otherwise the criteria are continually extended until 20 or more fits remain.

7) Rather than selecting a single representative fit, for any probability of exceedance, the 70th percentile from *all* retained fits is used.

The results of fits to individual 1 m/s bins for the A3W location are shown in Figure D-2 and Figure D-3, with the resulting IFORM contour shown in Figure D-4.
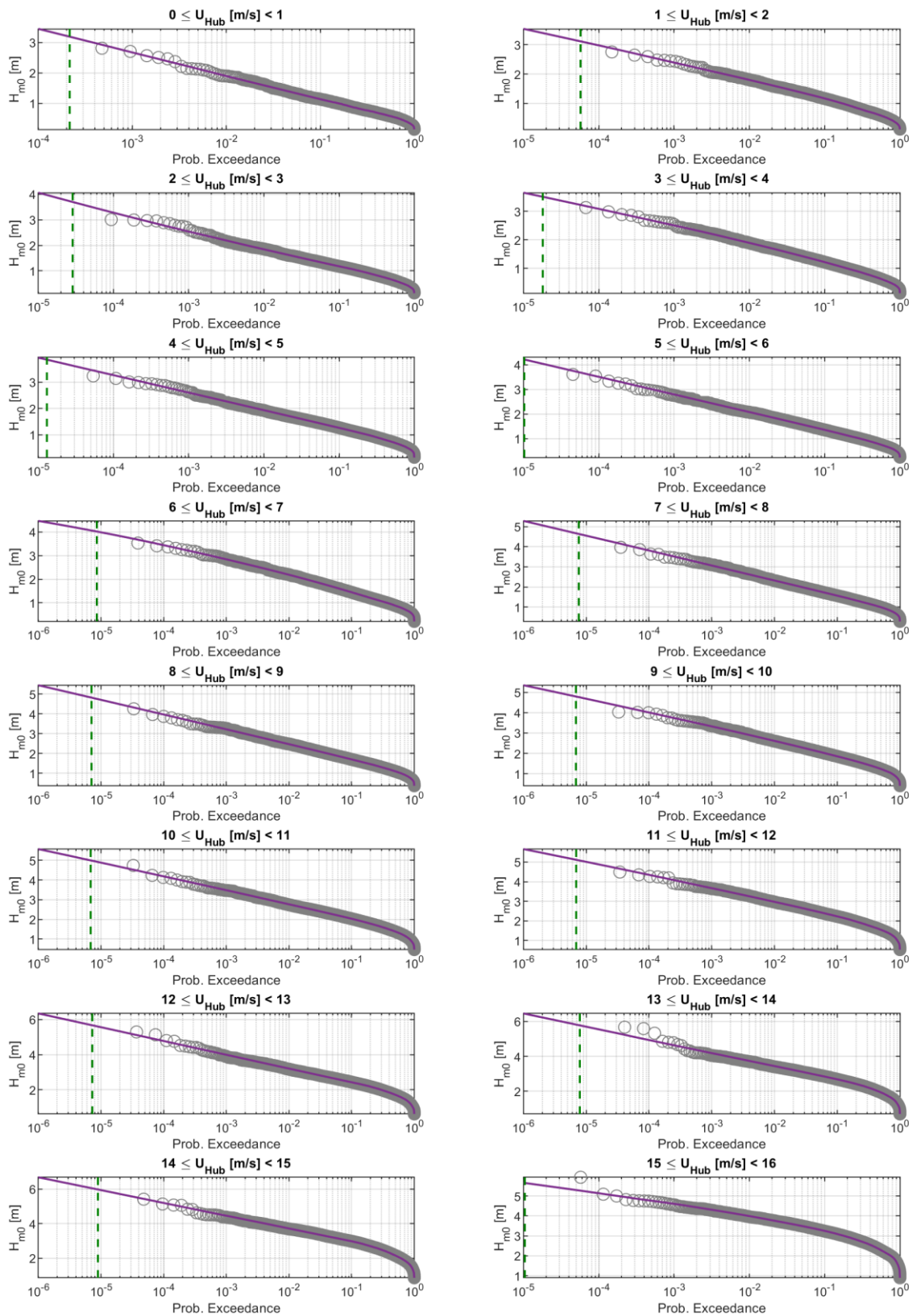
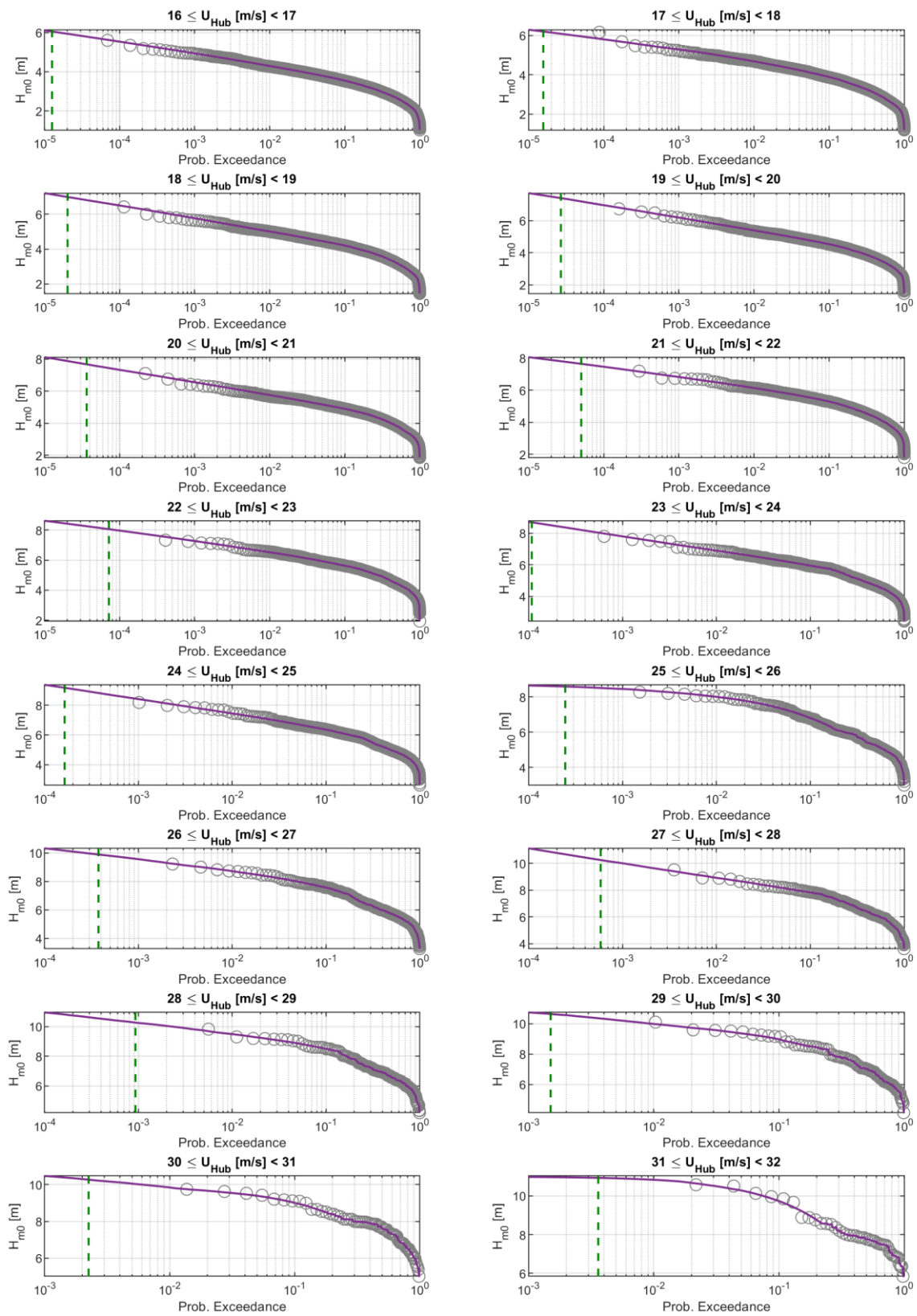Figure D-2: Hm0 binned automated upper tail fits, U_{hub} < 16 m/s, A3W.

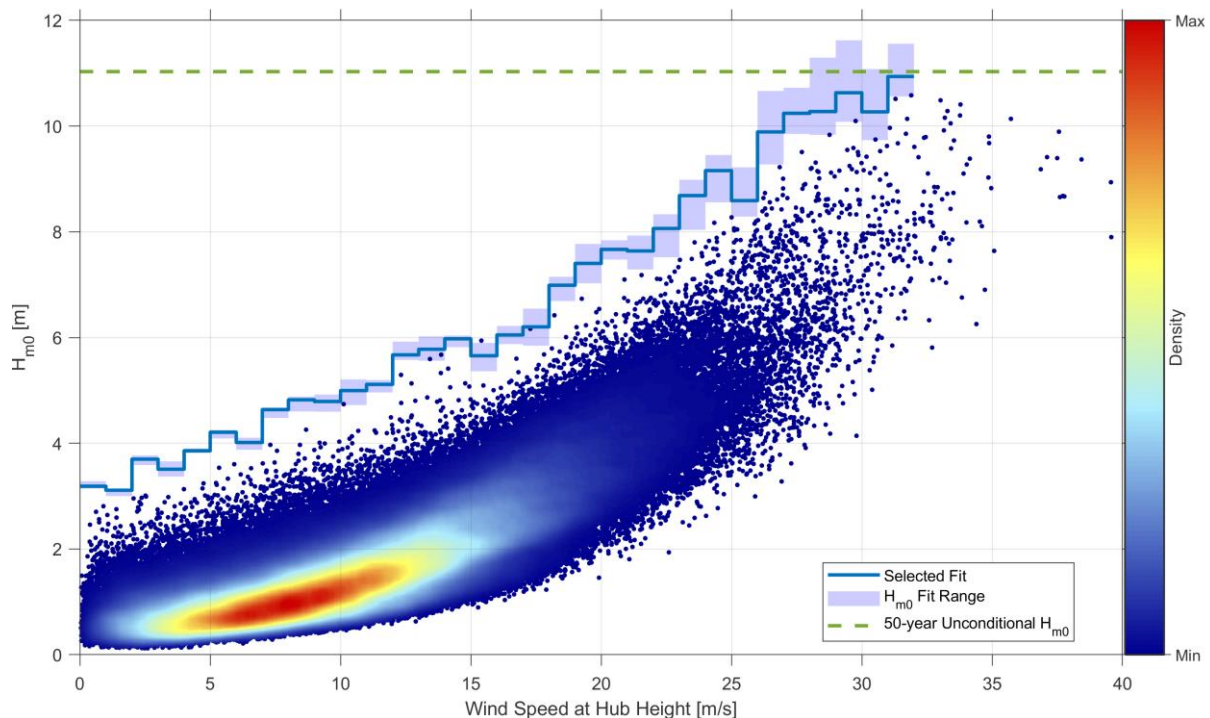Figure D-3: Hm0 binned automated upper tail fits, $U_{hub} \geq 16$ m/s, A3W.

Figure D-4: IFORM contour from automated upper tail Hm0 fits, A3W.

D.3.5 Smoothing and Final Adjustments

Throughout the previous Sections, each wind speed bin has been fitted independently. As this can lead to some discontinuities between neighbouring bins, smoothing of the contour may prove beneficial. As such, the following steps are used:

STEP 1: Fit a 4th order polynomial to the H_{m0} values for all bins

In order to smooth minor statistical variations between neighbouring bins, and allow estimates to be made at all wind speeds, a curve is fitted through the results for all bins. A 4th order polynomial provides a suitable balance between flexibility and smoothness in this regard, though a little caution is necessary to ensure any turning points at higher wind speeds are suitably addressed.

STEP 2: Add conservatisms to the polynomial

To ensure the H_{m0} values are conservative, the standard deviation of the residuals of the polynomial fit in STEP 1 are first added.

STEP 3: Limit the contour at the omni-directional 50-year H_{m0}

As noted in IEC 61400-3-1:

For all mean wind speeds, the unconditional extreme significant wave height, [$H_{m0,50}$]. with a return period of 50 Thus, the H_{m0} values on the contour should not pass above this value. For wind speed bins higher than those used in the fitting, i.e. where data is too sparse to obtain a suitable fit, this is also a suitable value for $H_{m0,SSS}$.

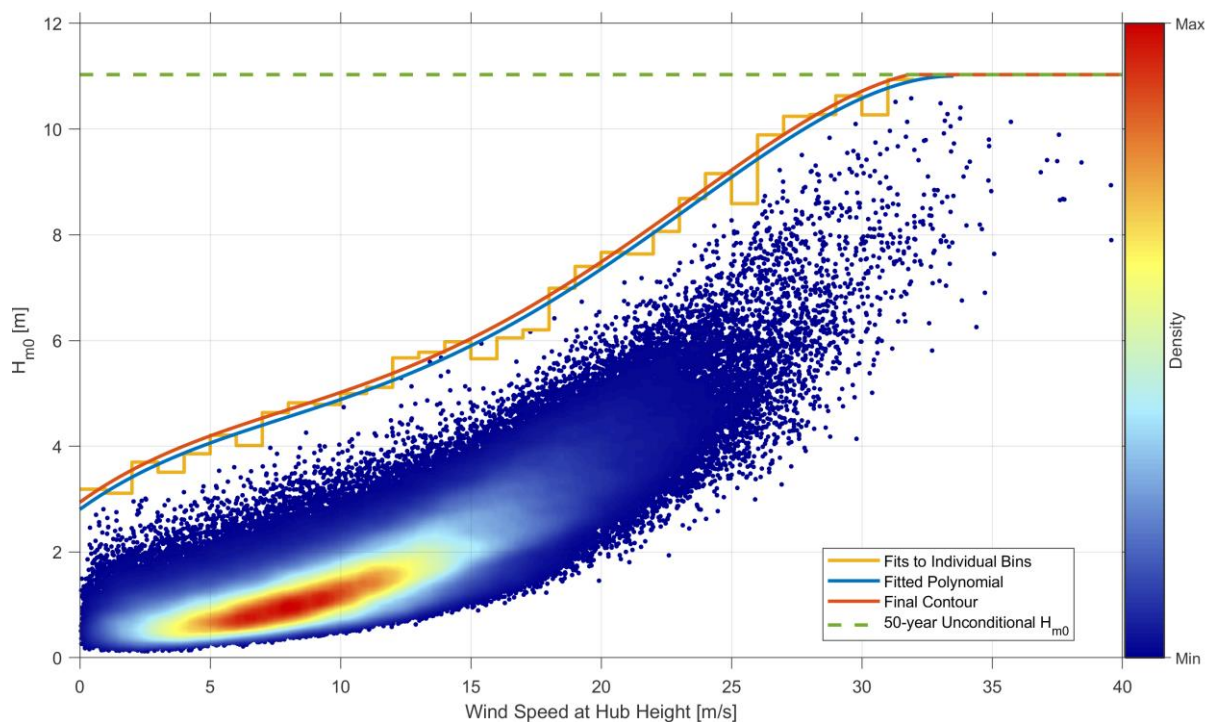The results of these final steps are shown below for the A3W in Figure D-5.

Figure D-5. Final SSS contour, A3W.

D.4   Associated Parameters

D.4.1   Peak Period (Tp)

Relationships between significant wave height (Hm0) and peak wave period (Tp) are determined by applying the conditional modelling approach (CMA) as described in Section 5.3, but only using data where Hm0 is amongst the highest 10% of values in an SSS wind speed bin. The relationship fitted is shown alongside the data in Figure D-6.

D.4.2   Associated Maximum Wave Height (Hmax)

Maximum wave heights associated with the contour are determined by a multiplier taken to be the largest ratio between Hmax and Hm0 found across return periods from 1 to 50 years for each location.

D.4.3   Associated with Hmax (Tass)

The lower, mid and upper estimates for the period associated with Hmax are taken to be 0.9 times the lower, mid and upper estimates for Tp, as explained in Section 5.3.1.
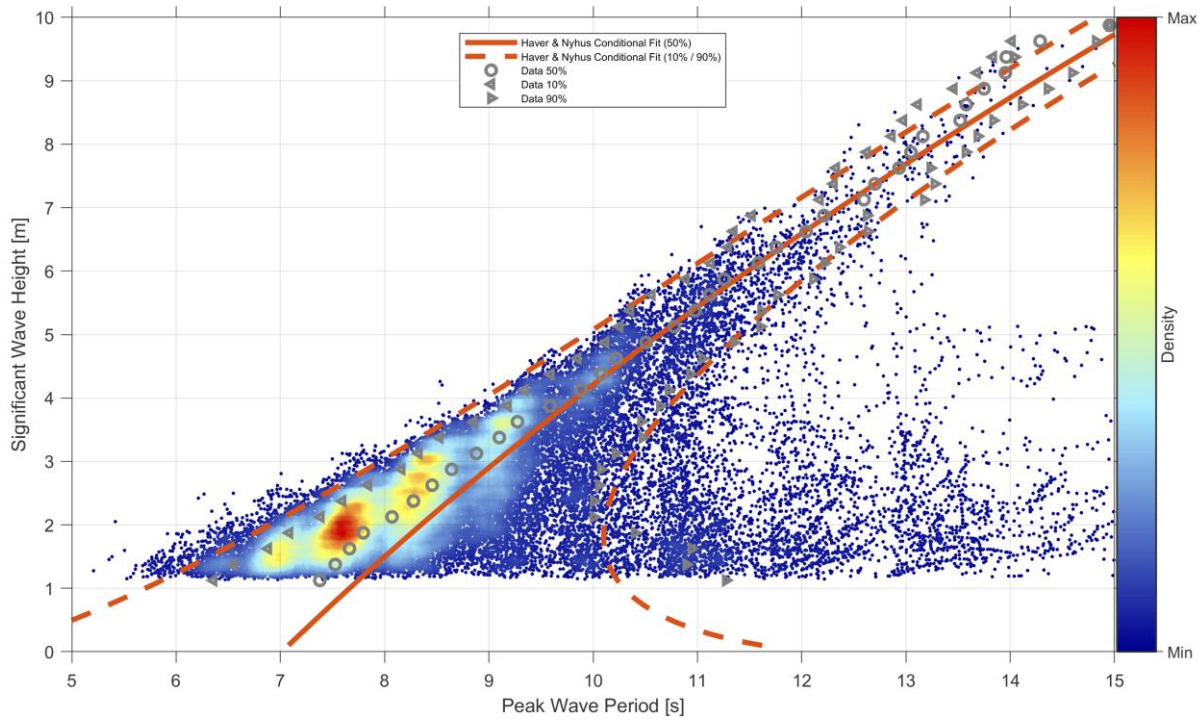
Figure D-6. Hm0 versus Tp relationship, A3W.